EXPLORING SUSTAINABLE SAND-WINNING IN THE WHITE VOLTA

ESTIMATING TRANSIENT STORAGE UPSTREAM OF RUN-OF-RIVER WEIRS FOR SAND WINNING PURPOSES VIA HEC-RAS 6, 1-D, FLUME MODELS

J. Arends

Witteveen + Bos

African Water Corridor

TU Delft

ESTIMATING POTENTIAL USE OF RUN-OF-RIVER WEIRS FOR SAND WINNING PURPOSES VIA HEC-RAS 6, 1-D, FLUME MODELS FOR DEEPER INSIGHTS INTO TRANSIENT STORAGE UPSTREAM OF A RUN-OF-RIVER WEIR

A thesis submitted to the Delft University of Technology in partial fulfillment of the requirements for the degree of

Master of Science in Civil Engineering and Geosciences

by

Jon Arends

December 2021

Jon Arends: *Estimating potential use of Run-of-River weirs for sand winning purposes via HEC-RAS 6, 1-D, flume models for deeper insights into transient storage upstream of a run-of-river weir* (2021)

ISBN 999–99–9999–999–9

The work in this thesis was made in the:

Water Resources group
Department of Water Management
Faculty of Civil Engineering and Geosciences
Delft University of Technology

Supervisors: Prof.dr. Nick van de Giesen
Dr. Miroslav Marence
ir. Marcel Wauben

ABSTRACT

This research aims to explore sediment transport behavior and accumulation caused by run-of-river weirs in order to examine there feasibility for sustainable sediment mining purposes in the White Volta River. Weirs are used to raise water levels upstream to increase water levels and storage, but their is little information regarding sediment continuity and transport over a weir. Observational research studies suggest that weirs do not have a 100% trapping efficiency, however, due to the reduced flows this study hypothesizes that sediment will settle upstream of the structure.

Based on data from the White Volta River, a 1D Flume model is created using HEC-RAS which tests several sediment transport functions and bed roughness parameters with constant bed slope, suspended and bed-load gradation in order to estimate sediment settling. The results suggest that during peak discharge events settled sediments are flushed up and over the weir. As peak discharges decrease, settling occurs based on particle diameter causing increased sediment storage upstream until the next flushing event. The volume of sediment stored ramp is highly variable with respect to bed roughness and the used transport function, suggesting river calibration is required for concrete estimates. Based on the model results, approximately $1 - 2\%$ of the White Volta's yearly suspended load settles in-front of the structure before the discharge flushing event.

ACKNOWLEDGEMENTS

This research is the final work done to obtain my masters of Science in Civil Engineering at the Delft University of Technology. I would like to thank Delft University for the education over the last three years, all the professors and fellow classmates for making the time special. A special thanks goes to Nick van de Giessen and Miroslav Marence my supervisors at the University. This research was done in collaboration with Witteveen+Bos, thus I would like to thank Jasper Schakel for introducing me to the African Water Corridor (AWC), and to the research topic. And a special thanks to Marcel Wauben, my supervisor at Witteveen+Bos for being there for all questions and for guiding me over the duration of this research. I would like to thank Job Udo from HKV for providing some of the data required for this research.

Lastly, I would like to thank my friends and those who have become my family during the course of my studies here in the Netherlands. You have turned this country into my home and have made my time here special in so many ways. I am forever grateful and blessed for you!

Jon Arends, 2021

...

CONTENTS

LIST OF FIGURES

LIST OF TABLES

ACRONYMS

1 INTRODUCTION

1.1 PREFACE

The city of Tamale is experiencing ecological dangers due to the changing morphological nature of the White Volta River. The increasingly urbanized city is being fueled by sediment mined from the river beds which is starting to create further issues in the region. Currently, sand mining is unregulated with verbal agreements to remain 100 meters from the river bed, however, news reports out of the region suggest that the Ghana Water Company (GWC) is struggling to supply Tamale with water due to the impacts of flooding and sand mining. During the dry season pumping station intakes are being clogged due to increased turbidity while during the wet season the pumps get flooded causing the intake point to shut down. A cause of these issues is reckoned to be sand winning due to the morphological impacts of its activities.

Ecological damages caused by sand winning is not uncommon, sand mining has destroyed river beds in other areas of the world rapidly changing the natural state of the river. Local communities are primarily affected as they depend on the river for farming, fishing, and acquiring drinking water. However, on a similar note, sand winning is a lucrative enterprise which provides income to local communities and helps drive the urban development of Tamale. Thus a sustainable win-win solution that both keeps the sustainability of the river and helps the local community is desired.

In the region, the AWC group has developed a mission for *"sustainable development through innovative sustainable implementation strategies to insure that water will not be a limiting factor in the development of human and natural resources in Sub-Saharan Africa"* [tud]. As an introductory study, the AWC group is investigating the implications of the construction of run-of-river weirs to help decrease flooding and potentially be used for sustainable sand winning. For further exploration of the topic see the research conducted by Kingma.

1.2 RESEARCH OBJECTIVE

The main objective of this research is to estimate the potential excess sediment accumulation immediately upstream of a single weir. The preliminary aim is to gain further understanding of sediment behavior, which includes the morphological behaviors of sediment and how the weir will alter its behavior. As morphological behavior is a dynamic process which requires a lot of field data, this study will be done based on available data that is found online. Therefore, predictions will be made to determine whether further investigations are of value. In practice, different methods of calculating sediment transport in rivers can give a wide variety of results. Models are often first created, and then calibrated to acquired data. As data can not be acquired at this time, a literature study of sediment transport methods will be conducted, which will then be modelled in a flume based on specifications from the White Volta River obtained from Udo and Klopstra, der Zwet, Akrasi. In

this research, HEC-RAS 6 will be used to create the model, input the parameters and predict the morphological behavior of a weir.

1.3 RESEARCH QUESTIONS

The primary question this research hopes to answer is **What is the estimated potential sediment accumulation and benefit resulting from a run-of-river weir on the White Volta River near Tamale?**. To solve this, the following sub-questions much be answered.

- What is the current volume of sediment transported through a typical cross section on the White Volta River?
  - How does the discharge of the river adjust the volume of sediment entering the system?
  - Using a sediment rating curve, what fractionalization of grain classes of sediment are transported through?
  - What is the current bed gradation of the White Volta River?
  - How does the discharge of the river alter the sedimentation behavior?
- With volumes of sediment known, how can sediment behavior be impacted by a weir?
  - How does the transport function, settling velocity, bed armoring, and roughness impact sediment transport behaviour?
  - After using the various methods of calculation, how will the weir change the behavior of the sediment with various flow conditions?

1.4 REPORT OUTLINE

- **Chapter 1** Includes the preamble, research objectives, and research questions.
- **Chapter 2** Begins with a brief introduction into sand mining and its impacts on the river and the water supply.
- **Chapter 3** Introduces the study area with further information about the region and river.
- **Chapter 4** Introduces the reader to the existing literature regarding the usage of a run-of-river weir for sand winning purposes
- **Chapter 5** Delves deep into the literature regarding sediment morphological behavior, transport functions, and calculations required to make accurate bed accumulation predictions.
- **Chapter 6** Shows how the model is created, which data is available to build the model and which information needs to be assumed.
- **Chapter 7** The results of the model are assessed.
- **Chapter 8** Recommendations for furthering research to explore the topic further are given.

2 PROBLEM STATEMENT

2.1 SAND MINING

Sand and gravel aggregates play an essential role in the production of concrete (cement, water, sand and gravel). Thus, these aggregates are essential for the formation of the urban environment as residential and commercial construction, roads, bridges, and walkways are primarily composed of concrete [56]. These aggregates come primarily from two sources: terrestrial and marine. Terrestrial sand includes residual soil deposits, river channel deposits, and flood plain alluvial deposits located primarily on mountain and river valleys. Marine sand comes from shore and offshore deposits [31]. Active river deposits of sediment are desirable for construction material as they are well sorted, durable, and located frequently near market and transportation routes [41]). Thus, they are genarally more desirable for construction than marine deposits. It is estimated that the total sand and gravel mined each year exceeds 40 billion tons, more than double the yearly sediment transported each year by every single river in the world [47]. Currently, sand and gravel is being extracted at volumes far exceeding its replenishment, a trend that is expected to continue due to population growth, rapid urbanization and an increased standards of living [47]. It is then expected that the extraction of sand will have significant environmental consequences without regulatory planning.

Sand and gravel can be easily extracted from river sources and do not require much processing to be used for building construction. The easy accessibility of river sand causes developing countries to be greatly dependent on river sources to meet aggregate requirements. Historically, the impacts of sand mining were of little consideration. However, it is beginning to be understood that sand mining can cause irreparable and irreversible damages to the ecological and socioeconomic environments of the rivers. Sand removal alters the sediment budget of the river, as well as changes the channel hydraulics [45].

In-stream sand mining can be severely damaging to the environment and ecosystem [54; 36]. Existing research on many river systems around the world show that sand mining has changed bed morphology, reduced flow velocities, increased erosion, and changes to the rivers sediment flux [36; 27]. Drastic changes to the sediment budget can lead to serious environmental hazards including habitat transformation, biodiversity changes, which may threaten the very existence of the river ecosystem. Reduction in sediment supply from upstream reaches and erosion can lead to loss of land, channel incision and the degradation of infrastructure structures. Which is confirmed with many studies conducted on dam impacts on bedload transport, with sediments being trapped in the upstream reservoir, effectively lowering reservoir capacity [48]. The release of sediment starved water leads to erosion and lowering of the channel bed downstream [48]). Removing sediment also lowers the water table, making it more difficult for stable drinking water supply and agriculture water use [47]. Not all sand removal activities are detrimental, with proper guidance sand mining can have net positive impact for flood plain management, increase reservoir storage, and can produce overall benefits [27]. However, when the rate of extraction of sand exceeds the rate that natural processes replenish the sediment long term damage begins to occur. Collins summarizes the impacts of

river sediment extractions with the following effects [22]:

- Extraction of bed material in excess of replenishment by transport upstream causes the bed to lower (degrade) upstream and downstream of the site of removal.
- Bed degradation can undermine bridge supports, pipelines, and other structures.
- Degradation may change the morphology of the riverbed, constituting one aspect of the aquatic habitat.
- Degradation can deplete the entire depth of sediment material, exposing other substrates that may underlie the sediment, which can in turn affect the quality of aquatic habitat.
- If floodplain aquifer drains to the stream, groundwater can be lowered as a result of bed degradation
- Lowering the water table can destroy riparian vegetation.
- Flooding is reduced as bed elevations and flood heights decrease, reducing hazard for human occupancy of floodplains and the chance damage of engineering works.
- The supply of over-bank sediments to floodplains is reduced as flood heights decrease.
- Rapid bed degradation may induce bank collapse and erosion by increasing heights of banks.
- Reduction in size or height of bars can cause adjacent banks to erode more rapidly or to stabilize, depending on how much gravel is removed, the distribution of gravel, and the geometry of the bend.
- Removal of sediment from bars may cause downstream bars to erode if fluvial transport of sediment from upstream is decreased.

Without proper regulation, sand mining will generate environmental problems usually stemming from more sediment being removed than the river system can replenish. All over the world, there are alarm bells sounding at the damage being done by unrestricted sand mining. However, with proper planning and employment of sustainable sand mining techniques, some researchers believe that the resulting negative consequences of sand mining can be reduced [27]. This is done by limiting the extraction of sediment to a portion of the bed-load that passes through the mining site on a given year.

2.2 IMPACT ON WATER SUPPLY

In-stream sand mining threatens water security resulting from decreased groundwater storage due to the lowering of the alluvial water table [44]. The Lake Country planning department in California estimated that the alluvial aquifer storage from river incision can decrease up to 15% [41]. In Tamale, large portions of the population are dependent on boreholes for fresh water supply, thus the lowering of the water table due to incision and extraction may strain rural populations. This effect is already being seen in the Northern Ghana region as residents are struggling to access fresh water [64]. In Tamale, the GWC told DW.com in an interview that “as a

result of sand mining, the river bed has degraded to the depth of excavation, causing the water table to lower near the river bed". The lowering of the water table also has the possibility of destroying native vegetation on the riparian habitats, however, studies have shown that pioneer vegetation species will develop after recovery of the landscape [41; 35].

Mining activities also deteriorates the water quality by increasing the turbidity downstream of the extraction sites. This has led to damage to the GWC's water intake pumps and increased the water treatment costs. The GWC proceeded to say that the river has been completely contaminated, with the water quality having the consistency of "groundnut soup" [5]. As a result, the GWC has been forced to shut down extraction for two days a week to service its water pumps. The turbidity increase also impacts fish populations, riparian vegetation, and the food web dynamics. Fish population diversity are reduced with those attuned to higher sediment concentrations becoming dominant in the river, while more sensitive fish struggle to survive [40]. The substrate removal also destroys fish spawning zones, however, with controlled volume removal at lower frequencies studies have shown that the disturbance on native wildlife can be limited to that of a regular flood event [51].

3 STUDY AREA

3.1 INTRODUCTION TO THE CITY OF TAMALE

This research focuses on the White Volta Basin, near the city of Tamale in the Northern Region of Ghana. The city of Tamale is a fast growing metropolis, quickly growing into the third largest urban center in Ghana with it population increasing from less than 2000 people in 1907 to an estimated 950,000 according to the Tamale Metropolitan Assembly [tam]. The city is located within latitudes 9°16'N and 9°34'N and longitudes 0°34'W and 0°57'W, in the Northern region of Ghana. Its climate is characterized by the Guinea Savanna Zone which consists mainly of grasses, shrubs, and a few trees. It experiences a rainy season between April and October with annual rainfall varying between 1000 and 1200 mm. The rainfall steadily increases from April with peak rainfall occurring in August and September. From November until March, the total rainfall rapidly decreases during the dry season, with the climate being primarily effected by a dry dust wind called the Harmattan Dust [15]. The mean annual maximum temperatures range from 33°C - 35°C, with a 22°C minimum and a mean of 27.8°C to 28.5°C [15]. The volume of rainfall experienced over the region has strong variability at annual, decadal, and longer timescales resulting in high variability in the discharge from the White Volta River 3.3.

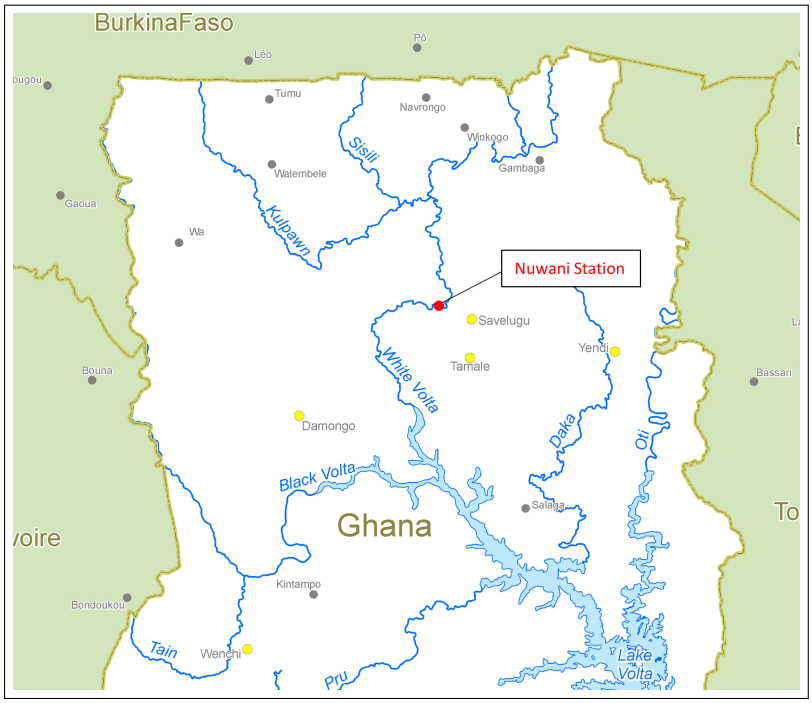

Figure 3.1: Location of Nuwani Guaging station on the White Volta River, Northern Region of Ghana

In Ghana the demand for sand aggregates is also growing, urban populations have increased from 9.4% to 50.9% in 80 years [34].The city of Ghana is rapidly urbanizing, which in turn has caused resource constraints. As the population is

quickly increasing, the need for housing, office space, industry and infrastructure continues to rapidly grow. One key material required to supply the rapid urbanization growth is sand. Currently, sand is produced illegally all over Ghana, with state security varying between cramping down on illegal sand winning or giving it a blind eye [9]. In Tamale, 50% of the sand is removed from the river walls of the White Volta, as the banks of the river consists of natural deposits of sand suitable for construction material. From a study from Abu and Peprah, of 6 monitored mining sites, an average of 54 tipper trucks per day carrying approximately $20m^3$ of sand each, leave each site. Therefore in total from the six sites, over $6000m^3$ of sand is removed daily from the river banks.

Figure 3.2: Ghanian Tipper truck

Currently, mining sand is not currently being strongly addressed by governmental policy and legislation. This has led to many ecological issues arising in Tamale due to sand mining activities [gov; 49; 67]. In addition, many residents near sand-winning sites have expressed desire for a regulatory body to help improve the social impacts of sand winning. In surveys conducted by Abu and Peprah, local respondents have reported that sand winners have used force to mine sand off of their lands which has caused destruction to their farm lands and has led to water shortages on their farms [9]. However, in many cases social bonds have formed between sand winners and local residents in which sand producers provided transportation services and attended community events.

While sand mining improves the development of infrastructure and provides livelihood opportunities, every nation is responsible to its succeeding generations in developing and conserving its natural resources in the best possible way. For this reason, this research aims to determine whether the construction of a river weir can have a positive impact in developing a sustainable sand mining economy with considerations for the long term health of the river ecosystem.

3.2 WHITE VOLTA RIVER HYDROLOGICAL INFORMATION

The White Volta River is an alluvial river making up one of the 3 main tributaries of the Volta River Basin. The Volta River Basin covers an area of $400,000km^2$ spanning across six countries: Benin, Burkina Faso, Cote d'Ivoire, Ghana, Mali, and Togo. The river snakes down from its source in Burkina Faso, to where it is discharged in Lake Volta. The study area is based on a location near Tamale, at the Nuwani Guaging station in Ghana. The river in the region of the Nuwani Guaging station has a very low slope ($0.00014m/m$) as it slowly meanders towards Lake Volta [59]. The discharge data used in this study were collected from Nawuni Gauging station in Ghana, by the Ghana Hydrological Services Department (GHSD) available at portal.grdc.bafg.de(Table 7.1). Quality assurance of the data was done by ensuring clearly abnormal errors were not present in the data. This study uses the assump-

tion that the data was collected accurately by the source, with no direct checks for accuracy at the gauging station. As seen in (Figure 7.2), discharge peaks at Nuwani station align with precipitation data, with short term high discharge peaks during the rainy season between May-October, and very low flows during the rest of the year.

**Note - Although not included in this research, the impacts that the creation of the Bagre Dam will have on discharge and sediment characteristics are not known, this research will be based on historical data with consideration to future hydraulic changes.*

Owner of Data	GHSD
Data Set Content	Mean Daily Discharge
Catchment Area km^2	92950
Longitude (DD)	-1.08
Latitude (DD)	9.7
Station	Nuwani
Country	Ghana
River	White Volta
Unit of Measure	m^3/s

Table 3.1: Data Reference information for Nuwani Station, Ghana taken from portal.grdc.bafg.de

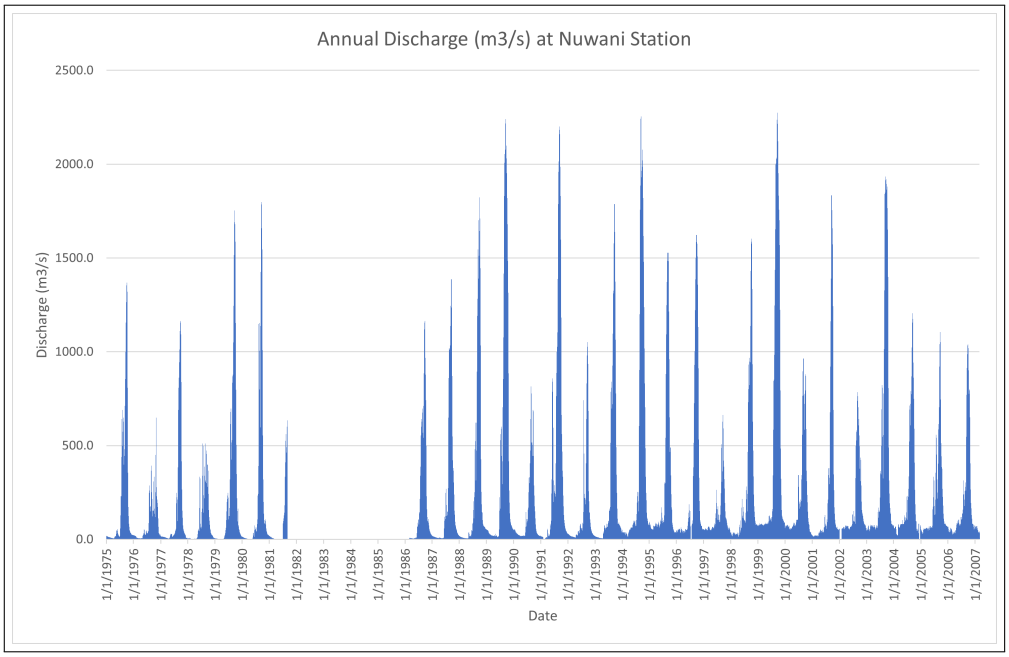

Figure 3.3: 1975-2007 Discharge measurements at Nuwani Guaging station north of Tamale. No data between 1982-1986

Years on Record	28
Average Max Yearly Discharge	1399.1
Standard Deviation	543.1
Skew	-0.51
90% Confidence	168.6

Year	**Annual Maximum Discharges** m^3/s	**Year**	**Annual Maximum Discharges** m^3/s
1975	1367.8	**1993**	1787.9
1976	648.4	**1994**	2279.3
1977	1163.7	**1995**	1528.5
1978	510.5	**1996**	1622.7
1979	1754.3	**1997**	663.7
1980	1797.3	**1998**	1602.3
1981	634.8	**1999**	2274.1
1986	1163.7	**2000**	964.1
1987	1387.0	**2001**	1835.0
1988	1823.2	**2002**	785.4
1989	2240.8	**2003**	1934.9
1990	816.2	**2004**	1206.5
1991	2200.8	**2005**	1106.2
1992	1051.2	**2006**	1038.4

Table 3.2: Annual Maximum Discharge for Nuwani Station

4 LITERATURE INVESTIGATIONS OF USING A WEIR FOR SEDIMENT CAPTURE

4.1 SEDIMENT BEHAVIOUR

In the rivers natural state, the river can be viewed as a conveyor belt, transporting erosional products to depositional sites below sea level. The transport of sediment is continuous, with channel bars and depositional zones having their grains replaced constantly by flowing sediment. This continuous flow will be altered by the creation of a weir. The effects of large dams is well known, with sediment trapping being nearly 100%, with exceptions made to flushing procedures. However, the influence of smaller run-of-river dams is less well studied. With the extent of run-of-river dams impact on channel morphology and bed material characteristics being for the most part, unclear [25]). A run-of-river dam is typically classified as a structure that extends across the river channel, doesn't have a mechanism that inhibits discharge of water over the structure, and is of a height that doesn't exceed the height of the channel banks upstream, with water being contained within the river channel [24]. The head upstream is usually less than a few meters, with short residence times upstream of the structure. The primary hydraulic targets of a weir is to regulate water levels upstream of the weir for navigation, increasing water supply for irrigation and drinking water, and also for low head energy production. Weirs produce lower velocity increased depth pools of water upstream of the weir. The dam increases the water levels upstream during periods of low flow, an effect that changes water surface profiles in an effect called backwater curve. For low gradient rivers, the distance of the backwater effect becomes significantly greater. At high stages the weir often becomes submerged as water flows directly over the structure, and the backwater effect is less pronounced.

Figure 4.1: Run-of-River weir on the Orange River in South Africa

The flow over the weir depends on the weir type, with broad, flat, sharp and ogee crests being the most common. As water flows over the weir crest, it will either free-fall or flow down the face of the weir in a high velocity stream of water as flow

becomes super-critical. Downstream of the weir, the depth starts to increase and velocity decreases as sub-critical flows are restored. Once the weir becomes submerged, the hydraulic jump decreases until there is no visible change in the water surface. As the height of the weir does not exceed the water banks, submergence of the dam will occur during the high discharge rainy season. During high stages when the weir is submerged, there is minimal backwater effect, thus water transport is dependent on downstream conditions. Due to the impact hydraulics have on sediment transport, and that the majority of sediment is transported during the high stage rainy season. Thus, understanding how sediments are transported around a weir during submerged flows is of critical importance in determining the trapping efficiency of the weir.

A weir will alter the flow patterns causing the river channel bed-load to adjust to the changed conditions [41]. In a study by Abdalla et al., the flow around an in-stream obstacle was numerically modelled and the flow lines are depicted in Figure 4.2, from this study it is observed that strong re-circulation currents form both upstream and downstream of the structure near the bed, creating a complex turbulent fluid pattern [24; 6]. In Figure 4.2, it can be observed that the velocity immediately upstream in front of the structure is greatly reduced. As the flow of sediments is dependent on the force of water acting on the particle, the low velocity zones should cause the sediment to aggregate in front of the structure. This aggregated sediment volume is sometimes referred to as "transient storage" or "sediment ramping" and has been observed in previous literature [25]. However, the dynamics and volumes of transient storage is still not widely understood. And therefore, their is no direct method of calculating the volume of transient storage sediment amassed infront of the structure. In addition, their is little information regarding the velocity required in the turbulent fluid zones to push the bed-load sediment into the high velocity streams Figure 4.2, up and over the structure.

During low stages, when the weir isn't completely submerged the deposition of sediments will be impacted by the decrease of velocity caused by the backwater curve. When the dam is completely submerged, only the flow immediately upstream and downstream of the weir are influenced by the flow [24]. Therefore, the trap efficiency of the weir is highly variable depending on the hydrological variability of the river. Therefore further testing on the influence of hydrological variability, sediment supply, hydraulical ability to lift bed material over the weir, bed material load, and the height of the weir is required. In a study done by Queen, he noted in a 1-D model that sediment is stored upstream of the dam rapidly increased linearly during initial filling, until it reaches an equilibrium where sediment is transported over the dam. The volumes of sediment stored upstream is dependent on the sediment input, with high inputs resulting in increased aggradation [50]. At higher water velocities, the storage upstream is decreased, suggesting the velocity in the re-circulation zone is high enough to transport sediment over the weir during high stages. Observations on Red Clay Creek show that sediment storage forms a characteristic sloping ramp from the floor of the impoundment to the crest of the dam [46]. However, after 200 years of modelling the structure only retained 25% of the weirs accommodation space. After an equilibrium is reached, sediment can be transported through the impoundment, up the ramp, and over the dam [46]. This is verified in RFID tracer studies, which have shown that sediment continuity is not broken by run-of-river dams, as D_{90} tracer particles are identified downstream of the weir structure [20].

Downstream of the weir we can expect scouring, as the high velocity flows due to the hydraulic drop will cause intense erosional forces. Trapping sediment by a weir will also create hungry water downstream of the weir which will have excess energy which will typically cause erosion to the bed and banks downstream to re-

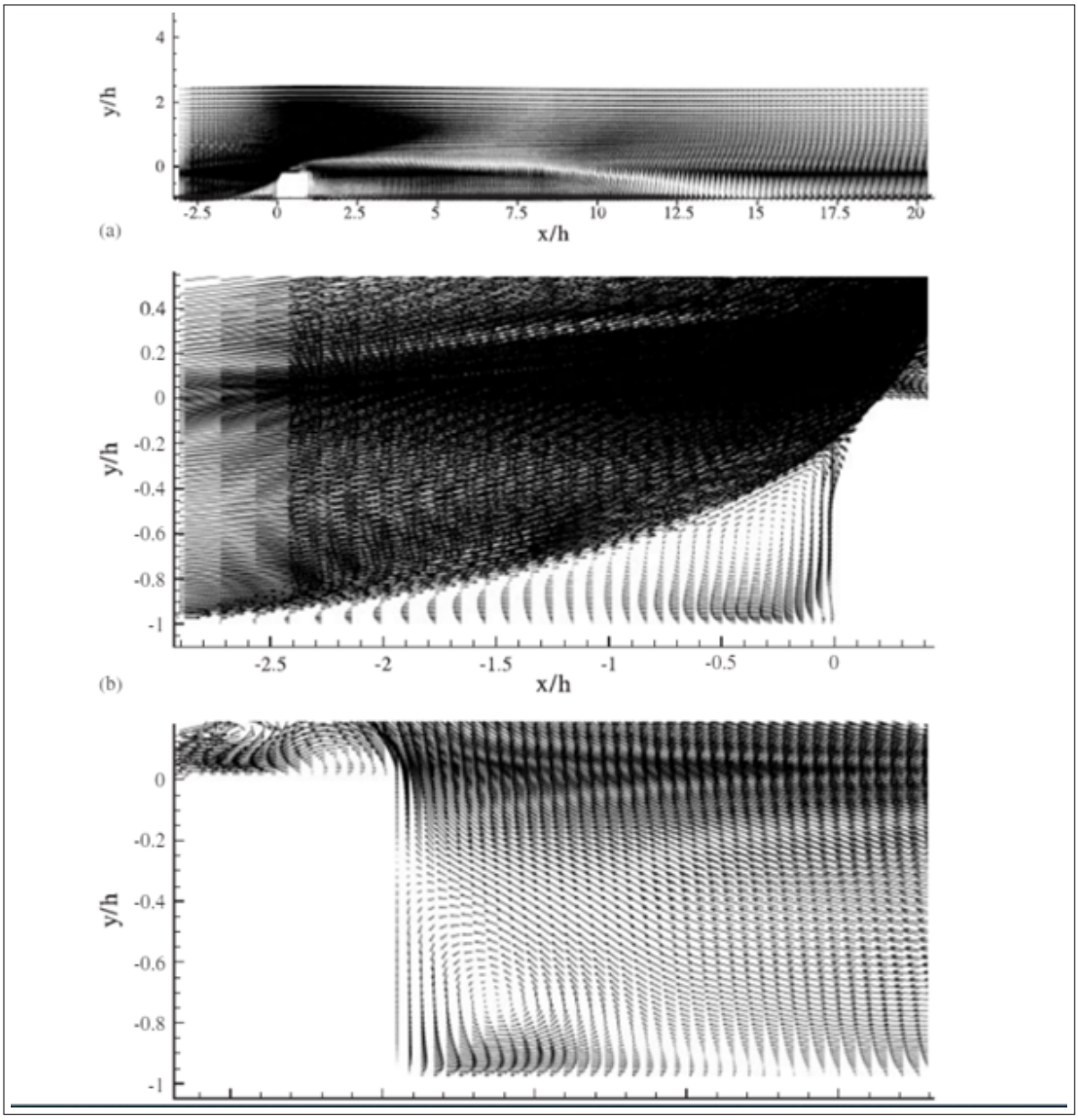

Figure 4.2: Figure 7.1 Numerically modelled flow lines over an in-stream obstacle credits to Ibrahim Abdalla (28), the top image (a) displays the full model results, while (b) and (c) depict the flow lines immediately in front and behind the obstacle.

gain its sediment load [41]. If infrastructure such as bridges are downstream of the weir, it may cause undercutting reducing the structures stability [41]). Therefore, locations for sand mining should be conducted outside of the range of influence on infrastructure. In practice, a protective zone or "apron" of concrete or large rocks will be built behind the weir for bed protection, effectively protecting the structural integrity of the structure [8] . However, as the trapping efficiency of run-of-river dams works with a different mechanism than a full reservoir, the net extent of erosion due to sediment starved water is unknown [25].

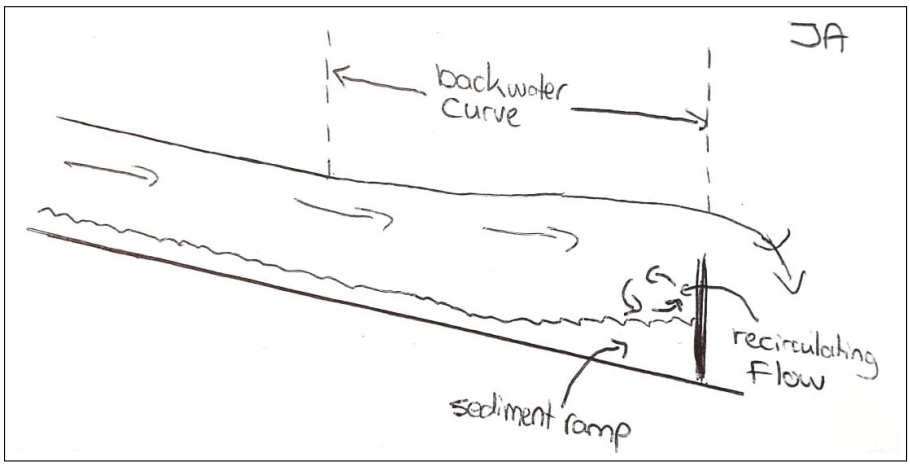

Figure 4.3: Sediment Ramping effect immediately upstream of the weir.

The sediment flow is highly variable due to the diverse processes included in its transport, therefore sediment models should be treated as basic attempts to represent sediment transport in a simplified fashion, a phenomenon that is very misunderstood [41]. In ideal cases, input values are often poorly derived as values are constantly shifting, with transport functions that have highly variable results. Therefore, the true nature of sediment flow in the Volta River requires consistent physical observations to verify the general simplified results of created models.

4.2 USING A WEIR FOR LOCALIZED SAND MINING

This model hopes to test the sediment ramping effect with a 1-D model using a variety of transport parameters to verify the sediment ramping effect using HEC-RAS, effectively estimating the yearly transient storage potential. It will calculate the sediment ramping formed for the 1994 discharge statistics on the White Volta River, using data obtained by Akrasi. In theory, if Queens hypothesis is correct, a specific volume of sediment will form in front of the weir quickly as it reaches its equilibrium point [50], but the sediment continuity of the river will not be significantly impacted [46; 50]). With the use of this model, we hope to determine an approximate volume of sediment that can be removed on a yearly during the low flow dry season that will be replenished quickly as transient storage during the yearly wet season without negatively impacting sediment continuity. It should be noted that weirs are not always positive, extensive studies have been done discussing the impact of weirs on water levels, discharge downstream, increase in flood risk, changes to fish migration patterns. These impacts are not discussed in this paper, but do require careful consideration in the design, construction, and management of the weir.

5 SEDIMENTATION MORPHOLOGY

5.1 SEDIMENT TRANSPORT FUNCTION

Sediment transport is the term used to describe the transport of particles(silt, sand, gravel, boulders) in rivers and streams. The transported material is called sediment load which is divided into two categories: Bedload and Suspended load. Sediment transport calculations are based on particle motion physics which is simplified to the core forces depicted in Figure 5.1.

The initiation of motion begins when the forces that promote movement on the particle are greater than the forces that hinder the particles movement. The main force that promotes movement is the force of velocity or fluid drag that flows over the particle. This force also gets underneath the particle and creates a lifting force causing the particle to become part of the suspended load. The primary resisting force is due to gravity, which holds the particle to the stream bed. And friction & electrostatic forces between grains.

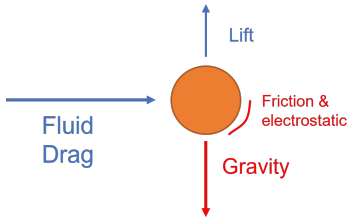

Figure 5.1: Primary forces acting on a particle

When the bed-shear velocity exceeds the critical value for initiation of motion, the bed-load particles will begin moving along the surface of the bed. For increasing bed-shear values, the particles will begin to have larger and more regular jumps called saltation's [52]. If bed-shear velocities exceed the fall velocity of a particle, the sediment particles will be lifted up by turbulent flow resulting in particles going into suspension.

Sediment flow is unpredictable in nature and the layers of complexity influencing river dynamics have resulted in a standardized sediment transport equation never being derived. However, the key forces to calculate are depicted in Figure. 5.1, which are dominantly impacted by bed slope, flow depth, velocity, sediment size, and particle fall velocity [30].

Most sediment transport function are based on the concept that of sediment motion occurs when the shear stress of the river bed is reached [30; 42; 63]. This means that the fluid force acting on the particle is greater than the resisting force caused by the particles weight and friction. Thus, generally at low velocities the bed does not move. As velocities increase, the dimensionless bed-shear stress τ (fluid force) is larger than the threshold critical shear stress (resisting force) τ_{cr} with shear stress being defined as follows:

$$\tau = \gamma D s \tag{5.1}$$

With γ being the weighted density of water, average water depth D, and the water surface slope s Thus, initiation of motion is derived as follows:

$$\tau \geq \tau_{cr} \tag{5.2}$$

The critical shields stress τ_{cr} can be calculated using the Shields equation [55].

$$\theta_{cr} = \frac{\tau_{cr}}{(\rho_s - \rho_f)gD} = f(\frac{u_* D}{\nu}) \tag{5.3}$$

With θ being most commonly defined by the Shields Function as a dimensionless relationship between shear stress τ (N/m^2), density of sediment ρ_s , density of fluid ρ_f , particle diameter D , gravity g, which is a function of the particle Reynolds number Re, kinematic viscosity ν, and shear velocity u_* derived as follows:

$$u_* = \sqrt{\frac{\tau}{\rho_f}} \tag{5.4}$$

Based on the Shields parameter the competence of flow μ_* can be determined, which determines which determines the velocity required to move particles as a function of critical shear stress and their diameters.

$$\mu_* = \theta_{cr}\sqrt{(\rho_s - \rho_f)gD} \tag{5.5}$$

With this in mind, during high discharge flood events large volumes of sediments are generally transported as the shear stress greatly exceeds the threshold shear stress. A prolonged flow slightly exceeding the critical value may have little significance in terms of the volume of bed material transported. While a brief flow greatly exceeding the critical value can transport large volumes of sediment [htt].

Alternatively, stream power is often used as a basis to determine sediment transport. First introduced by Bagnold, stream power suggests that the rate of energy used in transporting sediment can be related to the work being done in sediment transport [14]. Thus, stream power is the product of shear stress along the bed and the average flow velocity. Bagnold defined stream power as follows:

$$\omega = \frac{\rho_f g Q_s}{w} = \tau U \tag{5.6}$$

Where ω is the stream power per unit bed area, total discharge Q, width of flow w, and depth average velocity U. The critical depth averaged velocity is calculated as follows:

$$U_c = 5.75\log(\frac{12d_c}{D_b})\sqrt{\frac{\tau_{cr}}{\rho_W}} \tag{5.7}$$

And critical stream power per unit bed area:

$$\omega_{cr} = \tau_{cr} 5.75 \log\left(\frac{12 d_c}{D_b}\right) \sqrt{\frac{\tau_{cr}}{\rho_W}} \tag{5.8}$$

With d_c being depth of flow at critical motion.

To simplify, stream power is determined by the loss of potential energy as the water flows downstream Therefore, Bagnoldsuggests that it can also represent energy available to perform work in sediment transport, with the amount of sediment transported being determined by the rate of work i_b acting on the stream bed [14].

$$1_b = e_b(\omega - \omega_{cr}) \tag{5.9}$$

The uncertainty comes from e_b, which is the efficiency of the river in transporting sediment. However, stream power may have advantages over transport equations that require near bed velocities and bed shear stress data, as stream power can be approximated based on channel properties combined with discharge data. As these properties are more easily obtained, stream power equations may have a considerable practical advantage over locally variable parameters which require direct measurements. In this paper, the Shields critereon will be used to estimate the sediment input at the boundary condition of the model.
In practice, there are many forces acting on the particle including cohesive forces impacting soil structure and turbulent forces creating eddies, resulting in drag and lifting forces causing particles to bounce and skip along the bed. Because turbulence is random and irregular there is unpredictable flow patterns and geological conditions which causes complex sediment transport [htt]. The layers in complexity often result in the same formulae reported to have different ranges in accuracy by different authors for similar flow conditions [14]. The wide variability in results from sediment transport formulas make it difficult to correctly choose the correct sediment transport formula for specific functions. Therefore to obtain relatively accurate results and make smart predictions, it is crucial to properly define the river characteristics and the physical characteristics of the sediment. It should be acknowledged that for rivers, the spatial variability in the Shields Number, velocities, depth, slope, and grain size can be significant even in straight channels with uniform cross sections [38]. As one example, Wilcock estimates that the lateral topography of the bed alone change the transport rates by a factor 3. It is not practical to constantly sample in the field the bed-change variability, discharge or other variables and even with field sampling there can be many sources of error. Due to the unpredictable nature, transport functions based on natural stream measurements are few, as the difficulty in acquiring good measurements is great, thus most transport functions are derived in flume experiments.

This paper narrows down the selection of sediment transport functions for the White Volta River, which will then be tested in a HEC-RAS based flume study based on White Volta characteristics. The following 1D transport functions are included in HEC-RAS: Ackers & White, Engelund & Hansen, Meyer Peter and Muller, Yang, Wilcock & Crowe, and Toffaleti. Each one of these methods are developed in flume studies with different key parameters often reinforced with field data [61]. This research will include a process which narrows down the field of available transport functions based on literature to determine which transport functions are best suited for simulating the White Volta River based on Table 6.4.

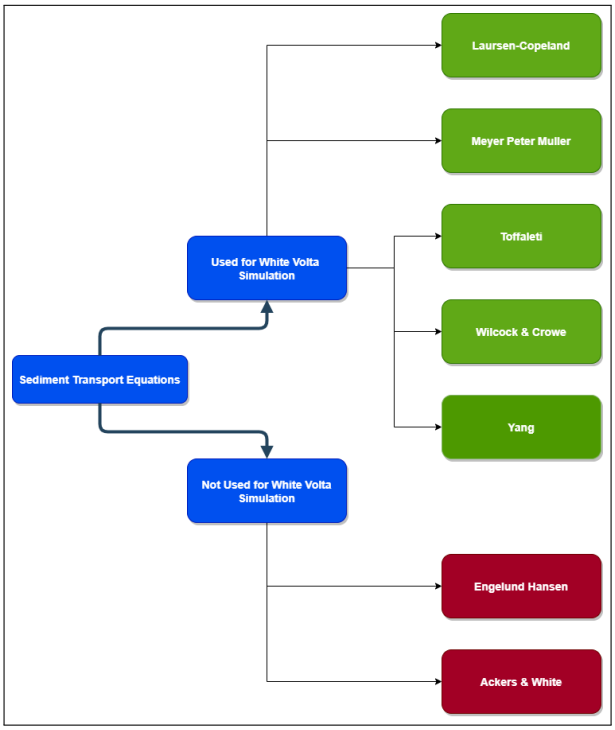

Figure 5.2: The depicted sediment transport equations are being used green and unused red in the Flume Models created for this research study. The chosen sediment equations will be further described in subsequent chapters.

5.2 TRANSPORT FUNCTIONS USED IN THIS STUDY

5.2.1 Laursen-Copeland

The Laursen-Copeland function is a modified version of Laursens transport function [43], The Laursen-Copeland equation was developed for a large range of sediment classes with both bed and sediment loads [23]. It measures the concentration of a particle class based on three parameters: excess shear stress, ratio of particle size to water depth, and the ratio of grain shear velocity u_* to grain fall velocity ω_p [23]. The equation differs from Shields as it replaces shear stress with grain shear stress $\tau^{'}$ which is based on the grain roughness $R^{'}$. Copelands equation also changes the way critical shear stress is calculated, which allows for initiation of motion of coarser particles at lower shear stresses, effectively increasing the transport potential of coarser particles. The grain shear stress $\tau^{'}$ becomes a function of grain roughness $R^{'}$, where V is velocity:

$$\tau^{'} = \frac{\rho V^2}{58}\left(\frac{d_{50}}{R^{'}}\right)^{1/3} \tag{5.10}$$

The transport of the bed-load is based on Shields critical shear stress which varies per particle grain class, with larger particles having a greater critical shear stress which the Laursen-Copeland equation defines as follows:

$$(\tau^{'}/\tau_{cr_i}) - 1 \tag{5.11}$$

The dynamic critical shear stress is determined using a combination of two methods which adjusts the Shields Parameters based on the value of the dimensionless shear

stress τ_o^*. When the dimensionless shear stress is above 0.05, a Shields value of 0.039 is used. However, when τ_o^* was below 0.05 the following equation is used:

$$\tau_o^* = \frac{\tau_o}{(\gamma_s - \gamma_w)} D_i \tag{5.12}$$

These adjustments results in the following equation:

$$C = 0.01\gamma(\frac{d}{D})^{7/6}(\frac{\tau^{'}}{\tau_c} - 1)f(\frac{u_*}{\omega_p}) \tag{5.13}$$

Laursen Copelands equation is suitable for a large range of particle classes 0.08mm - 29mm and velocities between 0.02 $\frac{m}{s}$ - 2.3 $\frac{m}{s}$ and will transport larger particle sizes much better than other functions [29].

5.2.2 Meyer Peter & Muller

HEC-RAS uses the Meyer-Peter & Muller (MPM) transport function based on Vanoni version which converts the MPM function to a dimensionless form allowing for unit volume calculations [18]. The transport function is one of the earliest developed and still one of the most widely used. It estimates the bed-load transport rate in an open channel as a function of excess shear stress caused by flowing water [18]. It is often used in research for comparative purposes with other transport functions as it is commonly used for engineering applications [63]. In its simplest form it reads:

$$q_b^* = 8(\tau^* - \tau_{cr}^*)^{3/2}; \tag{5.14}$$

Where: $\tau_{cr}^* = 0.047$
q_b^* and τ^* are the dimensionless transport and mobility parameters where:

$$q_b^* = \frac{q_b}{\sqrt{Rgd_m}d_m} \tag{5.15}$$

and:

$$\tau^* = \frac{\tau}{(\gamma_s - \gamma)} d_m \tag{5.16}$$

Vanoni's version of the MPM includes a drag form correction, $(\frac{k_r}{k_r^*})^{3/2}$ based on the roughness element ratio taken from Darcy-Weisbach bed friction factor. This adjustment isolates grain shear from bed shear which allows transport to be calculated based on the bed shear component acting only on specific particle grain classes. The equation is shown below:

$$Q_s \propto 8\left((\frac{k_r}{k_r^*})^{\frac{3}{2}}\tau^* - 0.047\right)^{\frac{3}{2}} \tag{5.17}$$

According to Kuriqi et al.; Karamisheva et al.; the MPM formula is best suited to larger sediment grain classes with higher bed-load rates. In sand or silt rivers, the MPM appears to give results that under predict the transport of finer materials [30]. Often its use is recommended in situations where the bed-load transport rate has never been calculated such as in the White Volta River.

5.2.3 Toffaleti

The Toffaleti function is a modified Einstein total load function that breaks the suspended load into three separate vertical zones (upper, lower, middle). It is not a shear velocity or bed shear dependent function. Instead sediment concentration is calculated for each of the three vertical zones as well as the bed zone. The three suspended zone concentrations are calculated using the Rouse number, based on the ratio of sediment fall velocity, upwards velocity, and shear velocity.
The three zones are calculated using the following equations where M is sediment concentration, hydraulic radius R, z is a relationship between sediment and hydraulic characteristics with r being depth, depth average velocity V, particle fall velocity ω, while g_{ss} represents suspended sediment transport, and n_v is a function of temperature T, and the slope S:

$$g_{ssUpper} = M\frac{(\frac{R}{11.24})^{0.244z}(\frac{R}{2.5})^{0.5z}\left[R^{1+n_v-1.5z} - (\frac{R}{2.5})^{1+n_v-1.5z}\right]}{1+n_v-1.5z} \tag{5.18}$$

$$g_{ssMiddle} = M\frac{(\frac{R}{11.24})^{0.244z}\left[(\frac{R}{2.5})^{1+n_v-z} - (\frac{R}{11.24})^{1+n_v-1.5z}\right]}{1+n_v-z} \tag{5.19}$$

$$g_{ssLower} = M\frac{(\frac{R}{11.24})^{1+n_v-0.756z} - (2d_m)^{1+n_p-0.756z}}{1+n_v-0.756} \tag{5.20}$$

$$g_{sBed} = M(2d_m)^{1+n_v-0756z} \longrightarrow orMPMforToffaletti \tag{5.21}$$

Where sediment concentration M, exponents z_i and n_v are defined as:

$$M_i = \frac{g_{ss}(1+n_v-0756z_i)}{(\frac{R}{11.24})^{1+n_v-0.756z_i} - (2d_{si})^{1+n_v-0.756z_i}} \tag{5.22}$$

$$z_i = \frac{\omega V}{(260.67-0.667T)rS} \tag{5.23}$$

$$n_v = 0.1198 + 0.000048T \tag{5.24}$$

The Toffelati Transport function can be used for particles between 0.062-4 mm, meaning it can span across multiple size classes. However, it is not developed for large particles or for systems with a wide gradient. Therefore, this function is better suited for large sand rivers [18].

5.2.4 Yang

Yang's equation is a total load transport equation which calculated transport based on stream power, the product of the mean flow velocity and energy slope [66]. Unlike Bagnold equation, the Yang equation related sediment transport to the energy

dissipation per unit weight of water. It is unique from other equations as it uses a critical flow velocity instead of a critical shear stress to determine particle motion. It correlates the total sediment concentration with effective stream power to estimate the sediment discharge which is expressed as follows:

$$\log C_t = A + B \log(VS - V_{cr}S) \tag{5.25}$$

The excess stream power relationship with The equation uses two separate relations for sand and gravel transport which take the following form.

For sand particles $d < 2mm$:

$$\log C_t = 5.435 - 0.286 \log \frac{\omega d_m}{\nu} - 0.457 \log \frac{u_*}{\omega} + \left(1.799 - 0.409 \frac{\omega d_m}{\nu} - 0.314 \log \frac{u_*}{\omega}\right) \log \left(\frac{VS}{\omega} - \frac{V_{cr}S}{\omega}\right) \tag{5.26}$$

For gravel particles $d > 2mm$:

$$\log C_t = 6.681 - 0.633 \log \frac{\omega d_m}{\nu} - 0.282 \log \frac{u_*}{\omega} + \left(2.784 - 0.305 \frac{\omega d_m}{\nu} - 0.282 \log \frac{u_*}{\omega}\right) \log \left(\frac{VS}{\omega} - \frac{V_{cr}S}{\omega}\right) \tag{5.27}$$

Therefore the motion of sediment is calculated for each sand grain size class using either of the two equations. The use of Yangs equation should be limited between the sediment diameters $0.15mm - 7mm$ as the coefficients were derived for this range based on extensive data bank and flume studies [65]. In modelling the Yang's equation often gives erroneous results at the transition diameters at the sand-gravel boundary.

5.2.5 Wilcock & Crowe

The Wilcock Crowe equation differentiates itself from traditional functions as it estimates the transport of sediment based on the quantity of each grain size present on the bed surface [62]. Generally, equations aren't created using bed-grain size as they data is difficult to acquire. The Wilcock & Crowe transport function was developed in flume studies, which includes concepts such as a hiding function and grain size distribution based on the ratio between the Shields number τ and the reference shear stress τ_{ri} , resulting in an excess shear stress function [62].

Wilcock and Crowe defines the ratio as follows:

$$\phi = \frac{\tau}{\tau_{ri}} \tag{5.28}$$

With transport for all size fractions calculated as follows:

When $\phi < 1.35$:

$$W_i^* = 0.002\phi^{7.5} \tag{5.29}$$

When $\phi \geq 1.35$:

$$W_i^* = 14\left(1 - \frac{0.894}{\phi^{0.5}}\right)^{4.5} \tag{5.30}$$

The reference stress for each grain class is calculated using the base reference shear stress for the median of the grain classes τ_{rm}^*, and the ratio of the grain class

particles d_i with the median bed surface grain size d_{sm}. Wilcock & Crowe's function is unique as it includes a hiding factor b that accounts for interdependence between grain sizes. For example, silty grains that are beneath gravel grains will require a greater shear stress to transport than silty grains on the surface of the bed. For uniform grain class distribution this interdependence can be ignored. However, for well mixed beds the transport function becomes increasingly inaccurate.

The ratio of reference shear stress with shear stress is calculated as follows:

$$\tau^*_{ri} = \tau^*_{rm}(\frac{d_i}{d_{sm}})^b \tag{5.31}$$

With hiding factor b calculated as:

$$b = \frac{0.67}{1 + \exp(1.5 - \frac{d_i}{d_{sm}})} \tag{5.32}$$

Using this equation, the Wilcock & Crowe function doesn't use a critical shear stress as a starting value for particle movement, but instead creates a reference shear stress in which the transport is trivial below the reference value. This equation is well utilized in situations where the surface bed gradation and discharge is known, and can provide the transport rates of sand and gravel for each grain class [18].

5.3 TRANSPORT FUNCTIONS NOT USED IN THIS STUDY: ACKERS & WHITE AND ENGELUND & HANSEN

The Ackers & White and Engelund & Hansen sediment transport equations were not tested in this research for the following reasons. The Ackers & White transport function grossly overestimates sediment transport for high velocities and grain sizes less than 0.04 mm [18]. While there are variations of coefficients added to the Ackers & White transport function to allow for use with varying grain sizes, they are not yet inputted into HEC-RAS [60]. As the majority of sediment transportation boundary condition inputs for the model of the White Volta primarily contains grain sizes below 0.04mm, the Ackers White function is not applicable for this research. The Engelund-Hansen formula will also not be used, it's the relation is designed to predict the sediment load for a single uniform grainsize, with the accuracy quickly decreasing with a wide sediment gradient. The function is limited for sediment sizes between 0.19 - 0.93 mm, meaning it will be inaccurate for the majority of the sediment input boundary conditions.

Note, these sediment transport functions are not used based on assumptions used for calculations and designs of the White Volta flume. However, once data is collected in the field it may change which functions are best suited.

5.4 FALL VELOCITY CALCULATIONS

When a pebble or grain of sand is dropped into water, it first experiences accelerating motion, but due to resistance of the water almost immediately experiences a uniform steady fall velocity [53]. The fall velocity is a balance between the net gravitational force F_g, defined as the difference of weight and buoyancy, and the drag force F_d acting on a particle as it moves through a fluid [28].

$$F_g = \frac{4}{3}\pi\rho R g\left(\frac{D}{2}\right)^3 \tag{5.33}$$

$$F_d = \frac{1}{2}\pi\rho c_D \left(\frac{D}{2}\right)^2 v_s^2 \tag{5.34}$$

This balance is dependent on the particle surface area, size, shape, relative velocity, density ρ and viscosity η. Particles with the same shape, but differing densities will behave differently in a fluid, with the higher density particle settling faster. The settling particle will have a resistance drag force slowing down the particle exerted on it by the fluid. As the relative velocity of the particle increases, so does the effective drag force. The particle will reach its terminal velocity when the net acceleration of the particle is equal to zero. This phenomena was first researched by Stokes, which is known commonly referred to as Stokes Law which defines particle fall velocity in fluid ω as follows:

$$\omega = \frac{\frac{1}{18}g(\rho_s - \rho_f)d^2}{\mu} \tag{5.35}$$

Stokes law shows that a particles velocity increases as a square of the diameter, so that larger particles settle faster than smaller. However, this relationship is not applicable to the entire range of sediment classes. This relationship also assumes that each particle is a sphere, for this reason many researchers have made adjustments to the Stokes equation to create a more applicable function for certain sediment classes [28].

The fall velocity equation used in this equation is the Ruby equation, as it is applicable for a large range of sediment diameters 0.00152 mm - 12.85 mm. It adjusts Stokes Equation by including an impact law which includes turbulent forces acting on particles. It determines a Reynolds number for the particle, and then uses this to derive the following equation for fall velocity [53].

$$\omega = \sqrt{\frac{(\frac{2}{3})g\rho_f(\rho_s - \rho_f)d^3 + 36\eta^2 - 6\eta}{\rho_f d}} \tag{5.36}$$

Ruby's equation is suitable as it is derived for a large range of sediment grain classes. It works well for silt, sand, and gravel and particles that have a specific gravity of 2.65, meaning the ratio of the sediments weight, to the weight of an equal volume of water.

5.5 BED ARMOURING & SORTING FUNCTION

5.5.1 Bed Sorting

During sediment transport, shear stress causes a drag force across the exposed surface area of the particles, while a gravity force acts on the particle weight as a function of volume and density. Therefore each grain class has a different transport rate which results in degradation or aggradation of the river bed. Large grain sizes are subject to a larger pull of gravity, this require greater shear to transport, while finer particles more likely to be dragged by the flow resulting in vertical, lateral, and longitudinal sorting of sediments [17].

As the stream power of the river exceeds the incipient motion certain grain size factions, the bed composition will change. If full sediment transport occurs in which critical shear stress for sediment transport is exceeded for all grain classes, all sediment grain sizes will be transported. During partial sediment transport, where the

critical shear stress isn't exceeded for larger particles, causes small particles to be transported away resulting in bed coarsening. commonly referred to as "armouring".

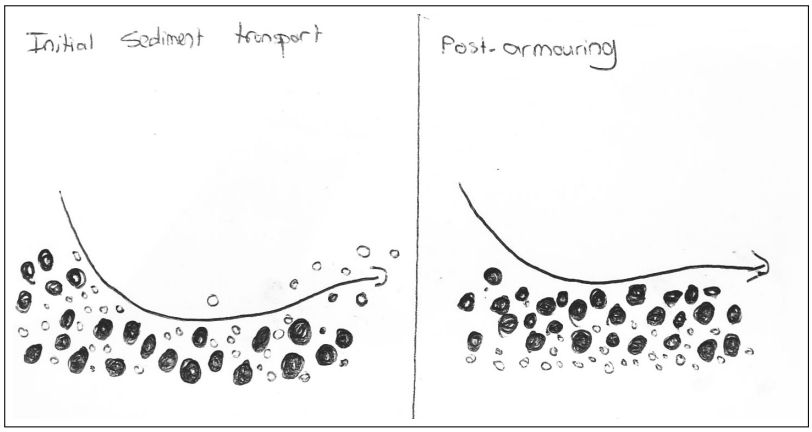

Figure 5.3: As finer sediments are transported away the bed layer coarsens and finer particles are trapped underneath the armouring layer.

Armouring has a significant influence on bed friction, sediment transport rate and scour depth[13; 17]. Armouring results in a decrease in erosion rates with time as a function of either deposition of coarser sediments on the bed or erosion of finer surface sediments [37]. As average particle diameter in the bed increases, erosion rates for a given shear stress decrease, describing how the coarsening of the bed reduces erosion rates [37]. Because the finer particles are more easily transported, the armor layer will begin to protect the sediment classes undisturbed by flow. This process effectively restricts the movement of sediment due to the hindrance caused by larger grain classes. Finer grains are often sheltered vertically in the coarser grains, meaning that coarser grains have greater exposure to the flow. This phenomenon is referred to as the "hiding factor" [57]. Thus during sediment armoring and sorting, two vertical layers are defined; an active layer and an inactive layer. The top layer, referred to as the "active layer or armor layer", is predominantly involved in the sediment transport process. The active layer interacts with the flow and determines the rate and composition of the transported sediment. The bottom layer is defined as the inactive layer or the substrate. The substrate is defined as a layer in which no transport occurs. In some functions a third layer is defined, the exchange layer, which is the layer in which the flux of sediment between the active layer and substrate occurs. This occurs when the active layer is eroded, the exchange layer "fluxes" to the active layer as it is now directly influenced by the flow. Likewise, if the active layer thickens due to deposition, the exchange layer will "flux" sediment from the active layer to the substrate.

Most sorting functions use an armoring ratio to define the rate at which sediment will be eroded based on the relative coarsening of the bed. The mass of each grain class is converted into a specific thickness which reduces erosion relative to average diameter of all grain classes. To determine how much sediment will erode the transport capacity of the river is measured with respect to the erodible supply. The capacity of transporting each grain class is determined, if available in the supply it will be eroded. If the erodible supply is fully eroded, the balance is taken from the inactive layer. In summation, the flux of sediment classes from the inactive layer to the active layer is aggregation and degradation.As sediment is transported from the inactive layer to the active layer it the river bed is degrading as the transport capacity is not being reached. Conversely, if sediment is being transported from the active layer to the inactive layer it is aggradation as the bed thickness is increasing. As

the diameters of the active layer increase the flux from active layer to inactive layer reduces until the armouring ratio becomes 0 and no more erosion occurs Figure. 5.4. In practice, this suggests that as erosion occurs, the average particle diameter in the active layer increases, causing an increase in the critical stress required for transport. Thus, at a certain bed thickness no erosion occurs. In conclusion, the armoring ratio determines the percentage of erosion of specific grain classes that can occur from the inactive layer[37].

HEC-RAS contains three bed sorting and armoring methods which will be compared in this research. The Active Layer method, Copeland Mixing Method, and Thomas Exner Mixing Method. The model will have drastically different results based on the applied bed sorting method, therefore choosing the proper sorting function in sediment modelling plays as large of a role in modelling sediment results as the transport equation [18].

Active Layer Mixing Method

The active layer mixing method in HEC-RAS is a two layered approach, with dividing the bed into an active layer, available for transport, and an inactive layer which has no impact on the computations. After each time step, the active layer is re-calibrated. If the bed erodes the inactive layer sends sediment back to the active layer to restore it, while during deposition the active layer resizes and sends the sediment back to the inactive layer. With erosion, the gradation of the bed layer will remain as specified, but will mix with the active layer sediment to create a new gradation in the active layer. Deposition is different, as the deposited material will have a different gradation than the defined bed gradation. In this case, HEC-RAS uses the 70-30 method in which 70% of deposited material and 30% of active layer material will be deposited into the active layer which maintains a course cover layer for armoring and allows for gradational evolution which is calculated as follows [57]:

$$\delta = 0.7d_i + 0.3a_i \tag{5.37}$$

Where δ is the transport of sediment to the inactive layer during aggregation, d_i is the fraction transported from deposited material, and a_i is the fraction of sediment deposited from the active layer.

The active layer method has several disadvantages in that it does not include an armoring factor and does not have clear vertical resolution. In HEC-RAS you must choose this function when using the Wilcock & Crowe transport function as it includes a hiding factor in the algorithm [18].

Thomas Mixing Method

The Thomas mixing method divides the active layer into a cover layer and a subsurface layer. Although the transport capacity is based on the data for the entire active layer, a cover layer coarsens independently which helps regulate erosion while maintaining a broadly graded active later [18]. At each time-step the Thomas method computes the active layer by computing the equilibrium depth D_{eq}, which is the smallest depth at which surface sediment does not move. The equilibrium depth is calculated based on a relationship between hydraulic energy, bed roughness and sediment transport intensity where D_{eq} is equilibrium depth, q is water discharge, and d_i is particle diamter:

$$D_{eq} = \left(\frac{q}{10.21 d_i^{\frac{1}{3}}} \right)^{6/7} \tag{5.38}$$

Using the D_{eq}, the armoring ratio is calculated where:

- $D_{eq} < 0.8$ = No Armoring effect, full grain class can be eroded from substrate
- $0.8 < D_{eq} < 2$ = Linearly interpolated armoring ratio between 0-1 between endpoints
- $D_{eq} > 2$ = Full armoring effect, no sediment is eroded

The equilibrium depth D_{eq} is calculated for each grain size, while setting the active layer thickness to the largest grain size. Using the newly calculated depth at each time step, HEC-RAS calculates a new active layer thickness, and recreates the subsurface layer. Using the armoring ratio, the percent of sediment removed is determined i.e.armoring ratio of 0.91 $\longrightarrow$ 91% of that sediment class is removed. In practice studies show that the Thomas method tends to over-predict armoring, and under predict erosion on finer grained systems [19].

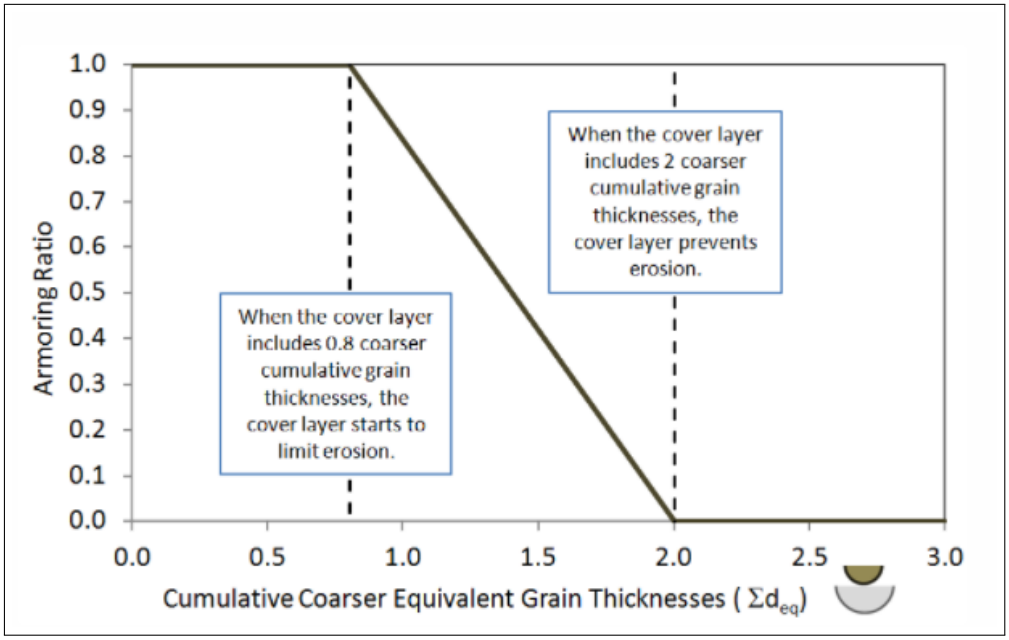

Figure 5.4: Armoring ratio as a function of D_{eq} [18]

Copeland Mixing Method

The Copeland Mixing method builds upon the Thomas method but is adjusted it to make it more applicable to sand beds. The armor layer is computed from a ratio based on the particle diameters of coarser grain classes, but it has a few adjustments which makes it better for large sand bed rivers. Firstly, the active layer is set to a thickness which is the greater between $2D_{90}$ or 15% of the water depth. Secondly, the armoring layer is limited to a maximum thickness of $3D_{90}$. Lastly, the armor ratio is changed start armoring at a smaller grain sizes. Instead of linearly interpolating the equivalent particle diameter between the two end points, Copeland uses the following polynomial:

$$0.8 < D_{eq} < 2 = AR = 0.026(\Sigma D_{eq})^3 + 0.28(\Sigma D_{eq})^2 - 1.07(\Sigma D_{eq}) + 1.40 \quad (5.39)$$

These changes allow for increased scouring and is better suited for sand systems as the armoring ratio decreases more gradually [18].

6 BUILDING THE MODEL VIA HEC-RAS

6.1 MODELERS NOTE

Data sources for the White Volta are extremely limited. Developing models for sediment transport at reach segment scale becomes difficult to accurately define. Although initiatives have been started for consistent sediment data acquisition, they have stopped as the cost has been too high to maintain [10]. For this reason, this model is being created to start a process in which the research objectives can be further developed when increased assets can be allocated to the project. The model here will be used as a starting point, to develop indicators that will determine the potential feasibility of using weirs for sediment entrapment. As the previously defined, even with perfect data, modelling sediment can create a wide variety of results. In practice, data is often first obtained for study, and a model is created to best fit the acquired data. From this point changes can be made to the model to study the impacts of various changes to the study reach. Due to Covid-19 travel restrictions, the full data required to develop a functional model has not been yet obtained, but in the further research this is expected.

In this research, the model will be created with all the current known data, with the missing data inputted as an assumption or range effectively creating a wide range of potential results. Future research can use the model results, match with gathered data to calibrate this research's conclusions. The data missing is Bed-load Sediment transport, Bathymetry, suspended sediment transport, and a hi-res DEM. For this reason, the model will be created 1-D, in a flume, to answer the research questions.

6.2 HOW THE MODEL WORKS

HEC-RAS 6 is a hydraulic model that computes hydrodynamics via computational increments. The flow duration is divided into computational increments during which the bed geometry, cross sections and hydraulic parameters are recalculated. During the computational increments, HEC-RAS updates the bed gradation, sorting, and armoring several times adjusting the grain classes several times during sediment transport calculations. The transport is measured using the Exner equation, in which the sediment entering or leaving a control volume must be stored or removed from storage. The Exner equations adjusts the difference between inflowing and outflowing sediment loads into bed change, erosion, or deposition as seen in Equation 6.1:

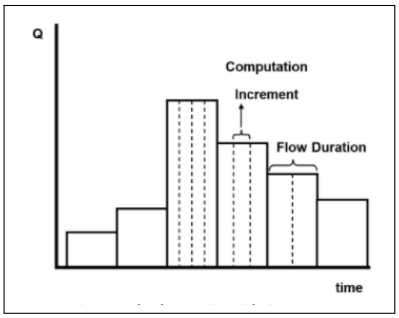

Figure 6.1: Quasi-Unsteady computation method, with multiple computation increments per flow duration

$$(1-\lambda_p)B\frac{\delta_\eta}{\delta_t} = -\frac{\delta Q_s}{\delta_x} \tag{6.1}$$

Where λ_p is porosity, B channel width, channel elevation η, time t, distance x, transported sediment load Q_s.
The HEC-RAS model computes the inflow sediment as the sediment entering the control volume from upstream control volumes. While the outflow sediment is calculated as a function of the sediment transport capacity, which computes the maximum sediment transported per grain class using hydrodynamics and sedimentation calculations. The hydrodynamic features transport capacity equations used are previously mentioned in Chapter 5.

6.3 GEOMETRY DESIGN

The White Volta will be modelled in a 1-D flume in order to determine the impact of a weir on sedimentation. In the model a 50 km long straight segment will be modelled with uniform cross sections. The width of the flume will be 120m, as measured approximately via Google Earth at the Nuwani discharge measuring station. As the bathymetry is unknown, the cross sections will be uniform with the bathymetry for each cross-section uniform as seen in Figure 6.2, with cross sections every 20 meters. The slope of the bottom is set at 0.00014 m/m as measured by HKV consultants for the reach section near Nuwani station [59].

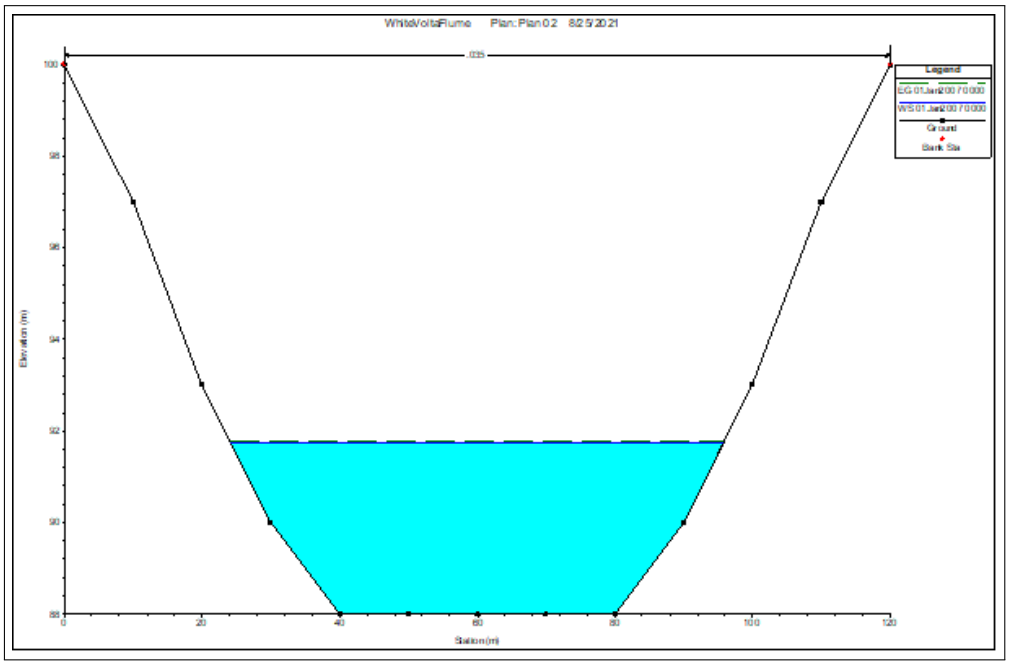

Figure 6.2: Uniform cross section bathymetry used for all cross sections along the flume.

The manning's value for a bed, especially sand beds, can be highly varied as bedforms move easily taking on drastically different configurations during high or low flows [12]. For example, during Low flows, bed forms may have little movement which results in much higher Manning's values. The Manning's values can be impacted by channel irregularities, alignment, obstructions, vegetation and meandering, each which will give a greater roughness value than in a straight bed. The degree of each factor on the roughness coefficient has been studied by Aldridge and Garrett, who created adjustment tables for increasing the Manning's N Value which

include: degree of irregularity, variation in channel cross sections, obstructions, vegetation, degree of meandering [11].

In future data collection of the Volta Basin when verifying results, these parameters should be implemented in the cross section manning values of the 1-D model with consideration for the dynamic bed form conditions. In this study, the obstruction will be included into the calculation. Similarly, with the other factors, each can play a significant role on the roughness of the bed. In this flume, the Manning's coefficient selected will be 0.017 based on Table 1 of Aldridge and Garrett's research, assuming the reach has smooth-roughly cultivated bed-forms [11]. The banks will be increased by 0.01 due to the impact of erosion and vegetation [12; 7]. As the impact of the roughness coefficient is so significant, further measurements must be monitored at the weir site at Nuwani station to calibrate the results. This model will run simulations with ±.005 for each parameter as depicted in Table 6.1.

Title	Left Bank (n)	Channel	Right Bank (n)
Geometric (1)	0.022	0.012	0.022
Geometric (2)	0.027	0.017	0.027
Geometric (3)	0.032	0.022	0.032

Table 6.1: Manning n value variation used as a comparison of the impact on sedimentation in simulations

6.4 QUASI-UNSTEADY FLOW DATA

The model uses the August 1994 - August 1995 discharge data from Nuwani station as its upper flow series boundary condition. This models the flood peak earlier in the simulation to reach a steady state in sediment at the duration endpoint resulting in the following hydrograph Figure 6.3.

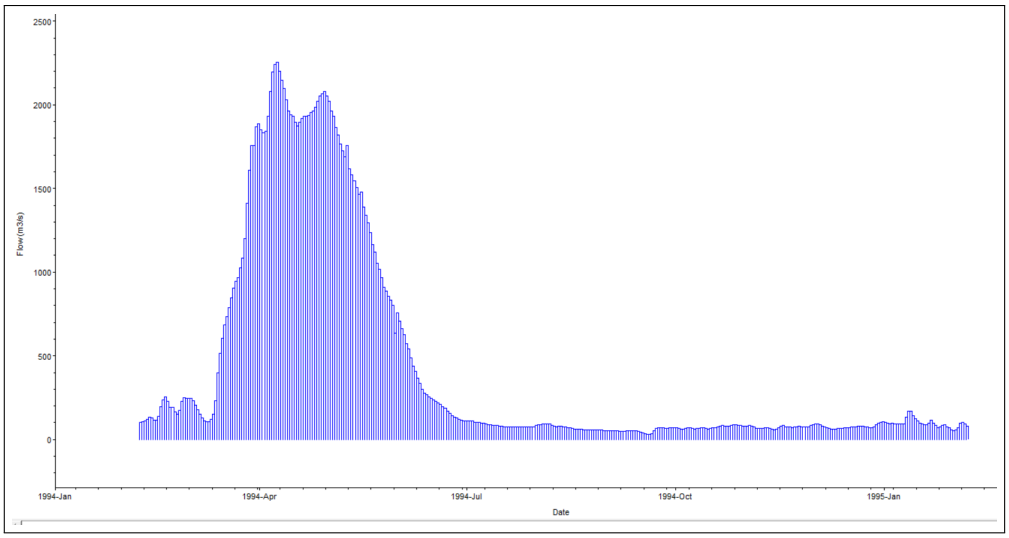

Figure 6.3: Hydrograph flow season August 1994-August 1995 measured at Nuwani Guaging Station

Based on the discharge, the computation increments (hours per flow duration (24 hrs)) were set as depicted in Table 6.2. The computation increments are selected to minimize oscillations in results. When increments set with too large of a duration between computations, the model is more likely to explode or give oscillating results. When the simulation timesteps are two small output file sizes and simulation

duration drastically increases. With finer computation increments the results of the model are smoother, however, in this case a rolling average will be used to reduce positive feedback.

Qlow	Qhigh	Computation Increment
0	50	6
50	100	4
100	250	1
250	500	0.75
500	1000	0.5
1000	1500	0.25
1500	2000	0.075
2000	2500	0.05

Table 6.2: Computation increments for each flow duration input. As daily means are chosen, flow duration is 24 hrs, while computation increments are how many hours between computations. At low discharges a computation is done every 6 hours, while at high discharges computations are done much more frequently with computations done every 0.05 hours

The lower boundary condition uses Normal Depth, which uses the friction slope of the river to determine model output. In this case the friction slope is set to $0.00014\frac{m}{m}$ as measured by [59]. As sediment transport calculations require temperature for measuring viscosity, the input flow temperature is set to 20°C for all flow durations.

6.5 MODELLING THE WEIR

The weir will be a broad crested weir located 3 km from the downstream boundary. In this research downstream conditions will not be strongly researched, with the primary focus being sediment behavior immediately upstream of the weir. Therefore stilling basins and erodible bed limits are not included in this research. A broad crested weir is used as it is more durable and requires less maintenance compared to a ogee or sharp crested weir. The discharge and head over the weir is based on the following equation for free flow:

$$Q = C_d L H^{\frac{3}{2}} \tag{6.2}$$

Where L is the length of the weir, C is the weir coefficient, and H is the head above the crest (m). When the weir is submerged the model reduces the C_D coefficient is reduced based on a percentage of submergance [18].

Parameters for the weir will just be standard with at 42% of the bank height with banks being 12 m as seen in Figure 6.2. Thus the weir height used is 5 meters. The width of the weir in the direction of the flow is also 5 meters, and a weir coefficient of 1.4. The weir coefficient is assumed at 1.4 as variations are found between a standard 1.6 for broad crested weirs [Claydon]. Or alternatively, approximately 1.2 as suggested by the United States Geological Survey [58].

The full dimensions are illustrated in Figure 6.4.

6.6 IMPLEMENTATION OF SEDIMENT PARAMETERS

The Sediment data will be inputted based on several measured data points but completed with assumptions made by the modeler. The parameters to be inputted

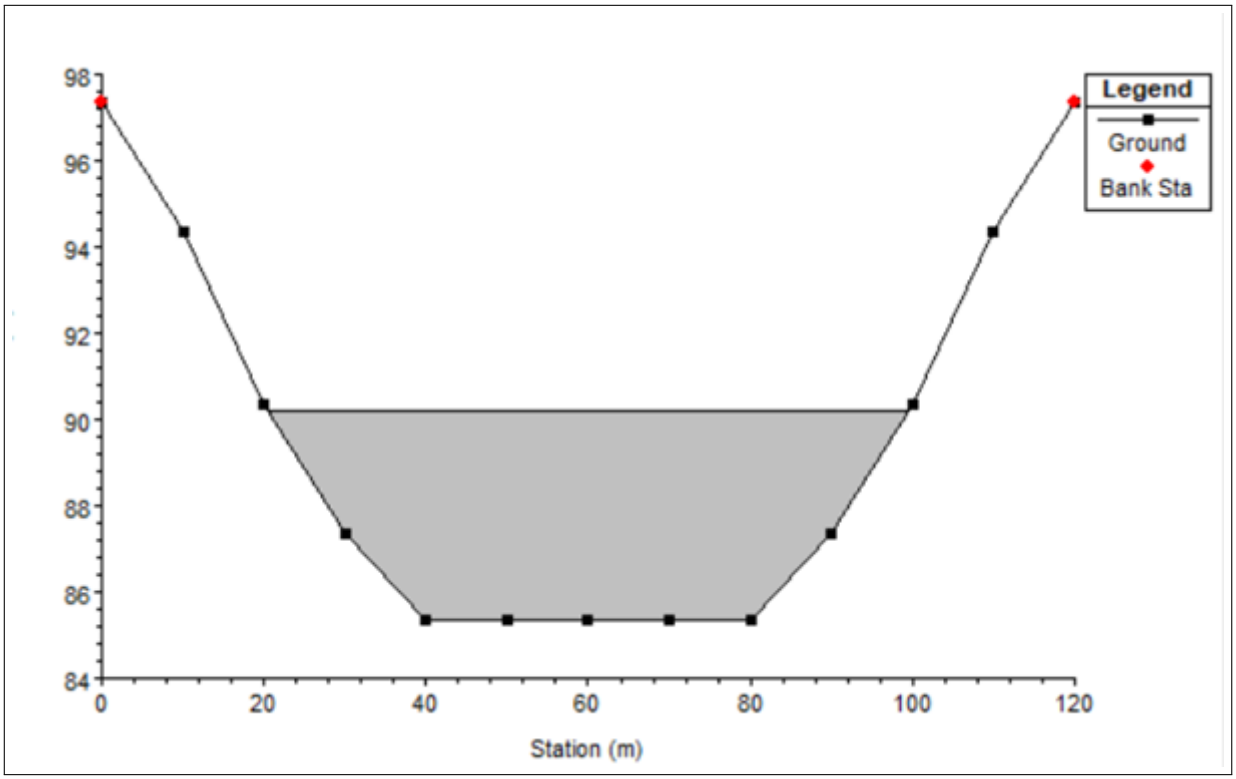

Figure 6.4: Geometry Design of the weir used in the simulations

include the transport functions, sorting method, fall velocity method, bed gradation, and sediment rating curves. The only known value is the bed gradation measured by HKV [59], and the sediment rating curve measured by Akrasi [10]. These measurements were taken at a single point in time, which may result in vast differences from the current practical situation. Due to the dynamic nature of sediment morphology these values are often subject to considerable changes in a given year which should be taken in consideration for the results of this study.

6.6.1 Bed Gradation

The bed gradation is defined as the percentages of sediment contained in the bed material for each grain class. HEC-RAS provides a template which allows the user to define a specific cross section with a certain sediment gradation. The grain classes are sorted from fine to coarse, with the classes being separated in % finer for the upper bound of the grain class. If the bed material is cohesive, the parameters can be adjusted for shear threshold, erosion rate, mass erosion threshold, however, observations at the Nuwani station observed that the bed material was non-cohesive so these adjustments will be ignored. HKV divided the grain classes into four classes which were measured at a sand bar in the center of the river with the results displayed in Figures 6.5, 6.6.

Figure 6.6's composition is defined with the following grain classes:

- Clay Diameter less than 0.002 mm
- Silt Diameter between 0.002 - 0.065 mm
- Sand Diameter between 0.065 - 2 mm
- Gravel Diameter greater than 2 mm

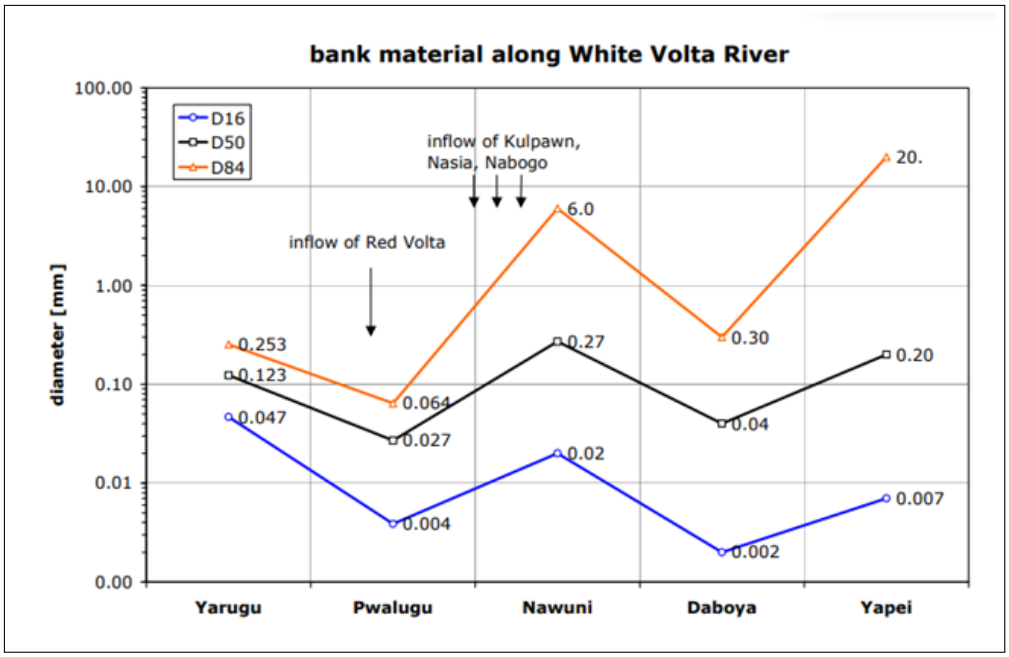

Figure 6.5: D16, D50, D84 values for bank material measured at measuring stations along the White Volta River [59]

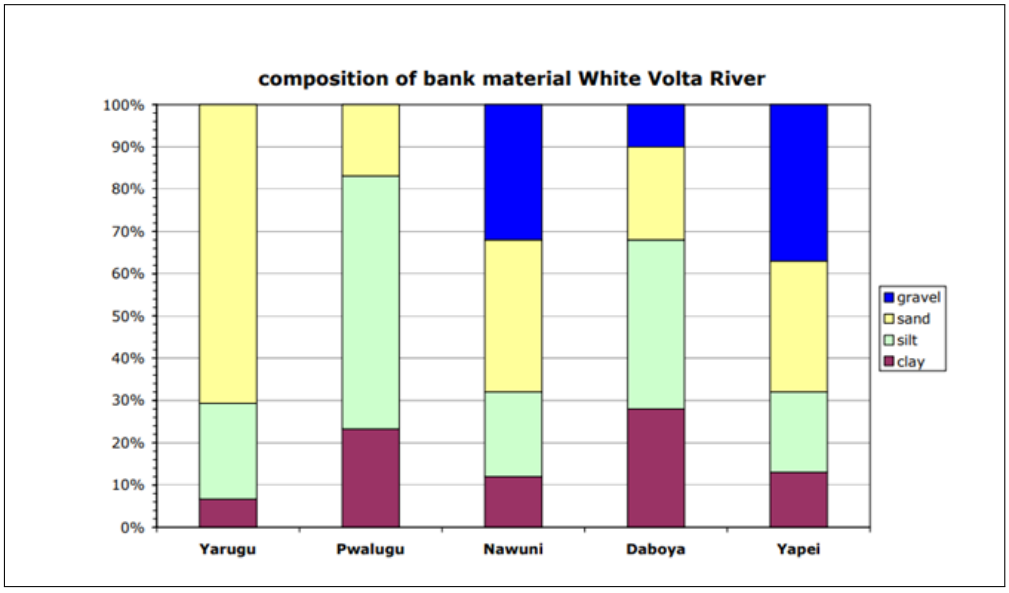

Figure 6.6: Measured Bank Material on the White Volta River at various river guaging stations. [59]

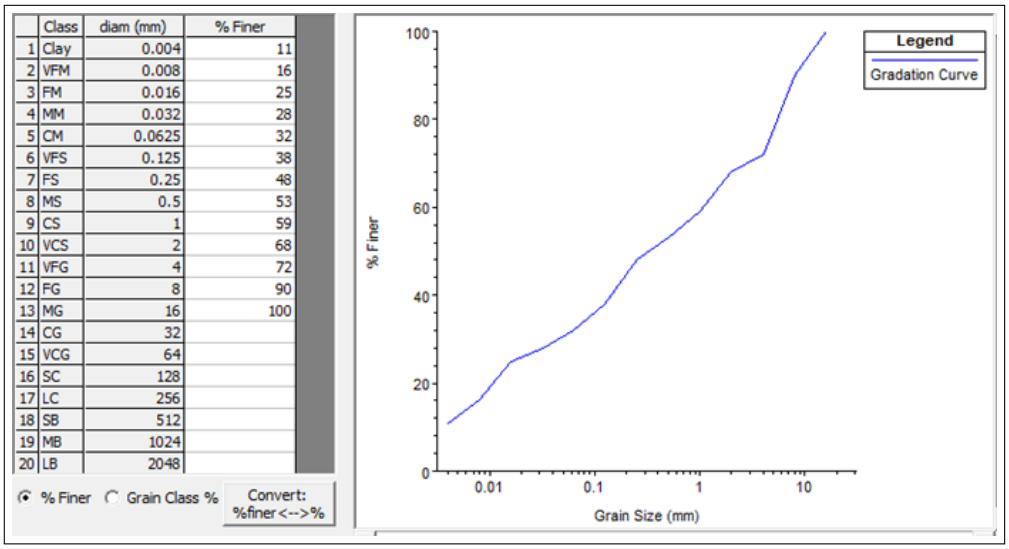

	Class	diam (mm)	% Finer
1	Clay	0.004	11
2	VFM	0.008	16
3	FM	0.016	25
4	MM	0.032	28
5	CM	0.0625	32
6	VFS	0.125	38
7	FS	0.25	48
8	MS	0.5	53
9	CS	1	59
10	VCS	2	68
11	VFG	4	72
12	FG	8	90
13	MG	16	100
14	CG	32	
15	VCG	64	
16	SC	128	
17	LC	256	
18	SB	512	
19	MB	1024	
20	LB	2048	

Figure 6.7: Model input Bed Gradation set for the intitial starting conditions, based on acquired HKV measurement data

This data has been translated to HEC-RAS to create the following Bed Gradations (Figure 6.7) with intermediary values being estimated. This bed gradation will be the entry point for all cross-sections along the 50 km channel. At each computation increment the bed composition will change when taken account the change of sediment in the control volume.

6.6.2 Sediment Rating Curve

The Sediment rating curve is used at the upper boundary measuring the input sediment into the modelled area of the reach. Load Gradation is one of the least certain to measure, but also one of the most sensitive inputs to the sediment model, therefore it is often used as a target calibration parameter of the model [33].Generally, rivers coarsen with increased flow until they reached a maximum grain sized limit and then remain constant beyond this threshold flow [32]. However, flow itself does not explain all the variability in the load data, which can also be impacted by hysteresis, storms and seasonal variations. In practice, the magnitude of sediment generally increases as a function of flow, but the load classes can both coarsen and fine, or remain relatively constant [32]. There is no accurate measured data for sediment load for the White Volta River, due to the high cost involved in gathering the necessary measurements on a daily or hourly basis over a long enough period of time for accurate sediment load estimations. The closest estimations that can be used are based on 89 dip measurements taken sporadically throughout the year on the White Volta conducted by Akrasi, in which a rating curve with a 25% correction factor was developed for mean concentration values across a specific cross section [10]. The rating curve technique developed by Walling is used which creates a relationship between sediment discharge and water discharge:

$$Q_s = aQ_w^b \tag{6.3}$$

Where Q_s is sediment discharge, Q_w water discharge and a,b are measured variables. The mean daily flow data is used to estimate the mean daily sediment discharge. This aligns with practice where suspended sediment flows are the greatest during periods of high flow during the flood season. Akrasi estimated the values of constant b and a were 1.345 and 3.230 at Nuwani station [10]. This data is then inputted into the rating curve information in HEC-RAS to estimate the total sediment

Discharge ($\frac{m^3}{s}$)	Sediment Load ($\frac{ton}{day}$)	Discharge ($\frac{m^3}{s}$)	Sediment Load ($\frac{ton}{day}$)
100	1582.0	1400	55048.4
200	4018.7	1500	60401.2
300	6933.2	1600	65878.5
400	10208.8	1700	71475.4
500	13782.2	1800	77187.0
600	17612.3	1900	83009.2
700	21670.0	2000	88938.1
800	25933.3	2100	94970.2
900	30385.0	2200	101102.3
1000	35010.8	2300	107331.3
1100	39799.3	2400	113654.5
1200	44740.5	2500	120069.3
1300	49826.0	2600	

Table 6.3: Sediment rating curve computed values for Sediment load based on Equation 6.3 with values constant values derived from Akrasi

load for specific discharges. Based on Akrasi's 1994 measurements, the estimated suspended load is $5.62 * 10^6$ tons in 1994 at the Nuwani Station [10], as other measurements aren't included for other years the discharge series used will also be from 1994. It should be noted that 1994 had a larger flood peak relative to other years, resulting in a greater suspended load than an average year. The total sediment load based on the rating curve constants of Akrasi using Equation 6.3.

However, there is no available measured data on sediment-load grain classes for the White Volta River which is required as an input for the sediment rating curve boundary conditions. For this model, assumptions must be made for the fractionalization of grain classes present in the suspended sediment load. Observational data upstream at Pwalugu noted that the majority of the suspended sediment load contained clay and silt, with very small amounts of sand [26].

In order to create reasonable estimations of grain classes entering the model, the input grain classes are fractionalized based on initiation of particle motion. In a steady flow analysis the shear stress of the bed was calculated without sediment flow using the quasi-unsteady flow data. Using the Shields Equation 5.3, the critical shields stress for each particle grain-class particle diameter was calculated. If shear stress was greater than the critical shear stress, it was assumed that the grain class was present in the input flow. If present, the fractions of each grain class were assumed, and remained consistent across all river discharges. Grain class inputs significant impact on the rate of aggradation and degradation, which will require further calibration of this model using measured data for practical applications.

	Flow (m3/s)	100	200
	Total Load (tonnes/day)	1582	4018.7
1	Clay (0.002-0.004)	0.3	0.3
2	VFM (0.004-0.008)	0.3	0.3
3	FM (0.008-0.016)	0.2	0.2
4	MM (0.016-0.032)	0.05	0.05
5	CM (0.032-0.0625)		
6	VFS (0.0625-0.125)		
7	FS (0.125-0.25)		
8	MS (0.25-0.5)		
9	CS (0.5-1)		
10	VCS (1-2)		
11	VFG (2-4)		
12	FG (4-8)		
13	MG (8-16)		
14	CG (16-32)		
15	VCG (32-64)		

(a) $flow < 200 \frac{m^3}{s}$

	Flow (m3/s)	300	400
	Total Load (tonnes/day)	6933.2	10208.8
1	Clay (0.002-0.004)	0.3	0.3
2	VFM (0.004-0.008)	0.3	0.3
3	FM (0.008-0.016)	2	0.2
4	MM (0.016-0.032)	0.13	0.13
5	CM (0.032-0.0625)	0.05	0.05
6	VFS (0.0625-0.125)		
7	FS (0.125-0.25)		
8	MS (0.25-0.5)		
9	CS (0.5-1)		
10	VCS (1-2)		
11	VFG (2-4)		
12	FG (4-8)		
13	MG (8-16)		
14	CG (16-32)		
15	VCG (32-64)		

(b) $200 < flow < 1800 \frac{m^3}{s}$

	Flow (m3/s)	1800	1900
	Total Load (tonnes/day)	77187	83009
1	Clay (0.002-0.004)	0.2	0.2
2	VFM (0.004-0.008)	0.3	0.3
3	FM (0.008-0.016)	0.3	0.3
4	MM (0.016-0.032)	0.2	0.2
5	CM (0.032-0.0625)	0.05	0.05
6	VFS (0.0625-0.125)		
7	FS (0.125-0.25)		
8	MS (0.25-0.5)		
9	CS (0.5-1)		
10	VCS (1-2)		
11	VFG (2-4)		
12	FG (4-8)		
13	MG (8-16)		
14	CG (16-32)		
15	VCG (32-64)		

(c) $flow > 1800 \frac{m^3}{s}$

Figure 6.8: Fractional grain class distribution for all sediment loads resulting from the sediment rating curve Equation 6.3. Fractions are estimated as a result from Shields Equation which are used for all sediment loads between the 1994 flow ranges.

6.7 TRANSPORT FUNCTIONS

As defined in Chapter 5, the bed load transport equations can compute a wide variation of results with respect to one another. It is important to verify the accuracy of a sediment transport function with measured data from the target stream. As the current river cannot be calibrated due to Covid-19, the functions that will be tested will be based on known characteristics to provide potential estimations of bed-load transport potential in the river. In sand-bed streams with high transport rates, the suspended load often is orders of magnitudes higher than that of gravel or rock rivers. As the Volta river bed gradation is primarily sand-bed, the equations used as a transport predictor will include suspended sediment in their measurements which include (Laursen & Copeland, Toffaleti, Wilcock & Crowe). Although Meyer-Peter Muller is used for rivers with coarse sediment, it will also be tested as HKV surveys suggest that Meyer-Peter Muller can be utilized for the White Volta [59]. In addition, Meter-Peter Muller is often used to estimate sediment transport when there is little data present. Lastly, Yangs' equation is used as it is a stream power function. Stream Power functions are much easier to acquire the necessary data to develop models. In Ghana, a simpler form of data acquisition will be more practical in sedimentation monitoring and design. Key parameters in choices of sediment transport function are illustrated in Table 6.4 in which, transport function use criteria is depicted from their respective authors.

Transport Function	Diameter (mm)	Uniform Grain Class	Velocity ($\frac{m}{s}$)	Channel Depth (m)
Laursen Copeland	0.08 - 0.7	No	0.2 - 2.37	0.2 - 16.2
Meyer Peter Muller	0.4 - 29	No	0.38 - 2.86	0.015 - 1.17
Toffaleti	0.062 - 4	No	0.21 - 2.37	0.024 - 16.8
Yang	0.15 - 1.7	Yes	0.24 - 1.95	0.024 - 15
Wilcock Crowe	0.06 - 4	No	Unspecified	Unspecified

Table 6.4: Conditions in which sediment transport conditions were derived

In the model, the Thomas Mixing Method will be used for Laursen Copeland, Meyer Peter Muller, Toffaleti and Yangs equation. For Wilcock & Crowe the active layer will be used, as it does not include the hiding factor in the equation. This is because Wilcock & Crowe includes a hiding factor in its sediment transport function. Rubey is used as the settling function. Rubey underestimates the settling velocity of large particles, however, the model is simulating largely smaller grain classes.

6.8 SUMMARIZING THE SIMULATIONS TO BE CONDUCTED ON HEC-RAS

All other parameters will remain at HEC-RAS system default. Therefore the simulations being conducted for this experiment can be seen in Table 6.6. As data acquired from the White Volta River is scarce, the range of simulations will be diverse to predict potential incomes of sediment accumulation in front of a weir. There will be five transport functions used: Laursen & Copeland, Meyer Peter & Muller, Toffaleti, Wilcock & Crowe, and Yang. Each transport function except for Wilcock & Crowe, which requires the Active Layer settling function will use the Thomas settling velocity equation. These variations will compare a range of manning values: (0.012, 0.017, 0.022), both with and without a weir. In total 30 simulations will be compared. The results of these simulations will be investigated to get a better understanding of the suitability of the function, as well as the practicality of the results. The simulations are labelled with the following Table 6.5:

Simulation	Transport Function	Settling Equation	Roughness	Weir
S	(1) Laursen & Copeland (2) Meyer Peter & Muller (3) Toffaleti (4) Yang (5) Wilcock & Crowe	(1) Thomas (3) Active Layer	(1) 0.012 (2) 0.017 (3) 0.022	(1) Yes (2) No

Table 6.5: Simulation key for comparisons conducted in this study

S1111	S2111	S3111	S4111	S5311
S1112	S2112	S3112	S4112	S5312
S1121	S2121	S3121	S4121	S5321
S1122	S2122	S3122	S4122	S5322
S1131	S2131	S3131	S4131	S5331
S1132	S2132	S3132	S4132	S5332

Table 6.6: Simulation Key for the Simulations conducted in this research, results for all categories will be placed in the appendix

7 MODEL RESULTS

7.1 TRANSPORT FUNCTION IMPACT ON SEDIMENT BEHAVIOUR UPSTREAM OF A WEIR

In Chapter 5, the transport functions used in this research were examined, as scientists have noted that a slight change in transport function can give a highly differing result due to the complex dynamic nature of sediment morphology. This complexity often makes it difficult to choose the correct transport function to use for practical applications of a sediment morphology model. Thus, in order to give proper estimations of the weirs net impact on the sediment balance, each transport function was simulated without a weir to ensure a realistic baseline. In this case, a function would be considered applicable if the non-weir simulations would provide an equilibrium style result. For each adjustment of the Mannings roughness coefficient, the baselines were assessed for use as depicted in Figures 7.1, 7.2, 7.3.

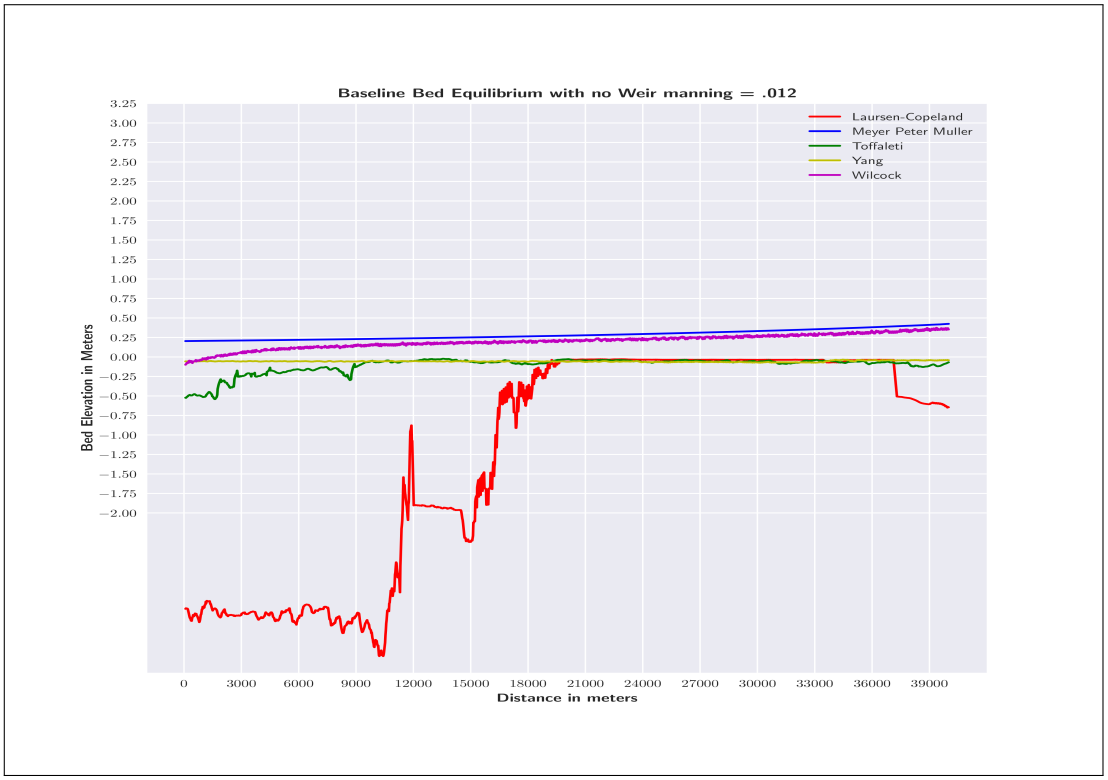

Figure 7.1: Change in Bed Elevation from 40,000 m upstream to the weir site for all transport functions

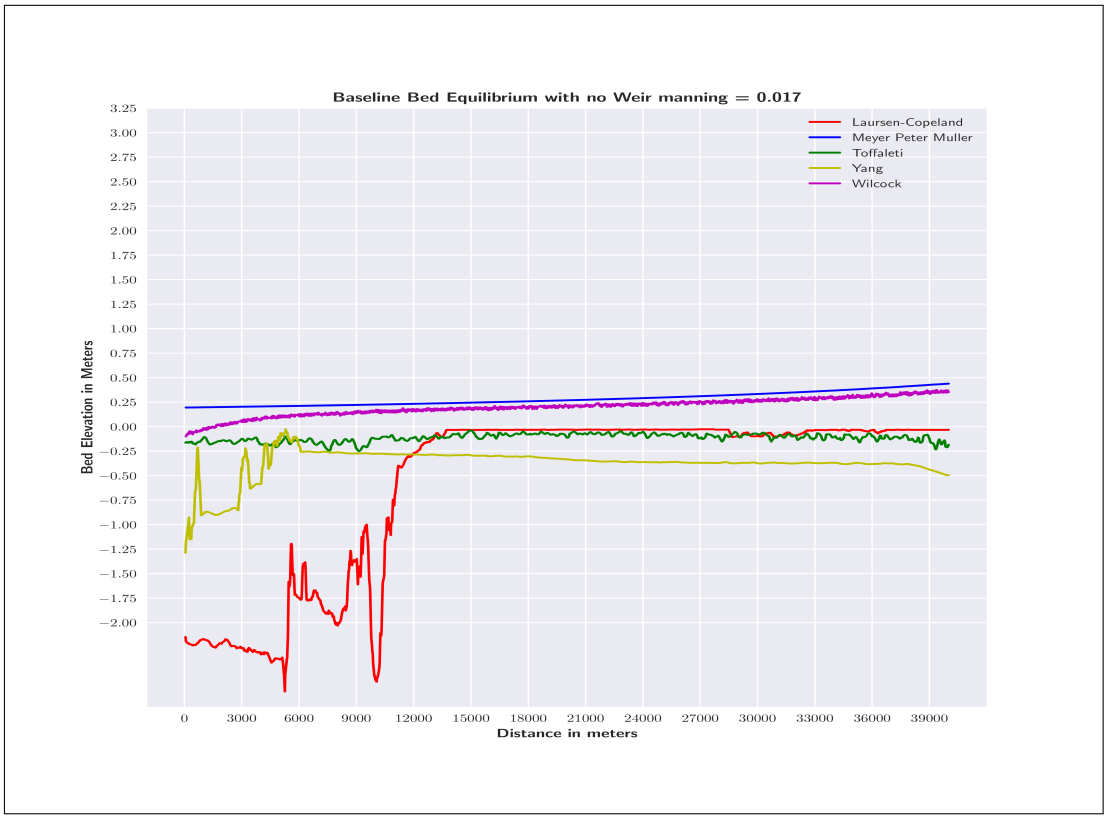

Figure 7.2: Change in Bed Elevation from 40,000 m upstream to the weir site for all transport functions

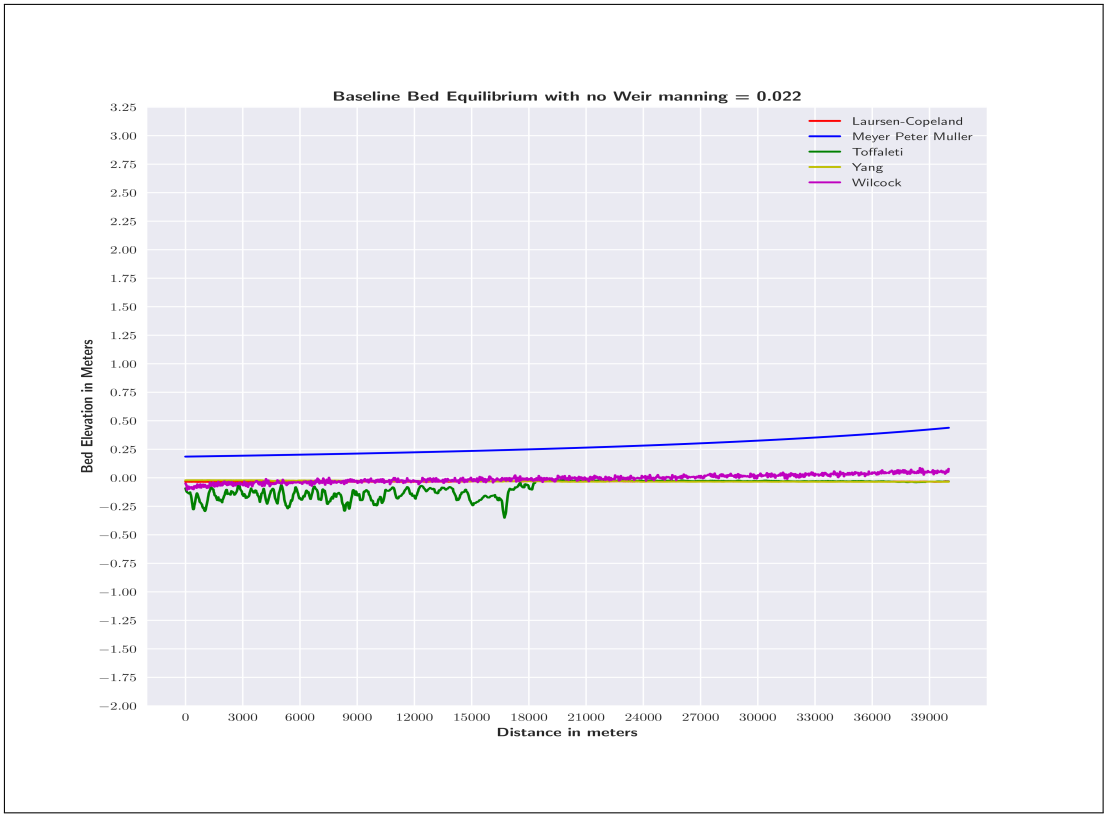

Figure 7.3: Change in Bed Elevation from 40,000 m upstream to the weir site for all transport functions

Based on the results of the Baseline simulations, in which all variables remain the same except the transport function, the variability of the transport function results is significant.

- **Laursen Copeland** - The Laursen-Copeland transport equation over estimates erosion significantly in baseline simulations. As the simulation duration increases, the bed levels are eroded to the non-erodible zone of the bed Appendix A.7. The volume of eroded sediment decreases with increasing manning values. The Laursen equation uses grain shear stress based on grain roughness, which may cause high erosion at lower manning roughness values in the bed. With the addition of a weir, their was an uptick in bed accumulation, however, this was not sediments from the incoming sediment load at the upper boundary but large diameter fragments $diameter > 0.125$ that were eroded and the upper boundary.

  The over calculation of erosion is illustrated in A.6. The Laursen & Copeland equation allows initiation of motion of coarser particles at lower shear stresses, which is resulting in a gross over estimation of sediment erosion. In the case of the model inputs, it was not suitable for assessing sediment accumulation in front of a weir.

- **Meyer Peter Muller** - Meyer Peter Muller transport function over estimates the settling of sediment from the incoming sediment load calculated from the rating curve. In this case, sediment immediately begins settling as they traverse across the system. This is because the function did not have the necessary stream power to properly transport the inbound sediment. This is why you can see the bed elevation linearly decreasing from the upper boundary condition. The MPM function does not cause any erosion of the bed gradation which is not observed in the field Appendix A.7. When a weir is included in the model, transient storage is not observed, although the bed elevation does increase as a greater percentage of the incoming sediment load settles.

  Reasons for this behaviour could be due to conditions in which these parameters were derived Table 6.4. The Meyer Peter & Muller formula was derived for particle grain classes with a diameters greater than 0.4 mm, which is significantly larger than the grain classes able to be moved using the initiation of motion calculations in Chapter 6.8. Thus, the formula could show poor sediment transport behaviour with smaller transport classes. The channel depth is also greater than derived conditions of the Meyer Peter formula, which may also cause unrealistic behavior. The Meyer Peter Muller formula is known for under predict transport of finer sediments, which is also observed in this model. Thus, for this research the results are not suitable for estimated bed accumulation.

- **Toffaleti** - The toffaleti equation maintains a relative equilibrium behavior in baseline conditions. Some erosion does occur which is largely composed of clay and very fine silt from the bed gradation Appendix A.7. Toffaleti does have some oscillations due to the complexity of the equation, which can be eliminated with smaller timesteps or cross section distance. As baseline values can be assumed to be similar to field values, this function will be used to estimate accumulation.

- **Yang** - Yangs equation maintains near perfect equilibrium in both the highest and lowest Mannings value. Similar to toffaleti, small amounts of clay and very fine silt is eroded from the bed gradation Appendix A.7, but then maintains a equilibrium through the year making it suitable to estimate the accumulation the weir provides.

- **Wilcock & Crowe** - This equation has similar behaviours to Meyer Peter Muller, in which the transport function predicts no erosion and slow settling of particles at lower roughness values. As roughness increases, the erosion increases. The addition of a weir causes settling behaviours as soon as the sediment enters the modelled river section, rather than seeing transient storage occur. This is likely due to the reduced velocity upstream which does not provide this function with enough stream power to transport sediments.

  While the derived grain class applicability of Wilcock & Crowe is much closer to the sediment rating curve see Table. 6.4, the function does not give a range for water depth or velocity in which it can be properly applied. In addition, when the bed contains a well mixed assortment of sediment grain classes, the results become increasingly inaccurate Chapter 5.2.5. As Wilcock & Crowe calculates sediment transport based on quantity of each grain class present in the surface of the bed, sources of error may arise as these values are estimated in this model.

Each transport function used in a simulation demonstrates differing bed change characteristics. While all of the used transport functions demonstrate an increase in bed elevation, and therefore bed mass accumulation upstream of the weir. For practical applications, we will only look at modelled behaviours that are likely to exist in the field. Toffaleti and Yang's transport functions demonstrate behavior that verifies transient storage upstream of the weir as Queen noted. In these results, the storage begins to increase approximately 20 kilometers upstream of the weir due to the decrease in river velocity. The settling rate of the various particles coincide with the initiation of motion calculations, with larger particles beginning to settle earlier than smaller particles before reaching a constant elevation.

7.1.1 Seasonal Variation in Sediment Continuity

Using Yang and Toffaleti's model results, the seasonal behavior of sediment transport can be examined. In this case a location is chosen 1 km upstream (for other distances see Appendix time series values) to demonstrate the change in sediment transport over the year in Figures 7.4, 7.5.

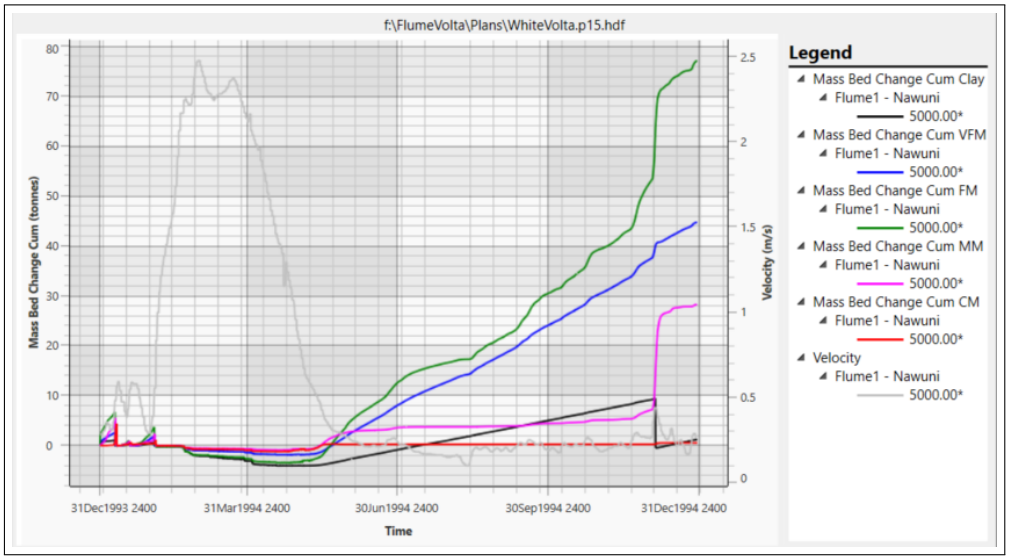

Figure 7.4: Sediment class behavior of Toffaleti Transport Function over time at 1000m upstream of the weir

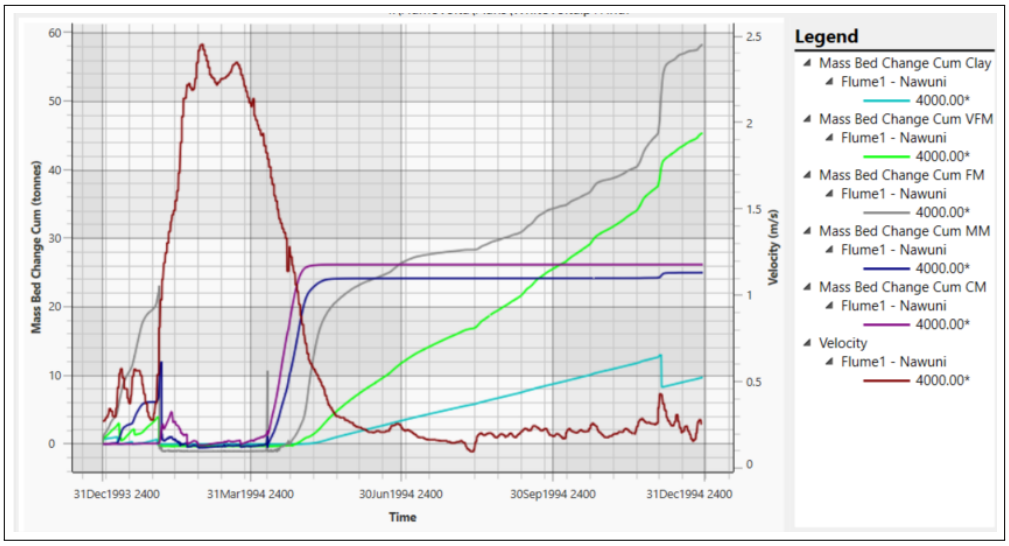

Figure 7.5: Sediment class behavior of Yang Transport Function over time at 1000m upstream of the weir

During the large peak flows, sediment continuity isn't hindered, as all grain classes are transported up and over the weir. As the velocity begins to decrease, sediment storage begins to accumulate over the course of the dry season. Grain classes CM, MM are no longer transported below $1.2\frac{m}{s}$ using Yangs equation while VFM, FM grain classes are slowly accumulating during the low flows. Toffaletis transport function demonstrates similar behaviour, with the finest grain classes VFM, FM, MM slowly accumulating during the low flow dry season, while the MM and CM grain classes are minimally transported during the dry season.

The results of both Yang and Toffaletis equations suggest that directly after the flood peak, a large volume of sediment will be accumulated behind the weir. Using Toffaletis equation the sediment will slowly accumulate over the duration of the dry season for the majority of sediment accumulated. Yangs equation suggests a transient storage period, in which as the flood peak is beginning to decrease there is an immediate settling of a large quantity of sediment, followed by a slow accumulation of the finer grain classes. If the behavior of the White Volta River is similar to the results of Yang's equations model, the construction of a weir will have a Transient Storage period which could potentially be optimized to maximize settling of particles during the 1 month period at the end of the rainy season.

While the change in bed elevation is being analyzed with respect to the starting bed elevation, in practice the net accumulation may be more accurate with a comparison of the increase in bed elevation with respect to total erosion behavior that occurred without the weir. For all simulations, these depictions are included in the Appendix for the respective simulations.

7.2 BEDMASS ACCUMULATION

The total mass of sediment that is accumulated upstream of the weir is calculated the sum of accumulation at each cross section A_n, where A is the 1st cross section immediately upstream of the weir, for the desired distance Equation 7.1:

$$Total = A + A_2 + A_3 + ...A_n \tag{7.1}$$

From the figure 7.6, the bed accumulation values for Toffaleti and Yang are of primary interest, as the morphological behavior is closer to what is expected in practice. With the addition of a weir that is 40 % of the bank height, the amount of sediment accumulated relative to erosional rates increases as it goes to further distances upstream of the weir. When the manning value increases the sediment accumulation decreases. Based on 10 kilometers upstream of the weir, using Toffaletis equation provides an estimated range between $\approx (30,000 - 115,000)$ tons of sediment will be accumulated. Using Yangs equation between $\approx (50,000 - 90,000)$ tons of sediment is accumulated. This values are likely a minimum estimate for total accumulated sediment upstream of the weir. Thus based on Yang's and Toffaletis sediment transport equations, the addition of a weir will provide between $30,000 - 115,000$ tons of sustainably sourced sediment without any disruption on the bottom levels of the river. This equates to approximately $1 - 2\%$ of the total incoming suspended sediment load. Thus, it is unlikely to cause hungry water nor negatively impact sediment continuity. This does have the additional benefit of lowering the total sediment entering the Aksombo Reservoir, reducing its filling time.

The majority of sand is accumulated at the end of the rainy season, this works ideally with the infrastructural limitations tipper truck drivers face, as often during the rainy seasons the roads are too muddy for the trucks to access, while during the dry season trucks can travel freely without hindrance. From an observational study by [9], from 6 mining sites an average of 250 total trucks per day were leaving with sediment. As 50 % of the mining sites are river sites, 125 trucks per day were leaving from river sites. This means that a weir will sustainably supply between 15-40 days supply for these trucks.

The average density of sand is 1620 kg per m^3, which means each m^3 of sand weights approximately 1.6 tons and a truck carries between 20-30 tons of sand. Thus, based on the results of the Toffaleti & Yang computations the weir will provide at minimum 1,200 ($\frac{25tons}{truck}$) truckloads of river sand and at maximum 4,600 ($\frac{25tons}{truck}$) truck loads of sand. A truckload of sand with an estimated $15 - 20m^3$ sells for 400 Ghanian Cedis (GHS) in Tamale. Thus the weir sand winning site can earn a revenue between (560,000 - 1,840,000 GHS). According to Abu and Peprah after expenses each truck earns approximately 182 GHS that is added to the local economy with (1 Euro = 6.96 GHS, 2021) [9].

Unfortunately, it is not known how much sediment is used in Tamale per day, so the net impact is not known in consideration of total sediment demand. However, even a small percentage of sustainable supply can be a starting point to mitigate damages until alternative or more sustainable building materials can be used.

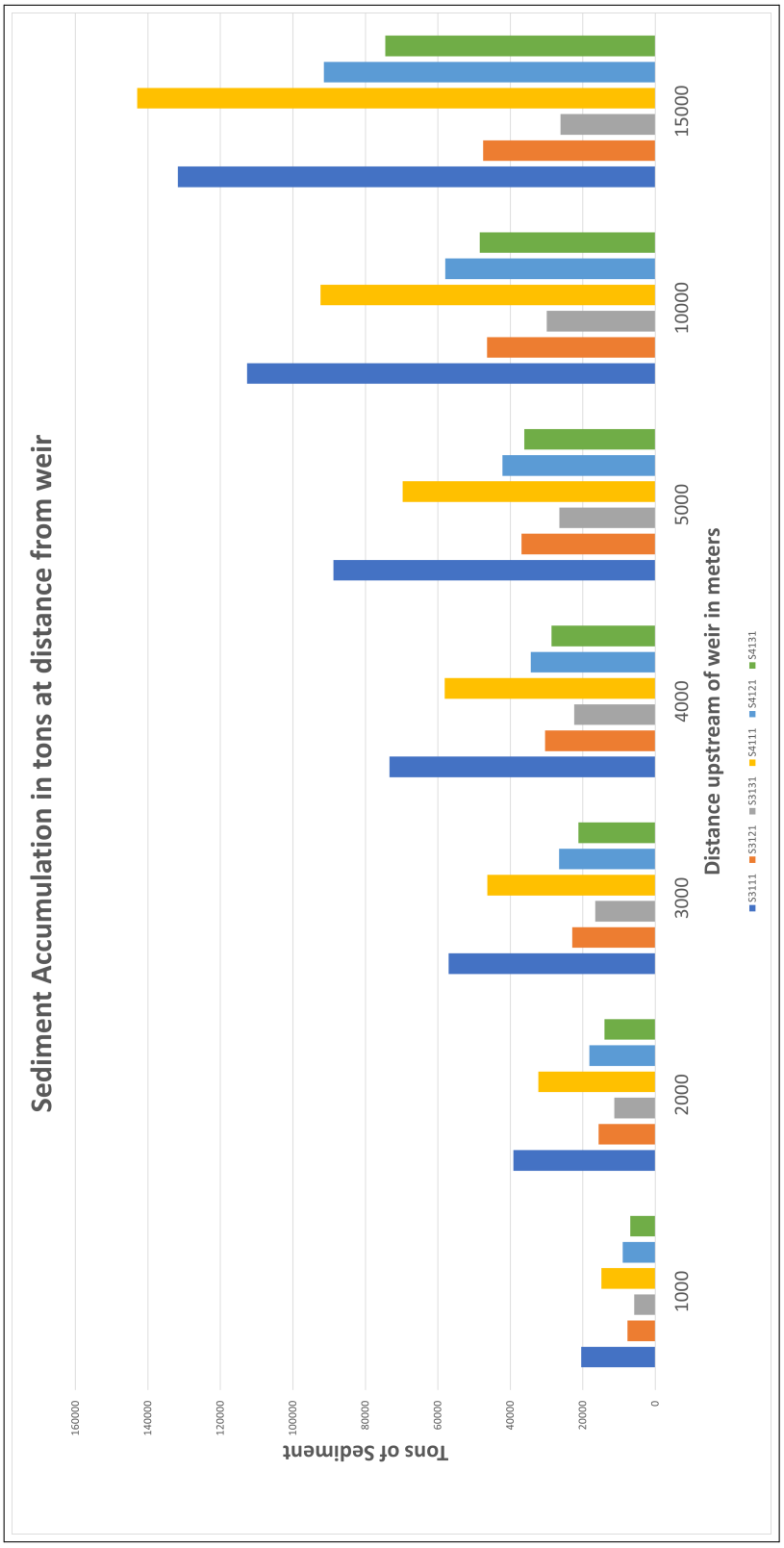

Figure 7.6: Total Sediment Accumulation in tons at differing distances from the weir using Toffaleti and Yang's transport functions.

8 CONCLUSIONS & RECOMMENDATIONS

The objective of this research was to gain a better understanding of sediment transport behavior around weirs to determine the potential excess sediment accumulation immediately upstream of a single weir implemented on the White Volta River. Based on the conclusions of this research, recommendations for practice and further research will be given.

8.1 CONCLUSIONS

Based on the literature study and the hydrological model, it can be noted that building a weir will create surplus sediment accumulation upstream of the weir with a transient storage effect. This transient storage zone is not immediately upstream of the structure, but goes many kilometers upstream due to the low slope of the channel bed. Depending on the method used for sediment transport, the variation in sediment accumulated is significant, with estimations between $30,000 - 115,000$ tons of surplus sediment derived from incoming suspended wash load. The large range in data demonstrates the difficulty in giving accurate predictions of sediment transport and accumulation based on the many assumptions that were made in creating the mode.

8.1.1 Sediment Behavior - Transient Storage

This thesis hoped to examine sediment behavior when introduced to a run-of-river weir. The literature study concluded that their was very little information regarding methods to calculate the trapping efficiency of a weir. This was due to the complex behavior of sediment transport. Observational studies have shown that weirs do not have a 100 % trapping efficiency like a hydro-powered dam, which transports all sediment except those which are flushed. The stream-bed upstream of a weir did not increase to the same height as the weir, therefore their is a mechanism that caused sediments to be transported up and over the weir. This was observed to be a sediment ramping effect, in which sediments settled to form a ramp, until the stream power is sufficient to pull sediment up and over the weir.

This observed continuity was also observed in the model. The addition of a weir only trapped 1-2 % of the incoming sediment load into the river section, the majority of this trapping occured at the offset of the rainy season, during a period where the heavy incoming wash load and eroded sediment settled as the velocity of the flow decreased. During the peak flows, sediments pulled up and over the weir, and little accumulation is observed. Thus during the heaviest flows a sediment ramp was not required for sediment to be pulled over the weir. Instead, the weir increases the water levels upstream. A maximum increase in water level occurs directly upstream of the structure, and decreases proportionately with the backwater curve caused by the weir. The increased water level lowers the velocity and effectively causes settling of sediments. The heavier sediments will begin to settle at higher velocities and will begin to settle further upstream of the weir Appendix A.26, while the closer to the weir as velocities continue to decrease the finer sediments will settle. HEC-RAS computes these as classes with a sediment range, thus you can see a "stair-like"

effect but the nature spread of grain classes is smoother and will effectively create a ramping effect.

The height of the ramping does not reach until the height of the weir, but to a fraction of the weir height. Based on these behaviours, that fraction will likely increase with a steeper slope due to the greater impact a weir has on stream velocity. However, in rivers with a heavy flood peak, the ramping behavior will be flushed out as seen in Appendix A.30. Therefore, weirs can be used to trap sediments after the rainy season, with volumes that increase with increasing slope.

Lastly, sediment transport is a dynamic process with many different variables having large impacts on transport volumes. The 1-D models confirmed this behavior, with simply changes to stream roughness or transport calculation methods completely changing the outcome of the simulation while many of the model inputs were identical. Rivers themselves also aren't uniform in their behaviours. However, improving the data available for study will allow for much better predictions of sediment transport behaviour.

8.2 ADVICE TO AWC

If weirs are being built for drinking water purposes, using the structure for sediment mining based on these predictions does not provide enough sediment to meet the massive demand of the growing city of Tamale. However, the potential for a sustainable supply should be considered further, only to prevent long term damages to the river. As earlier stated, this model predictions are a likely minimum of the total sediment that will be captured. In addition, current extraction methods only consider the excess of a single year, without optimizing dredging events to maximize sediment captured. Sand winning can be optimized to maximize settling of suspended loads with the creation of pits to further slow down the flow which will trap a higher volumes of sediment. If illegal sand mining continues to create increasingly devastating damages, using these pits could be a way to start the industry into a more sustainable direction. As the primary sediment type suspended in the White Volta River is silt, it would need to be mixed with larger diameter sands sourced from other locations. If the topic is of interest, there is much more research and testing to be done, including in the field in Ghana to develop more robust knowledge of the river and resource availability of sediments for long term use.

8.3 RECOMMENDATIONS FOR FURTHER RESEARCH

8.3.1 Expanding this model to a fully modelled system on the White Volta

As the AWC is looking to sustainably develop the water corridor in the Tamale region, a precise hydrological model of the reach near Tamale should be developed to allow further research. Data for the White Volta is sorely lacking, with the only data available being discharge data. In order to calibrate the findings of this research field data must be collected. First digital elevation model (DEM)'s are required with the necessary precision to model flood risk and sediment transport. To date, medium resolution data ($30m - 90m$) can by found online via ASTER or SRTM, but this resolution is not high enough for flood mapping and sediment transport purposes. Data acquisition using satellite-borne LIDAR or SAR are not practical for small scale application, as the data collected is at lower resolution over larger areas unless data is purchased from private companies. Drone technology has im-

proved to produce high resolution DEM by stitching together hundreds of photos creating an orthomosiac via LiDAR and photogrammetry. The second set of vital data missing is the bathymetric data across the river cross sections. This can be done using echo-sounders which all the bed elevations at various cross sections be determined in the White Volta River. Using multi-beam echo-sounders, the entire channel bed elevation can be determined, this method is also the most effective method of estimating bed-load transport as point based measurements are highly inaccurate. Or for a cheaper method, using a boat and a measuring stick relative to the bank height. At low flows, drone based DEM could also potential obtain stream bottom elevations as well. Improving the cross section from a flume to realistic data for the White Volta will provide better velocity computations, which has a significant impact on which sediment can be transported and the amount of sediment that will be deposited.

With an accurate Digital Elevation Model, the realistic reach of the river can be modelled for fine tuned research. For sediment transport, sediment fractions for the sediment rating curve should be obtained. As the sediment class has a large impact on settling behavior, a measured sediment rating curve with class fractions will provide a much better prediction of total accumulation upstream of the weir. The models can be calibrated with echo-sounding surveys which can measure seasonal changes in aggradation and deposition, Acquiring this data, or even more will allow water planners for the water corridor a much better understanding of the hydro-logical system to determine if weirs can be used to sustainabilize Tamales sand mining operations.

In addition, in the coming years the Bagre Dam construction will be complete in Northern Ghana, this will reduce the supply of sediment downstream in the Tamale region. Studies done before and after the Bagre Dam completion will be interesting to analyze in developing the sediment balance of the White Volta River.

8.3.2 Behavior of sediment in front of large scale run of river weirs

The behavior of sediment upstream of large obstructions is still largely unstudied. Outside of observational evidence and tracer studies, their is no derived method of calculating the estimated accumulation of bed material as a function of particle diameter, velocity of flow, bed roughness, weir height, and channel slope. The methods of calculation is complex, and the procedure to estimate the transient storage or sediment ramp is not defined. This is likely due to the dynamic behavior of the river. Small eddies and currents can create a whirl pooling effect which is hard to predict, and will often pull sediment up and over the weir. Engineers assume the velocity in front of a weir is zero, in reality there is a turbulent flow at the bed in front of the weir, with undefined sediment behavior Queen. For better predictions of the bed mass accumulation a flume can be created using various sediment classes, slopes, and velocities to model the behavior of sediment in front of the weir structure. Bases on these flume experiments, perhaps a simplified estimated method can be derived which can predict increase in bed levels as a function of grain class, slope, and velocity.

8.3.3 Using local cheap infrastructures for weirs

In prediction models by Vera Kingma, it is estimated that building a weir in the White Volta will cause increased flooding to communities surrounding the river [39]. While mitigation measures such as bank protection, dikes, and levees could be built upstream of the structure for additional flood protection, another possible solution could be temporary weir like structures. A temporary weir, a potential

example being gambions, can be installed that could be removed if the river experiences peak floods higher than usual which would minimize the flood risk to local communities. Flume experiments can be conducted to estimate the difference in sediment accumulation and water storage upstream with a temporary structure and a permanent structure. Gabions will accumulate sediment upstream of the structure but the morphological behavior relative to permanent structures is still relatively understudied [16]. Tests can be conducted in a flume to determine the efficiency of sediment capture using gabions with different filling materials (concrete, large rocks, earth).

8.4 SUMMARY

There are a lot of gaps in this research to provide concrete answers in helping to develop a sustainable sand winning system for Tamale. Sand mining is increasingly causing concern worldwide due to the long replenishment times of river based sediment. My goal was that this paper will help others wanting to get introduced to sediment transport, its mechanisms, and perhaps spark ideas in helping solve this issue. This research acknowledges these gaps, and I am hoping that some of the information here can help assist others in researching this topic further. Thank you for your interest.

BIBLIOGRAPHY

African water corridor.

Transmission of sediment by water.

(2021). Current turbidity of our rivers destroying our pumps - water company ltd.

Abdalla, I. E., Cook, M. J., and Yang, Z. (2007). Numerical study of transitional separated–reattached flow over surface-mounted obstacles using large-eddy simulation. *International journal for numerical methods in fluids*, 54(2):175–206.

Abed, A. D. and Jaafer, S. M. (2021). Detect the water flow characteristic of the tigris river by using hfc-ras program. In *IOP Conference Series: Earth and Environmental Science*, volume 754, page 012003. IOP Publishing.

Abozeid, G., E Mohamed, W., and ME Osman, N. (2019). Experimental study on bed scour and its protection behind standing wave weirs considering combined flow over weir crestand bottom pipes. *JES. Journal of Engineering Sciences*, 47(4):461–474.

Abu, I. and Peprah, K. (2020). Application of ecological modernisation in sand winning in building construction in tamale, ghana. *Ghana Journal of Development Studies*, 17(2):1–22.

Akrasi, S. A. (2005). The assessment of suspended sediment inputs to volta lake. *Lakes & Reservoirs: Research & Management*, 10(3):179–186.

Aldridge, B. N. and Garrett, J. M. (1973). Roughness coefficients for stream channels in arizona. Technical report, US Geological Survey.

Arcement, G. J. and Schneider, V. R. (1989). Guide for selecting manning's roughness coefficients for natural channels and flood plains.

Baar, A. W., Weisscher, S. A., and Kleinhans, M. G. (2020). Interaction between lateral sorting in river bends and vertical sorting in dunes. *Sedimentology*, 67(1):606–626.

Bagnold, R. A. (1966). *An approach to the sediment transport problem from general physics*. US government printing office.

Barry, B., Obuobie, E., Andreini, M., Andah, W., and Pluquet, M. (2005). Comprehensive assessment of water management in agriculture (comparative study of river basin development and management. *International Water management institute IWMI*.

Berney, O., Charman, J., Kostov, L., Minetti, L., Stoutesdijk, J., and Tricoli, D. (2001). Small dams and weirs in earth and gabion materials. *Rome: Food and Agriculture Organization of the United Nations*.

Blom, A. and Parker, G. (2004). Vertical sorting and the morphodynamics of bed form–dominated rivers: A modeling framework. *Journal of Geophysical Research: Earth Surface*, 109(F2).

Brunner, G. W. (2016). *HEC-RAS, RIVER ANALYSIS SYSTEM HYDRAULIC REFERENCE MANUAL*. US ARMY CORPS OF ENGINEERS.

Brunner, G. W. and Gibson, S. (2005). Sediment transport modeling in hec ras. In *Impacts of Global Climate Change*, pages 1–12.

Casserly, C. M., Turner, J. N., O'Sullivan, J. J., Bruen, M., Bullock, C., Atkinson, S., and Kelly-Quinn, M. (2020). Impact of low-head dams on bedload transport rates in coarse-bedded streams. *Science of The Total Environment*, 716:136908.

Claydon, J.

Collins, B. and Dunne, T. (1990). Fluvial geomorphology and river-gravel mining: A guide for planners, case studies included. special publication 98. *Calif. Div. Mines and Geol*.

Copeland, R. R., Thomas, W. A., et al. (1989). Corte madera creek sedimentation study: Numerical model investigation.

Csiki, S. and Rhoads, B. L. (2010). Hydraulic and geomorphological effects of run-of-river dams. *Progress in physical geography*, 34(6):755–780.

Csiki, S. J. and Rhoads, B. L. (2014). Influence of four run-of-river dams on channel morphology and sediment characteristics in illinois, usa. *Geomorphology*, 206:215–229.

der Zwet, J. V. (20012). The creation of a reservoir in the white volta river, ghana: An analysis of the impact on river morphology. Master's thesis, Technical University Delft, the Netherlands.

DID (2009). River sand mining management guideline.

Farrell, E. J. and Sherman, D. J. (2015). A new relationship between grain size and fall (settling) velocity in air. *Progress in Physical Geography*, 39(3):361–387.

Flynn, R. H. (2011). *Analysis of the transport of sediment by the Suncook River in Epsom, Pembroke, and Allenstown, New Hampshire, after the May 2006 flood*. US Department of the Interior, US Geological Survey.

Garcia, M. (2008). Sedimentation engineering: processes, measurements, modeling, and practice. American Society of Civil Engineers.

Gavriletea, M. D. (2017). Environmental impacts of sand exploitation. analysis of sand market. *Sustainability*, 9(7):1118.

Gibson, S. and Cai, C. (2017). Flow dependence of suspended sediment gradations. *Water Resources Research*, 53(11):9546–9563.

Gibson, S. and Pridal, D. (2015). Negotiating hydrologic uncertainty in long term reservoir sediment models: simulating arghandab reservoir deposition with hec-ras. In *SEDHyd: 10 th Interagency Federal Sedimentation Conference*.

GSS (2012). 2010 population and housing census: summary report of final results.

Gumiero, B., Rinaldi, M., Belletti, B., Lenzi, D., and Puppi, G. (2015). Riparian vegetation as indicator of channel adjustments and environmental conditions: the case of the panaro river (northern italy). *Aquatic Sciences*, 77(4):563–582.

Hackney, C. R., Darby, S. E., Parsons, D. R., Leyland, J., Best, J. L., Aalto, R., Nicholas, A. P., and Houseago, R. C. (2020). River bank instability from unsustainable sand mining in the lower mekong river. *Nature Sustainability*, 3(3):217–225.

James, S. C., Jones, C. A., Grace, M. D., and Roberts, J. D. (2010). Advances in sediment transport modelling. *Journal of Hydraulic research*, 48(6):754–763.

Karamisheva, R. D., Lyness, J. F., Myers, W. R. C., and O'Sullivan, J. (2006). Sediment discharge prediction in meandering compound channels. *Journal of hydraulic research*, 44(5):603–613.

Kingma, V. (20021). Tthe creation of a reservoir in the white volta river, ghana: An analysis of the impact on river morphologyhe creation of a reservoir in the white volta river, ghana: An analysis of the impact on river morphology. Master's thesis, Technical University Delft, the Netherlands.

Koehnken, L., Rintoul, M. S., Goichot, M., Tickner, D., Loftus, A.-C., and Acreman, M. C. (2020). Impacts of riverine sand mining on freshwater ecosystems: A review of the scientific evidence and guidance for future research. *River Research and Applications*, 36(3):362–370.

Kondolf, G. M. (1994). Geomorphic and environmental effects of instream gravel mining. *Landscape and Urban planning*, 28(2-3):225–243.

Kuriqi, A., Koçileri, G., and Ardiçlioğlu, M. (2020). Potential of meyer-peter and müller approach for estimation of bed-load sediment transport under different hydraulic regimes. *Modeling Earth Systems and Environment*, 6(1):129–137.

Laursen, E. M. (1958). The total sediment load of streams. *Journal of the Hydraulics Division*, 84(1):1–36.

Madyise, T. (2013). *Case studies of environmental impacts of sand mining and gravel extraction for urban development in Gaborone*. PhD thesis, Citeseer.

Padmalal, D. and Maya, K. (2014). *Sand mining: environmental impacts and selected case studies*. Springer.

Pearson, A. J. and Pizzuto, J. (2015). Bedload transport over run-of-river dams, delaware, usa. *Geomorphology*, 248:382–395.

Peduzzi, P. (2014). Sand, rarer than one thinks. *Environmental Development*, 11:208–218.

Peeters, A., Houbrechts, G., Hallot, E., Van Campenhout, J., Gob, F., and Petit, F. (2020). Can coarse bedload pass through weirs? *Geomorphology*, 359:107131.

PrimeNewsGhana (2017). Sand winning causing water challenges in tamale - gwcl warns.

Queen, R. W. (2018). *Morphodynamic Modeling of Flow and Sediment Transport over Low-head, Run-of-river Dams*. PhD thesis, Colorado State University.

Rempel, L. L. and Church, M. (2009). Physical and ecological response to disturbance by gravel mining in a large alluvial river. *Canadian Journal of Fisheries and Aquatic Sciences*, 66(1):52–71.

Rijn, L. C. v. (1984). Sediment transport, part ii: suspended load transport. *Journal of hydraulic engineering*, 110(11):1613–1641.

Ruby, W. (1933). Settling velocities of gravel, sand and silt particles. *American Journal of Science*, 25:325–338.

Santo, E. and Sánchez, L. (2002). Gis applied to determine environmental impact indicators made by sand mining in a floodplain in southeastern brazil. *Environmental Geology*, 41(6):628–637.

Shields, A. (1936). Application of similarity principles and turbulence research to bed-load movement.

Sumani, J. B. B. (2019). Possible environmental and socio-economic ramifications of sand and gravel winning in danko, upper west region of ghana. *Ghana Journal of Geography*, 11(2):27–51.

Toro-Escobar, C. M., Paola, C., and Parker, G. (1996). Transfer function for the deposition of poorly sorted gravel in response to streambed aggradation. *Journal of Hydraulic Research*, 34(1):35–53.

Tracy, H. J. (1957). *Discharge characteristics of broad-crested weirs*, volume 397. US Department of the Interior, Geological Survey.

Udo, J. and Klopstra, D. (2012). North ghana sustainable development, disaster prevention and water resources management flood hazard assessment white volta.

Voogt, L., Van Rijn, L., and Van den Berg, J. (1991). Bed roughness and transport of fine sands at high velocities. *Journal of Hydraulic Engineering, ASCE*, 117(7):869–890.

Wilcock, P. R. (2001). Toward a practical method for estimating sediment-transport rates in gravel-bed rivers. *Earth Surface Processes and Landforms*, 26(13):1395–1408.

Wilcock, P. R. and Crowe, J. C. (2003). Surface-based transport model for mixed-size sediment. *Journal of hydraulic engineering*, 129(2):120–128.

Wong, M. and Parker, G. (2006). Reanalysis and correction of bed-load relation of meyer-peter and müller using their own database. *Journal of Hydraulic Engineering*, 132(11):1159–1168.

(www.dw.com), D. W. World water day: Northern ghana grapples with water shortages: Dw: 22.03.2016.

Yang, C. T. (1973). Incipient motion and sediment transport. *Journal of the hydraulics division*, 99(10):1679–1704.

Yang, C. T. (1984). Unit stream power equation for gravel. *Journal of Hydraulic Engineering*, 110(12):1783–1797.

Yeleliere, E., Cobbina, S., and Duwiejuah, A. (2018). Review of ghana's water resources: the quality and management with particular focus on freshwater resources. *Applied Water Science*, 8(3):1–12.

A SIMULATION RESULTS

A.1 TRANSPORT BASELINES

Figure A.1: Changes in Bed Elevation with respect to differing Manning Values

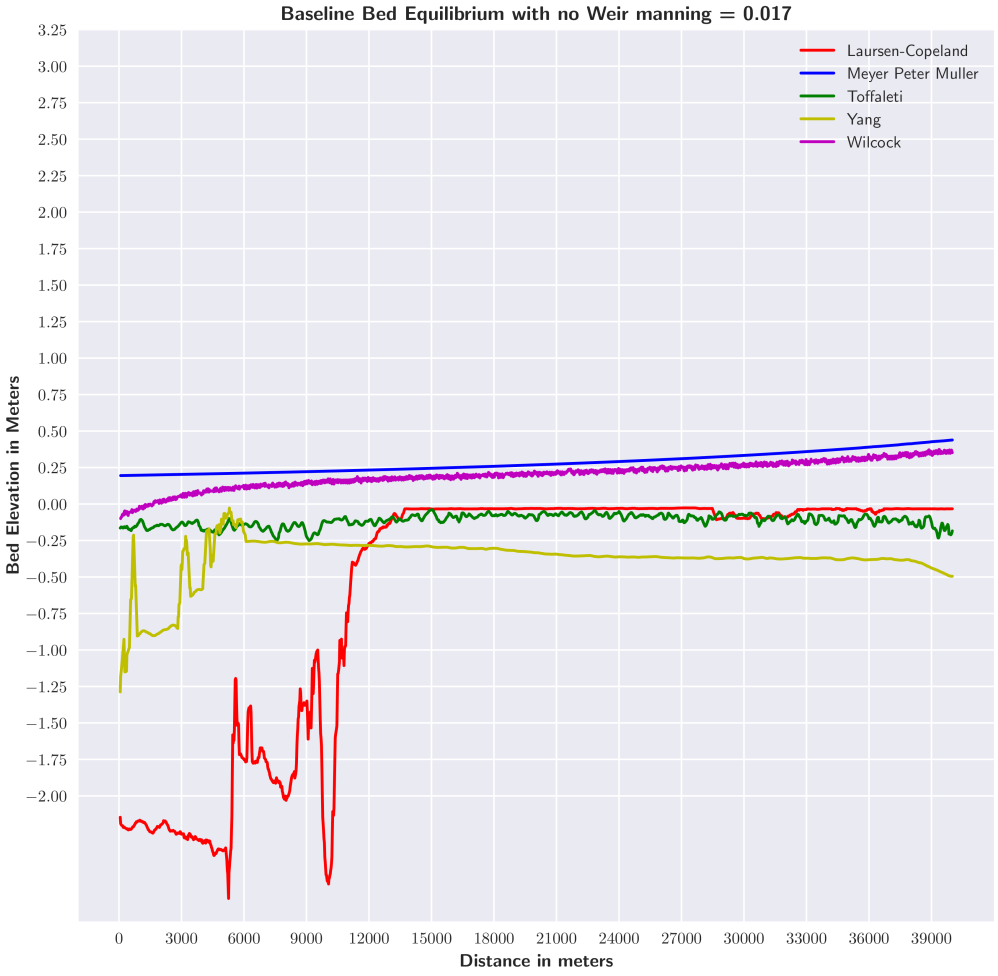

Figure A.2: Changes in Bed Elevation with respect to differing Manning Values

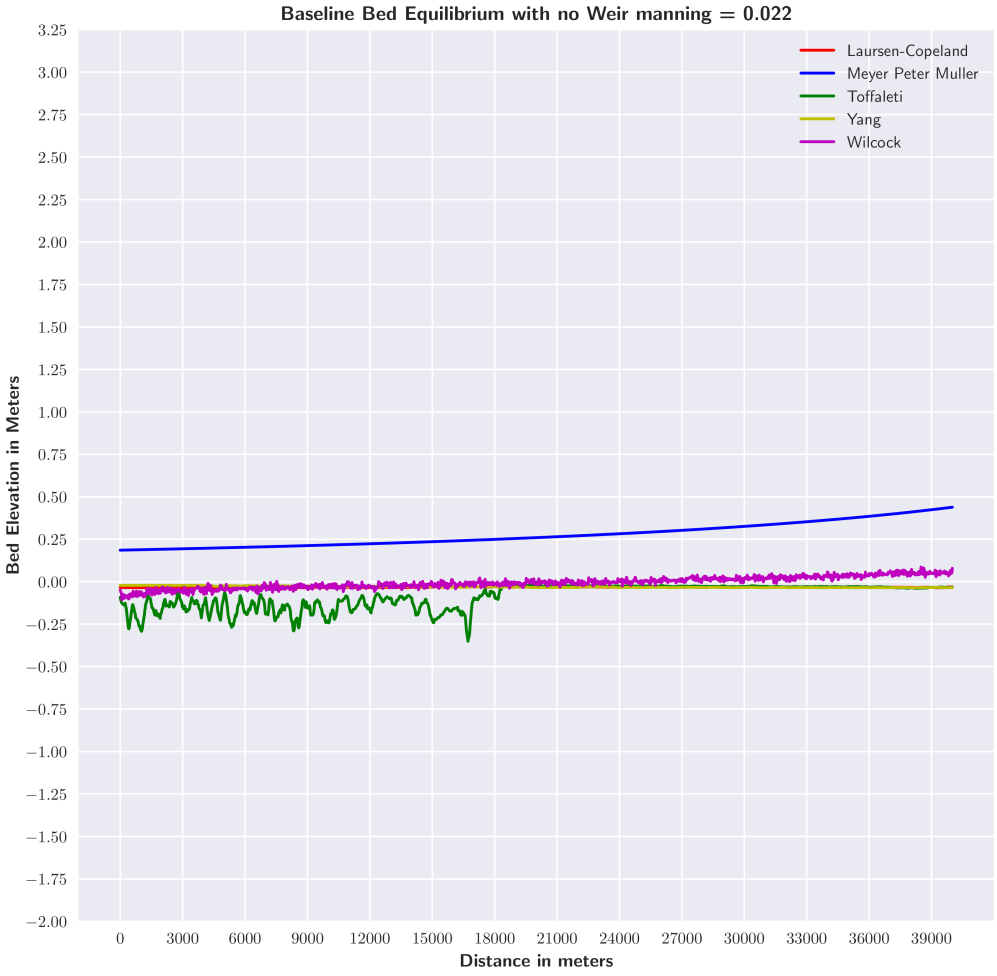

Figure A.3: Changes in Bed Elevation with respect to differing Manning Values

A.2 MODEL RESULTS: LAURSEN COPELAND

A.2.1 Invert Change

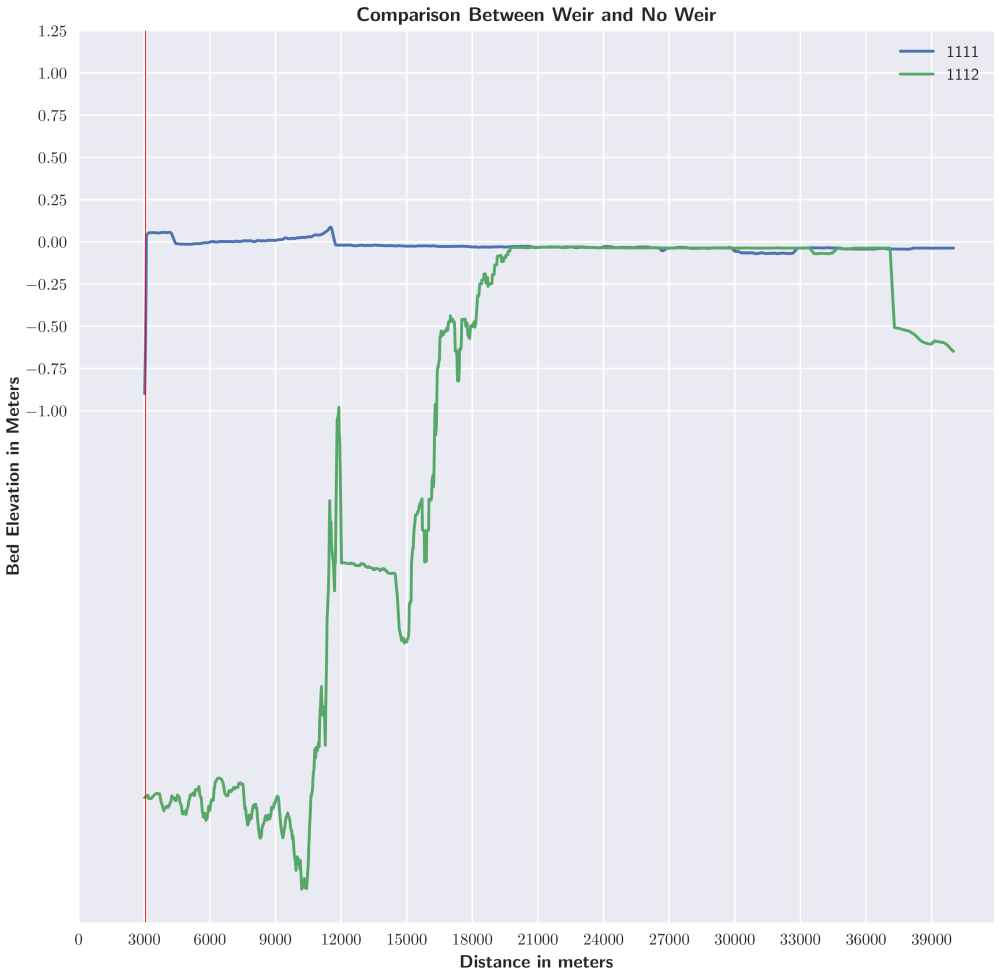

Figure A.4: Bed Elevation Comparison between 1111 & 1112: Manning Value 0.012

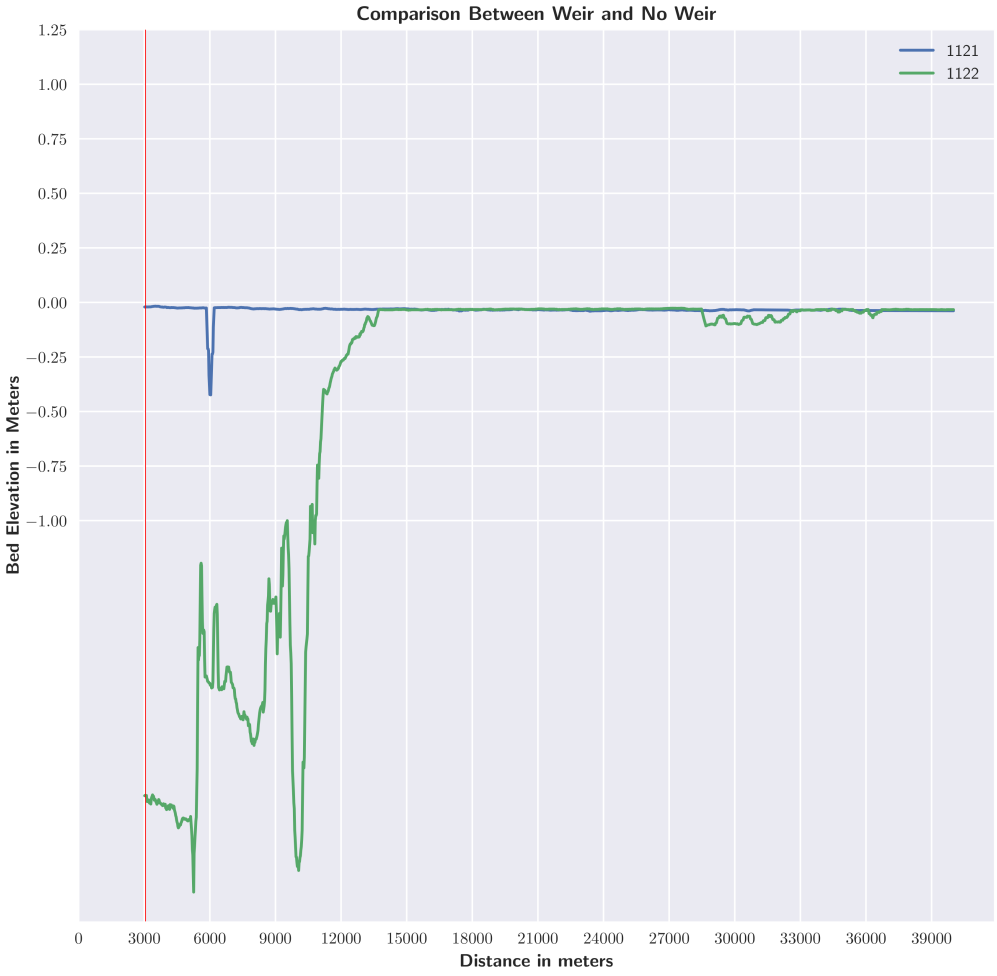

Figure A.5: Bed Elevation Comparison between 1121 & 1122: Manning Value 0.017

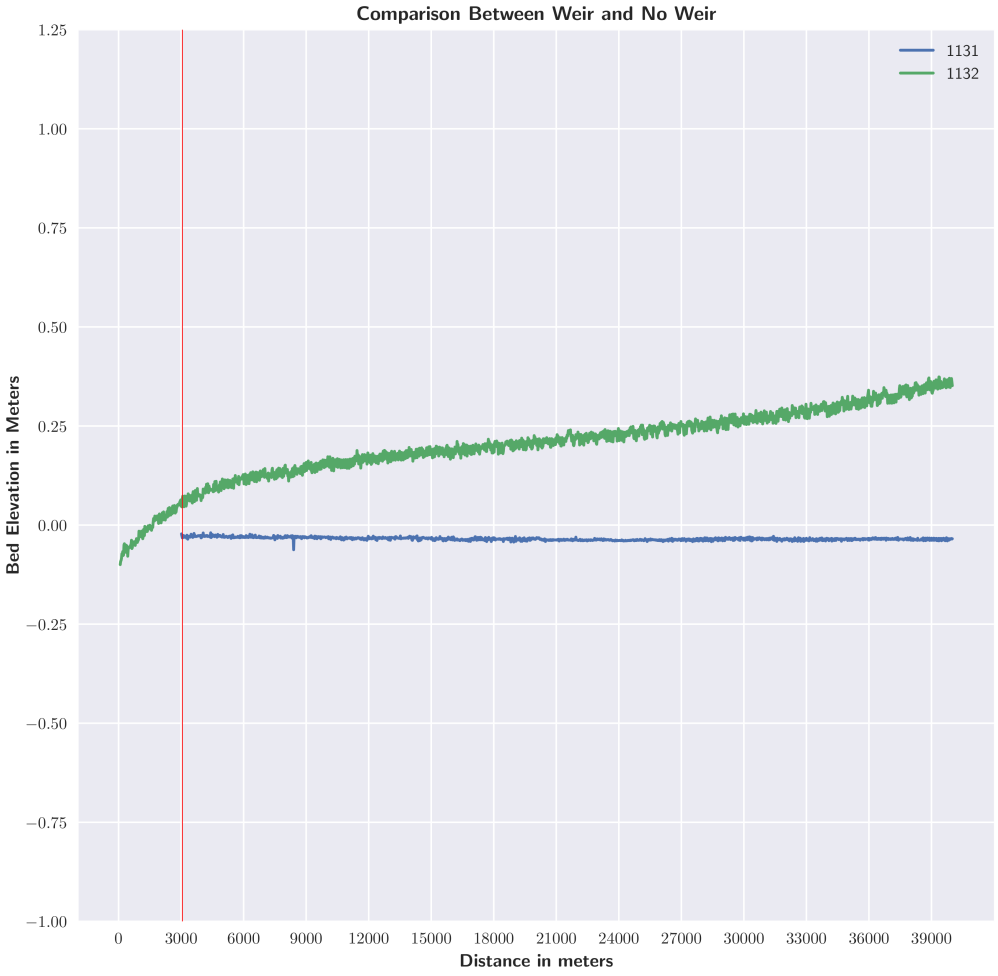

Figure A.6: Bed Elevation Comparison between 1131 & 1132: Manning Value 0.022

A.2.2 Bed Mass Change

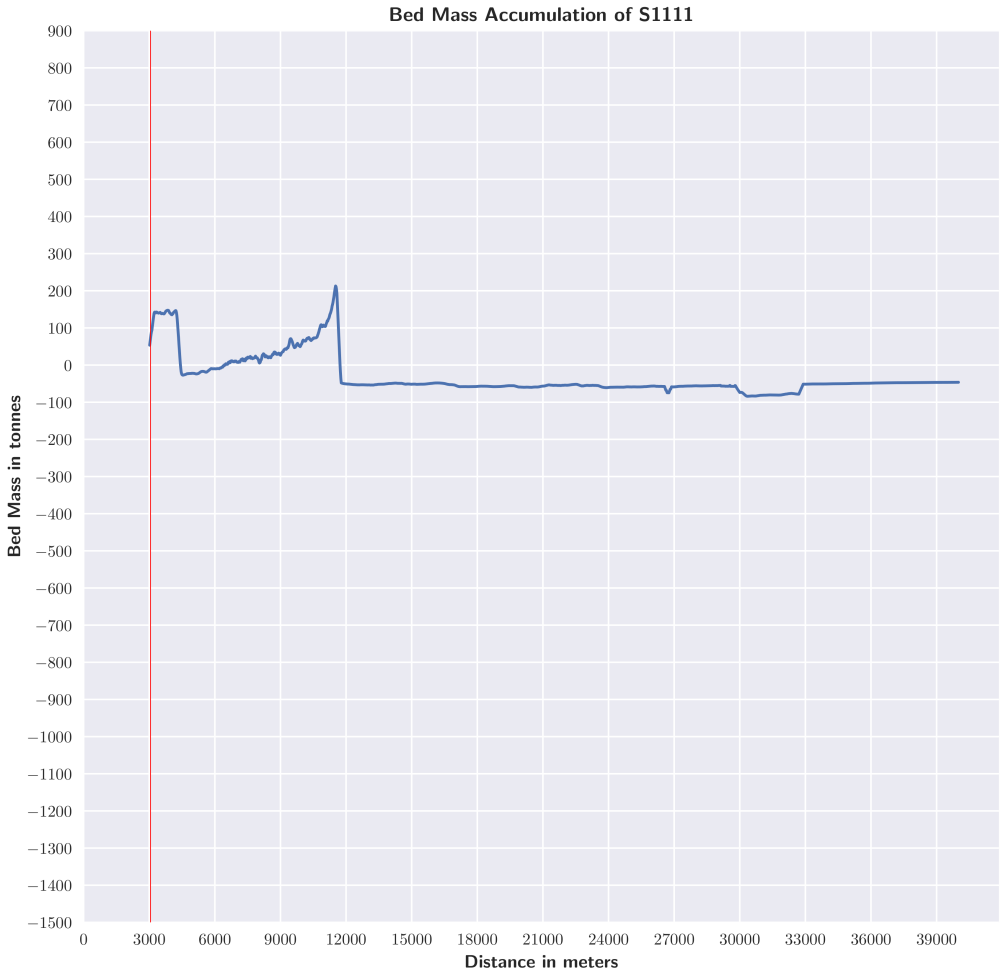

Figure A.7: Bed Mass Accumulation in Tonnes S1111

A.2.3 Time Series Upstream of Weir 20, 40, 100, 200, 500, 1000m

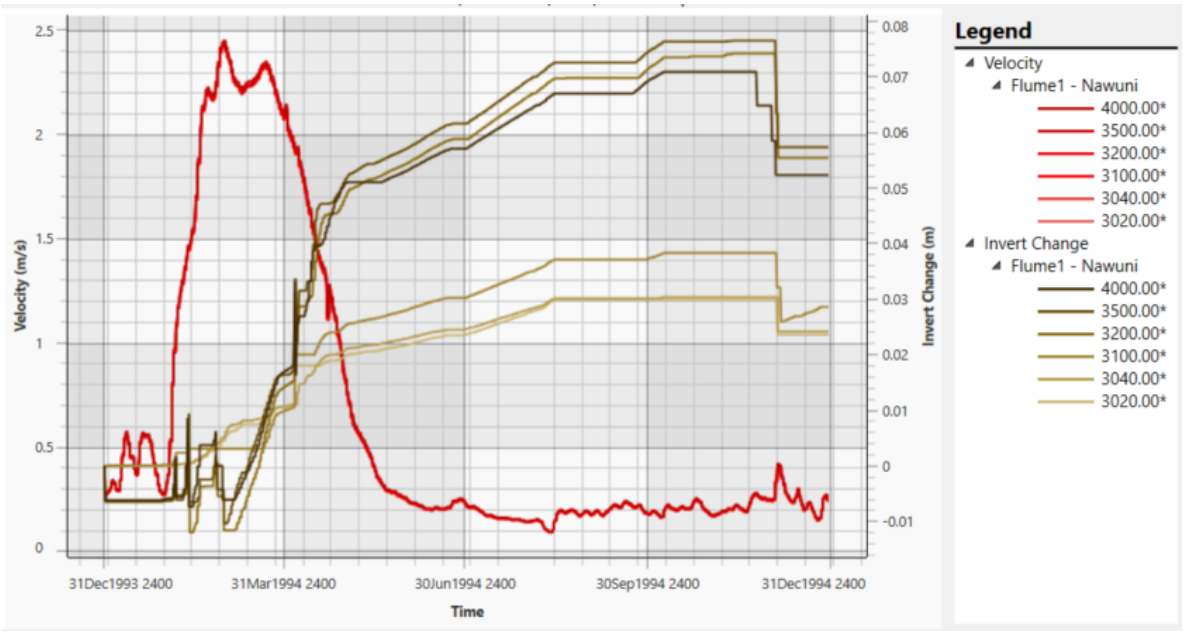

Figure A.8: Time Series Data for S1111 at locations upstream of the weir

A.2.4 Total Sediment Accumulation upstream of weir

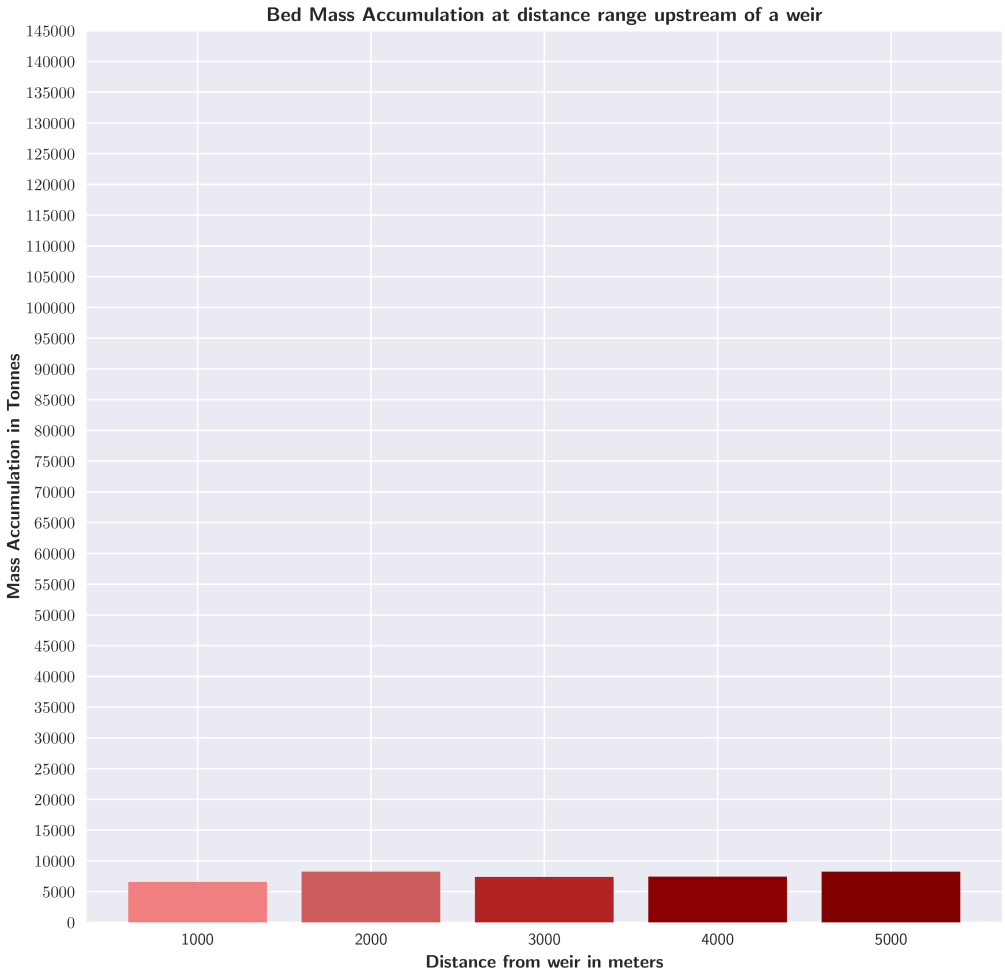

Figure A.9: Sediment Accumulation above "om" baseline levels in tons at distances upstream of a weir

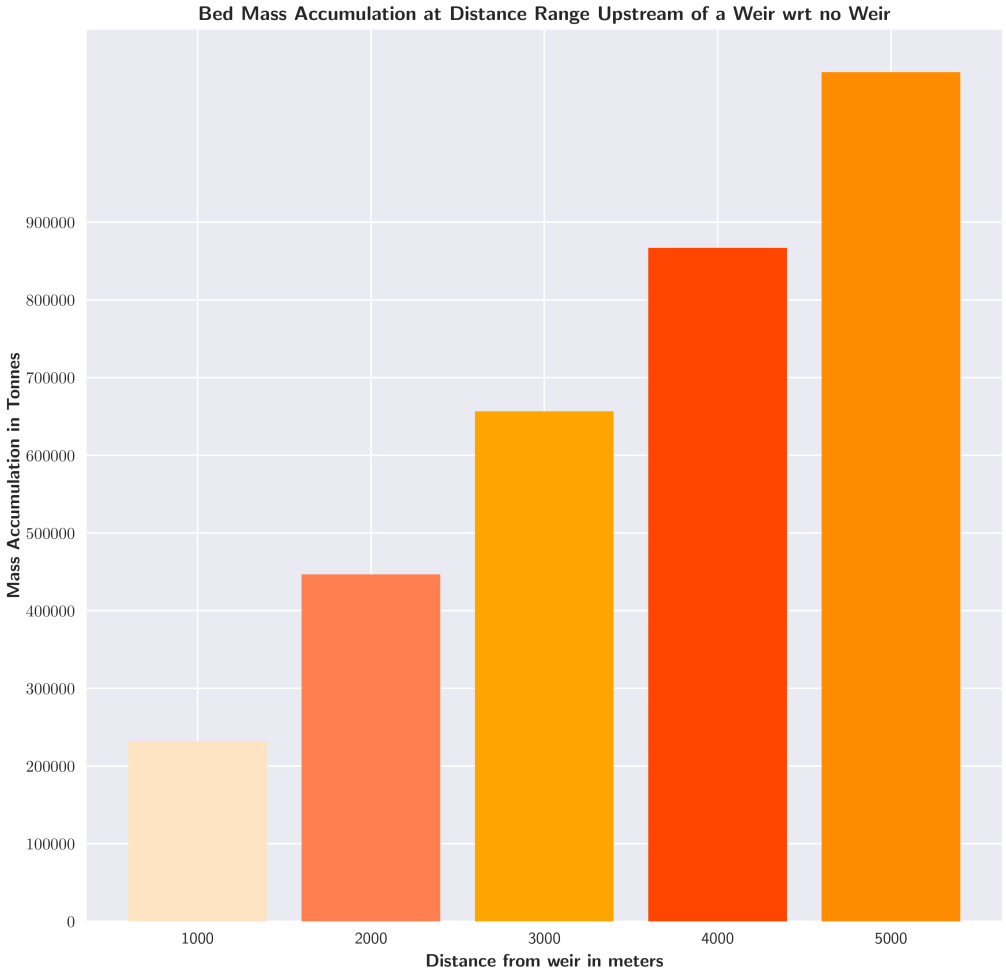

Figure A.10: Sediment Accumulation relative to erosion based on no weir at distances upstream of a weir

A.3 MODEL RESULTS: MEYER PETER MULLER

A.3.1 Invert Change

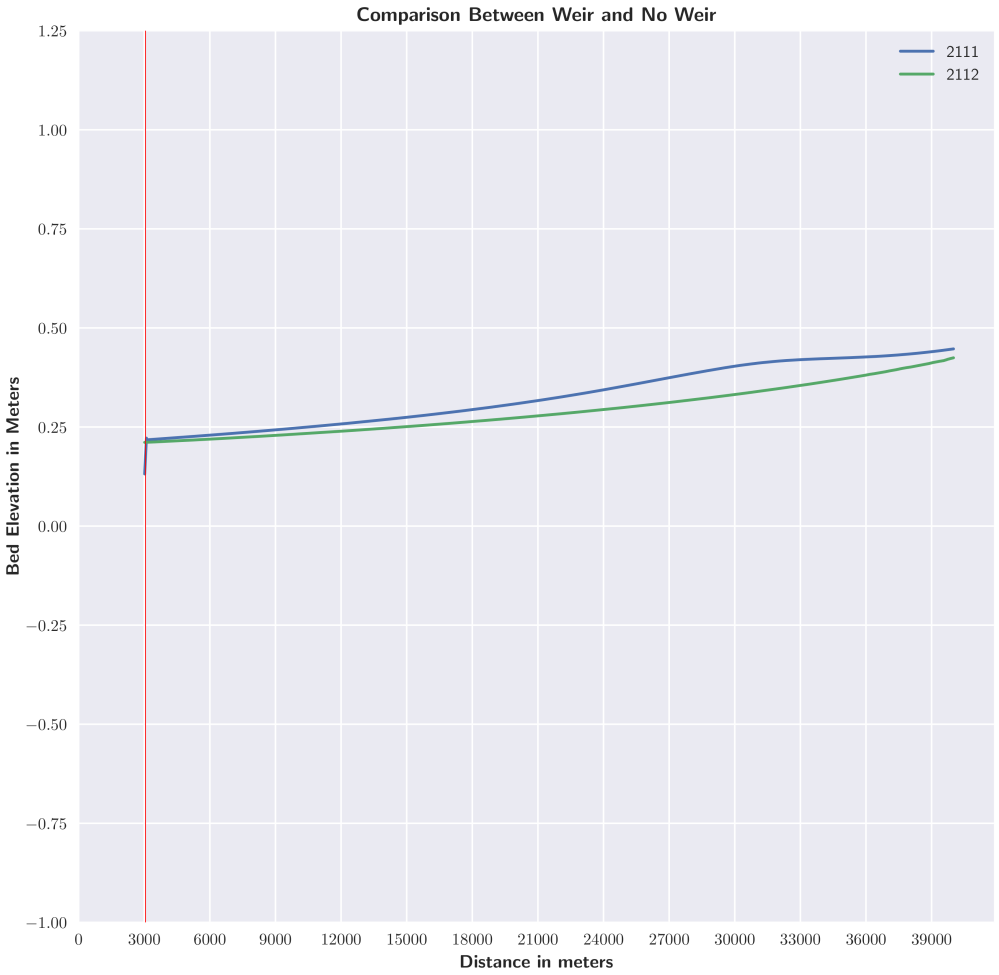

Figure A.11: Bed Elevation Comparison between 2111 & 2112: Manning value 0.012

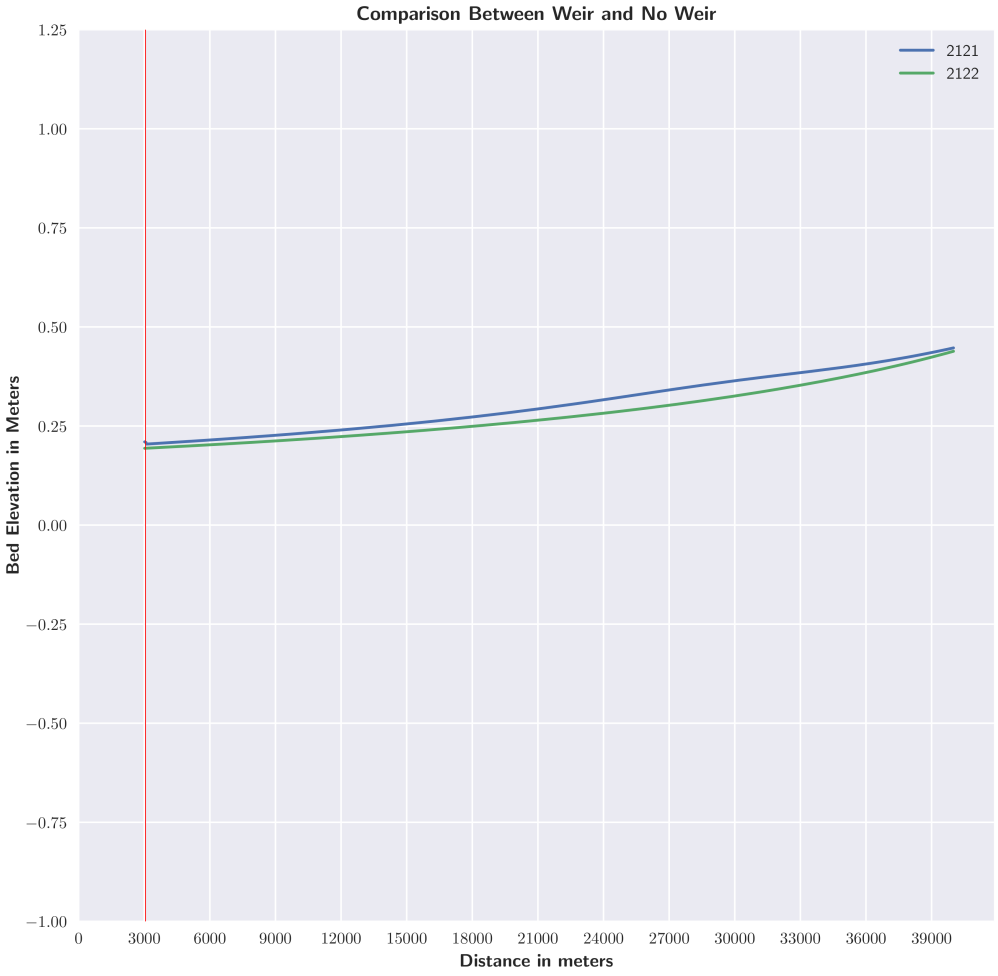

Figure A.12: Bed Elevation Comparison between 2121 & 2122: Manning Value 0.017

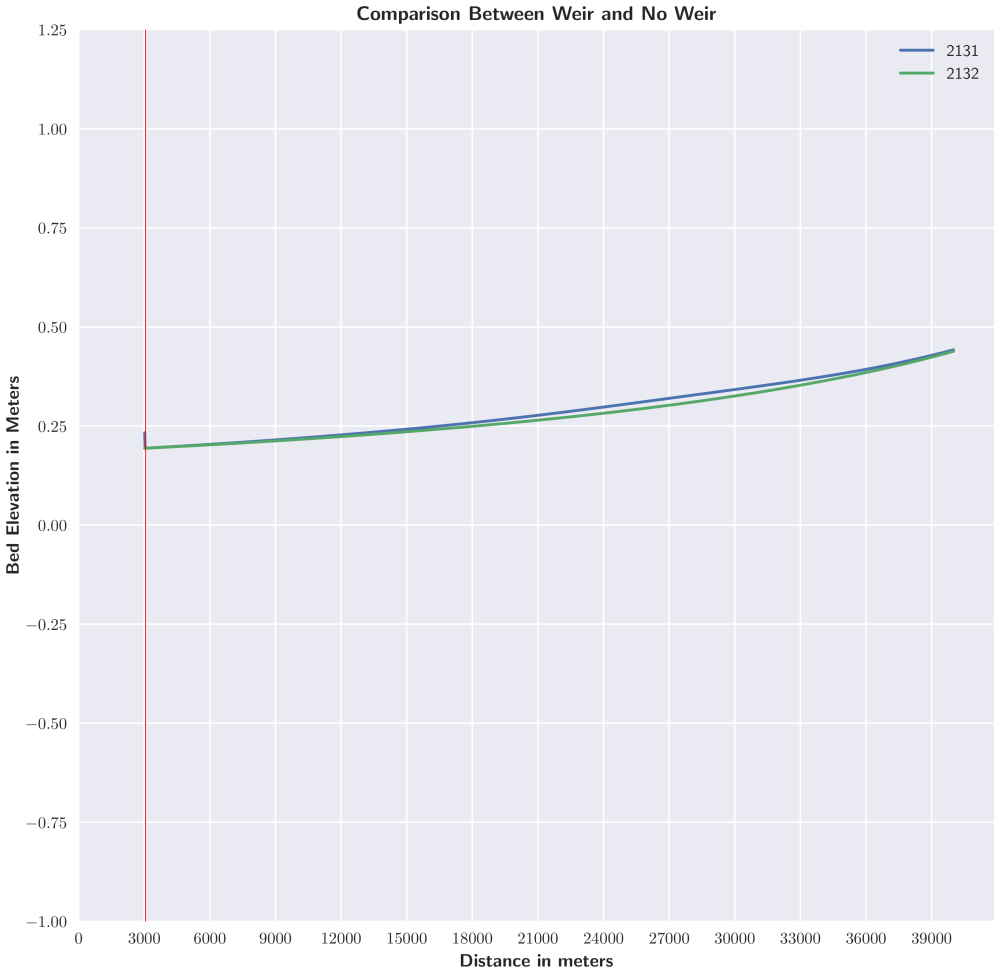

Figure A.13: Bed Elevation Comparison between 2131 & 2132: Manning Value 0.022

A.3.2 Bed Mass Change

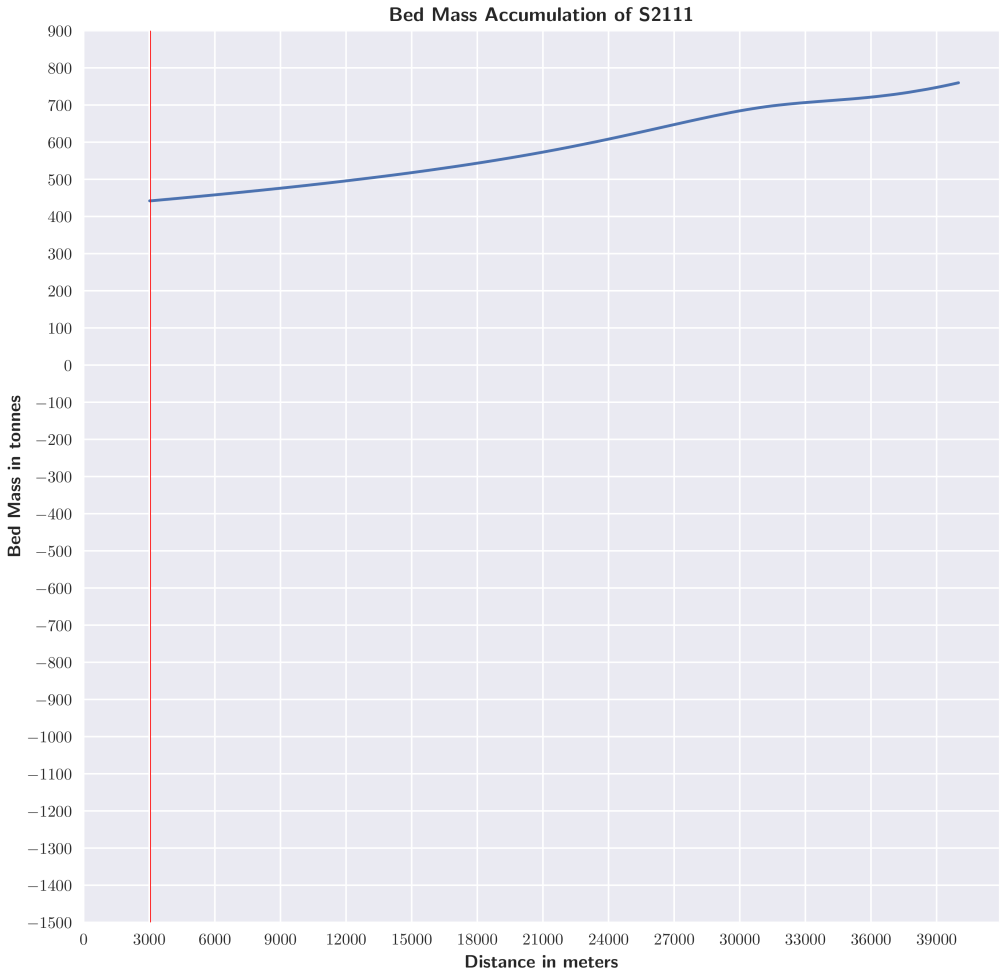

Figure A.14: Bed Mass Accumulation in Tonnes S2111

A.3.3 Time Series Upstream of Weir 20, 40, 100, 200, 500, 1000m

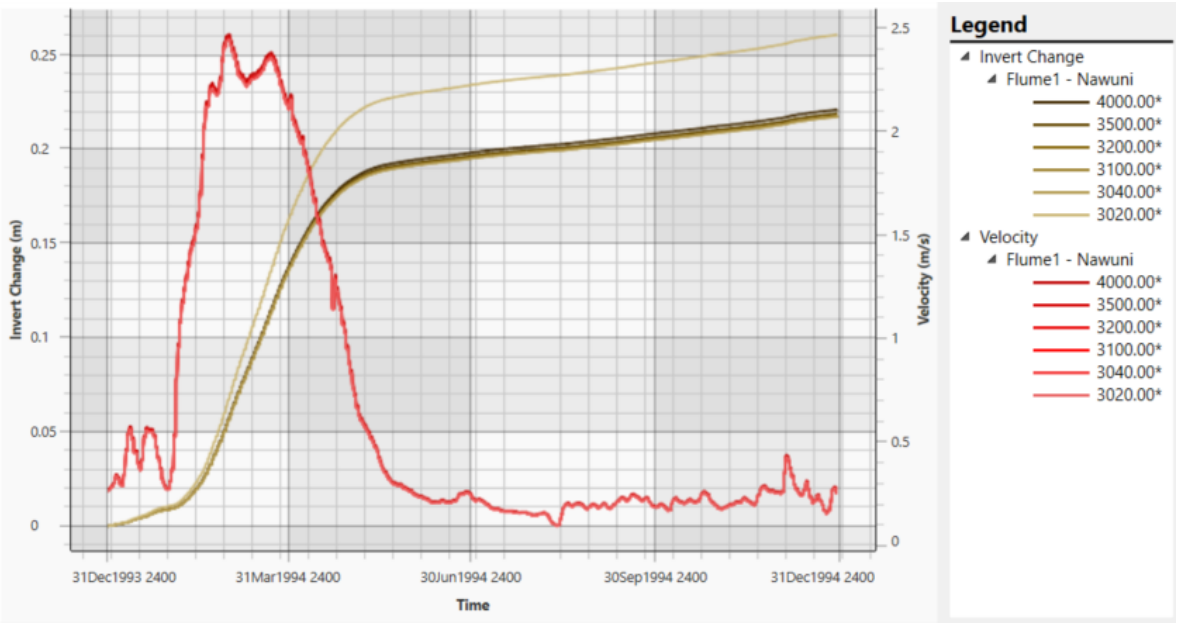

Figure A.15: Time Series Data for S2111 at locations upstream of the weir

A.3.4 Total Sediment Accumulation upstream of weir

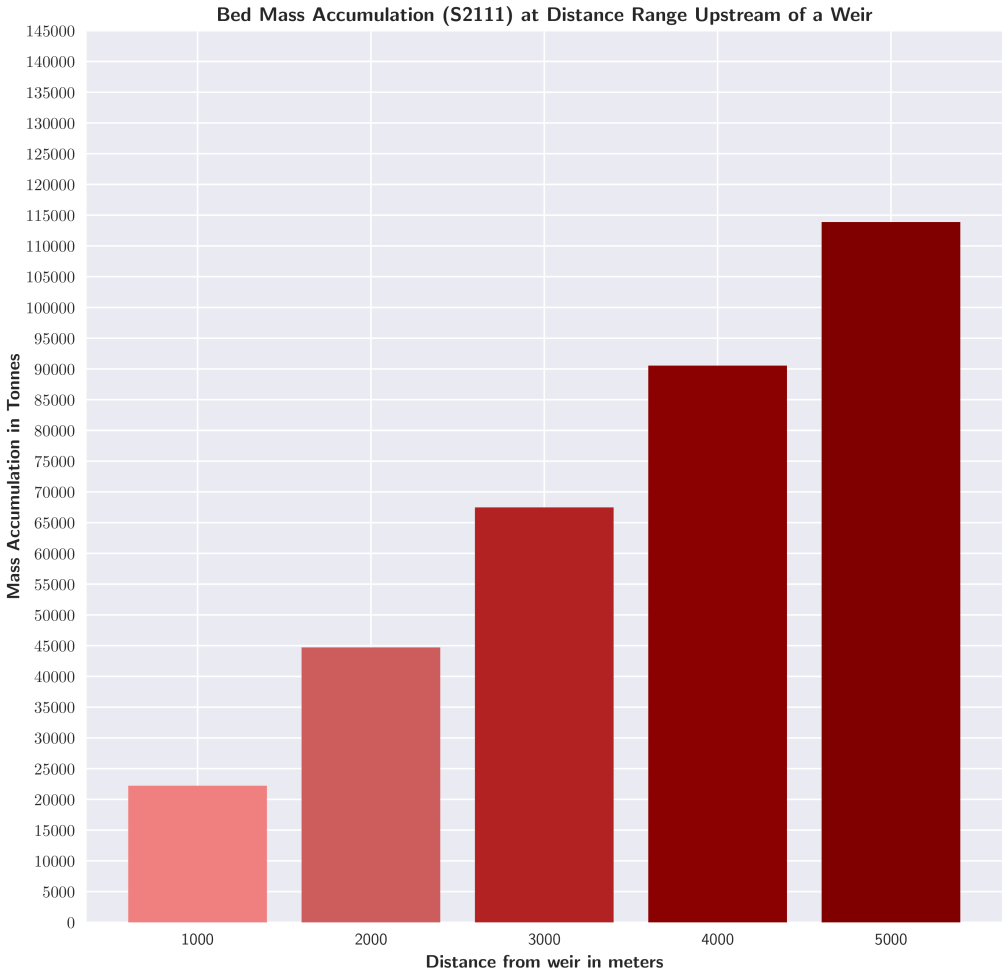

Figure A.16: Sediment Accumulation above baseline levels in tons at distances upstream of a weir

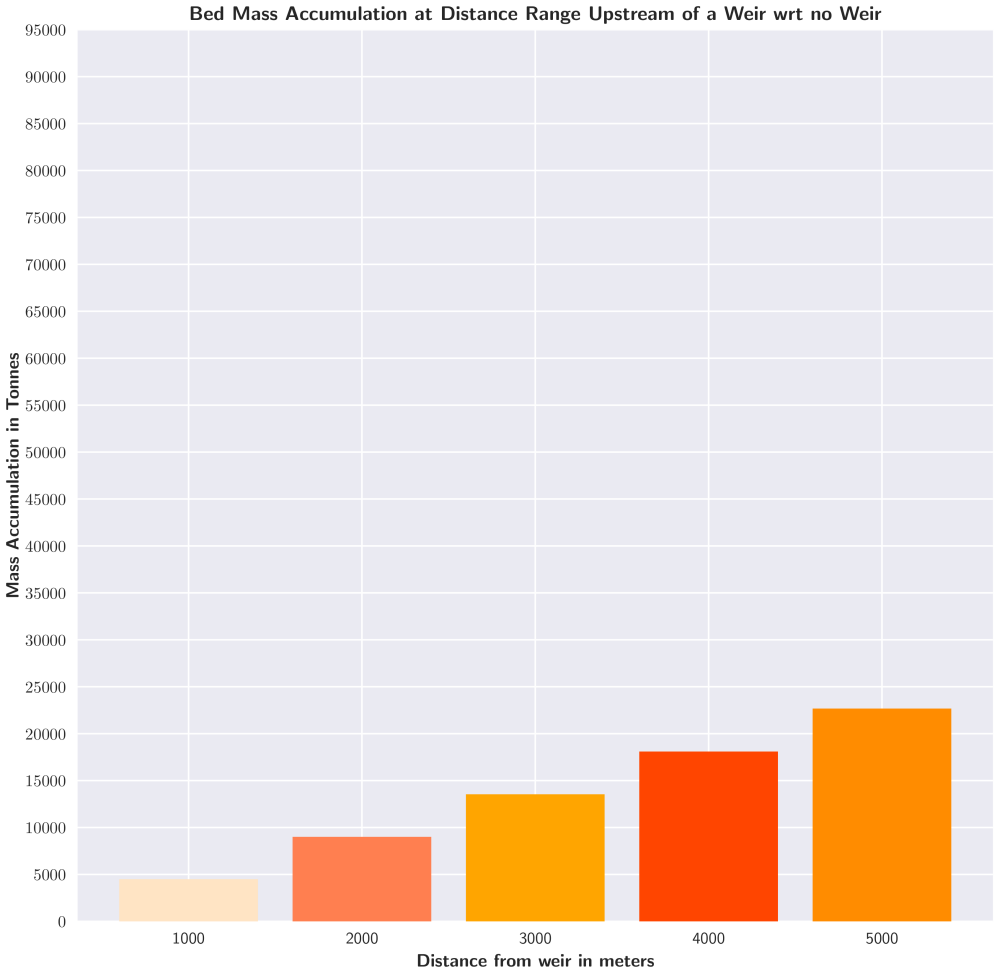

Figure A.17: Sediment Accumulation relative to erosion based on no weir at distances upstream of a weir

A.4 MODEL RESULTS: TOFFALETI

A.4.1 Invert Change

Figure A.18: Bed Elevation Comparison between 3111 & 3112: Manning Value 0.012

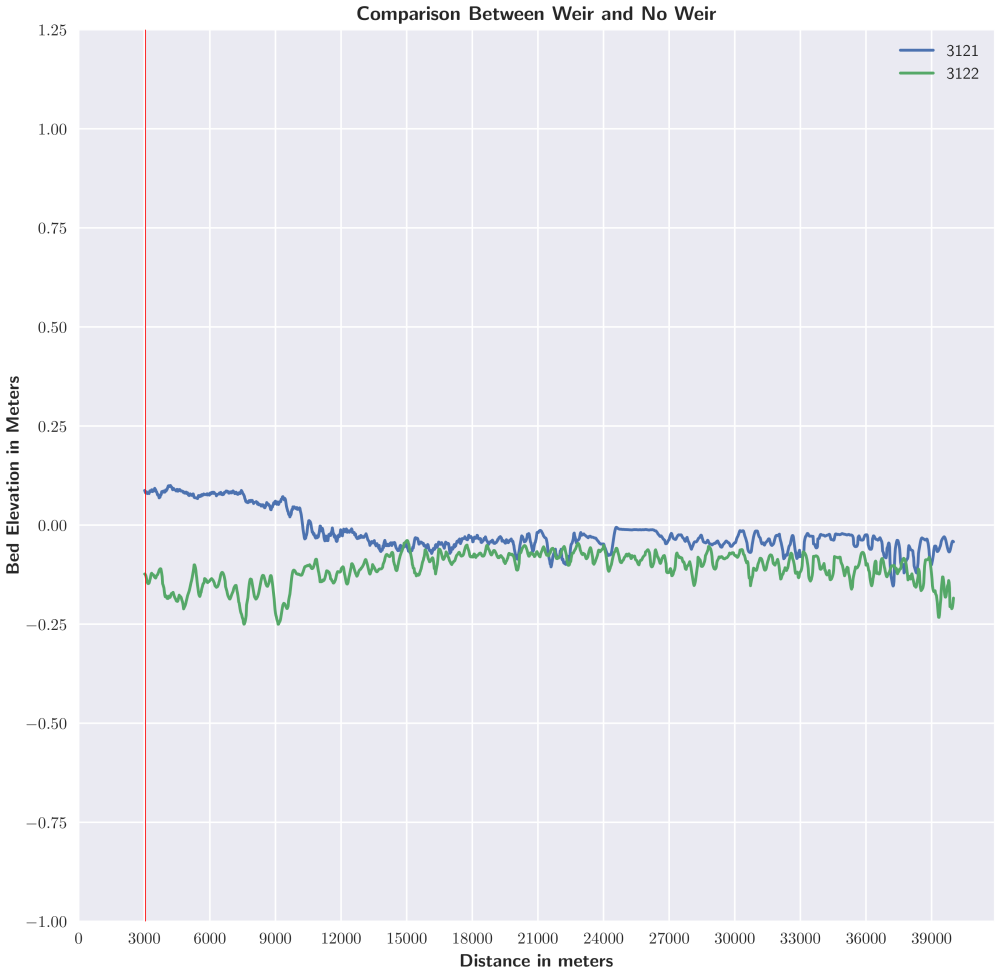

Figure A.19: Bed Elevation Comparison between 3121 & 3122: Manning Value 0.017

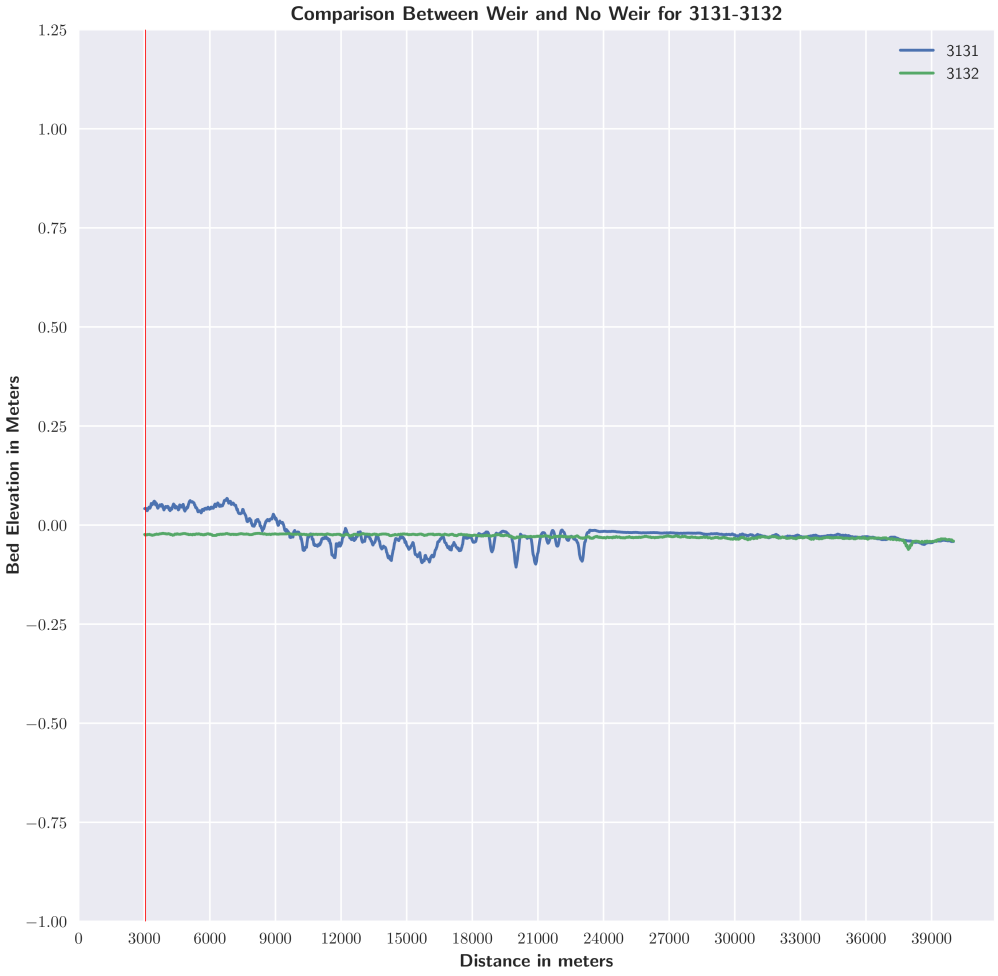

Figure A.20: Bed Elevation Comparison between 3131 & 3132: Manning Value 0.022

A.4.2 Bed Mass Change

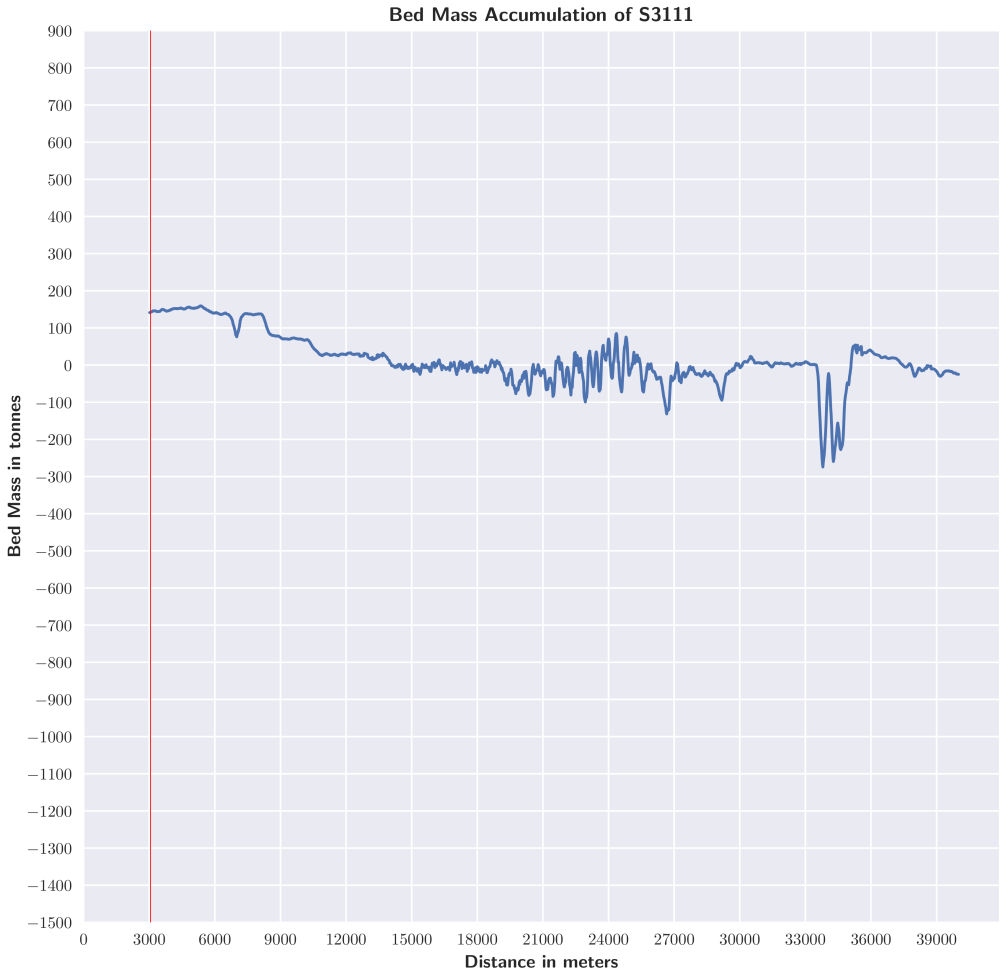

Figure A.21: Bed Mass Accumulation in Tonnes S3111

A.4.3 Time Series Upstream of Weir 20, 40, 100, 200, 500, 1000m

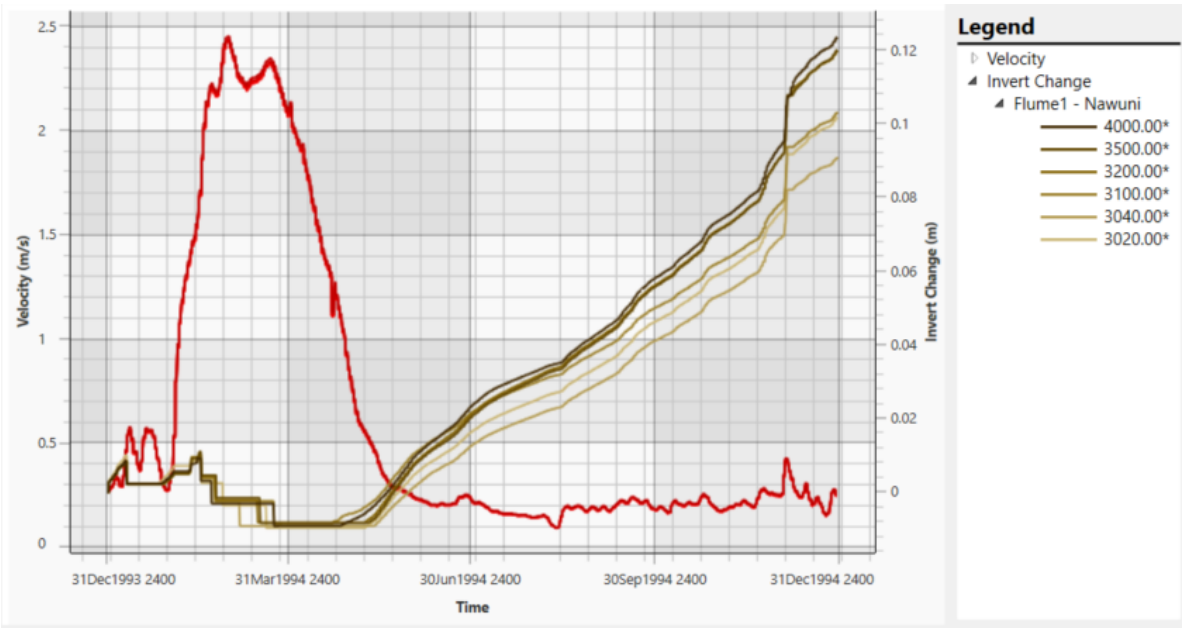

Figure A.22: Time Series Data for S3111 at locations upstream of the weir

A.4.4 Total Sediment Accumulation upstream of weir

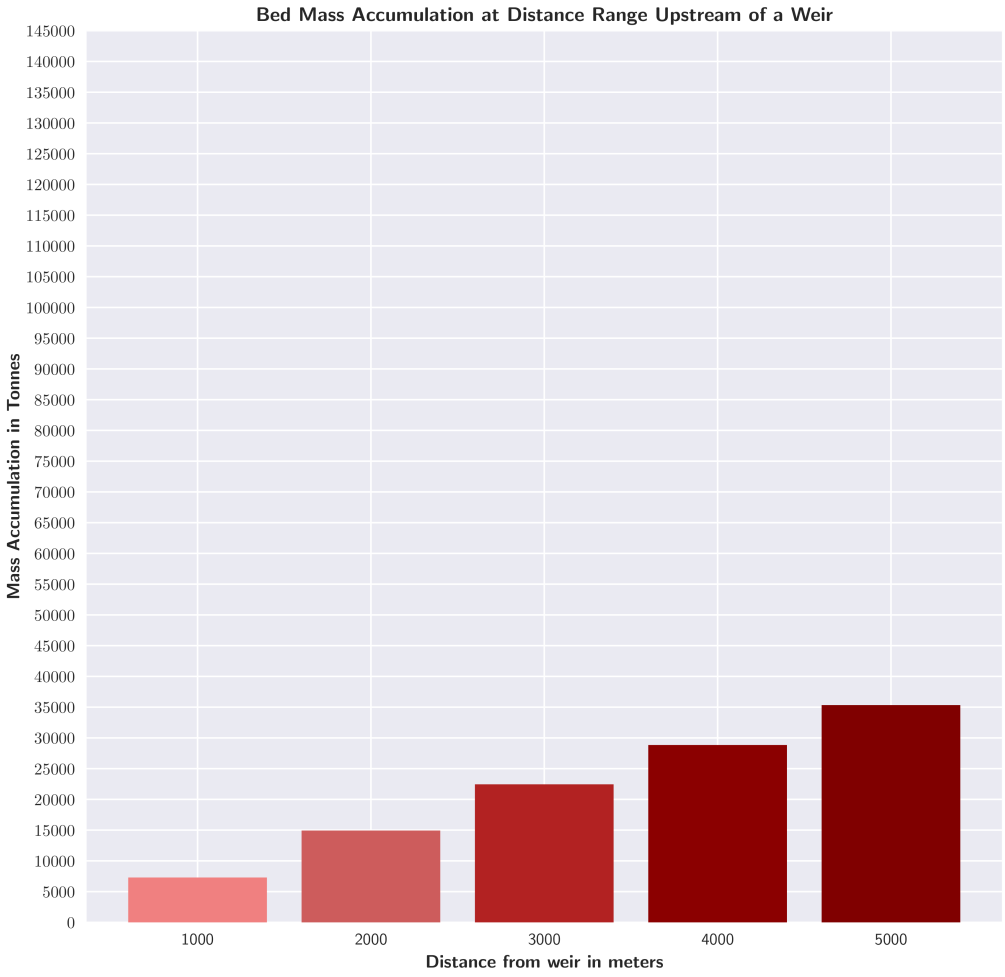

Figure A.23: Sediment Accumulation above baseline levels in tons at distances upstream of a weir

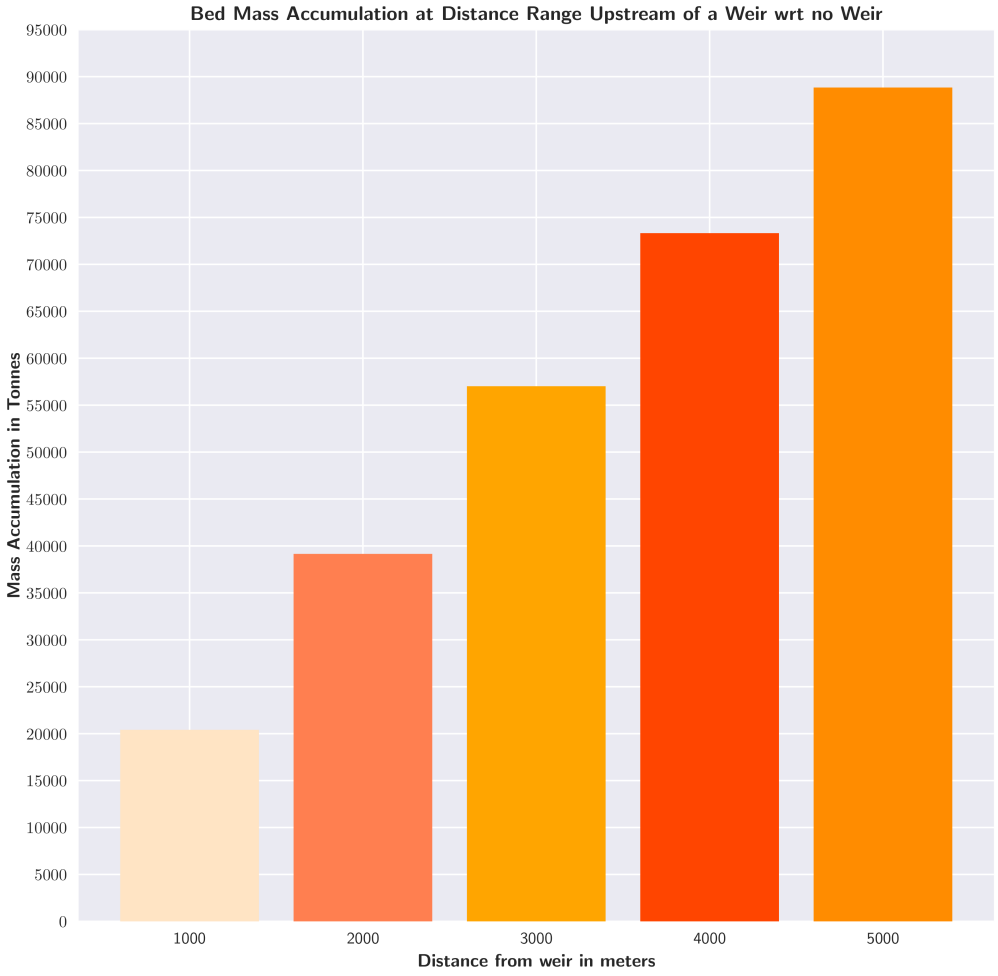

Figure A.24: Sediment Accumulation relative to erosion based on no weir at distances upstream of a weir

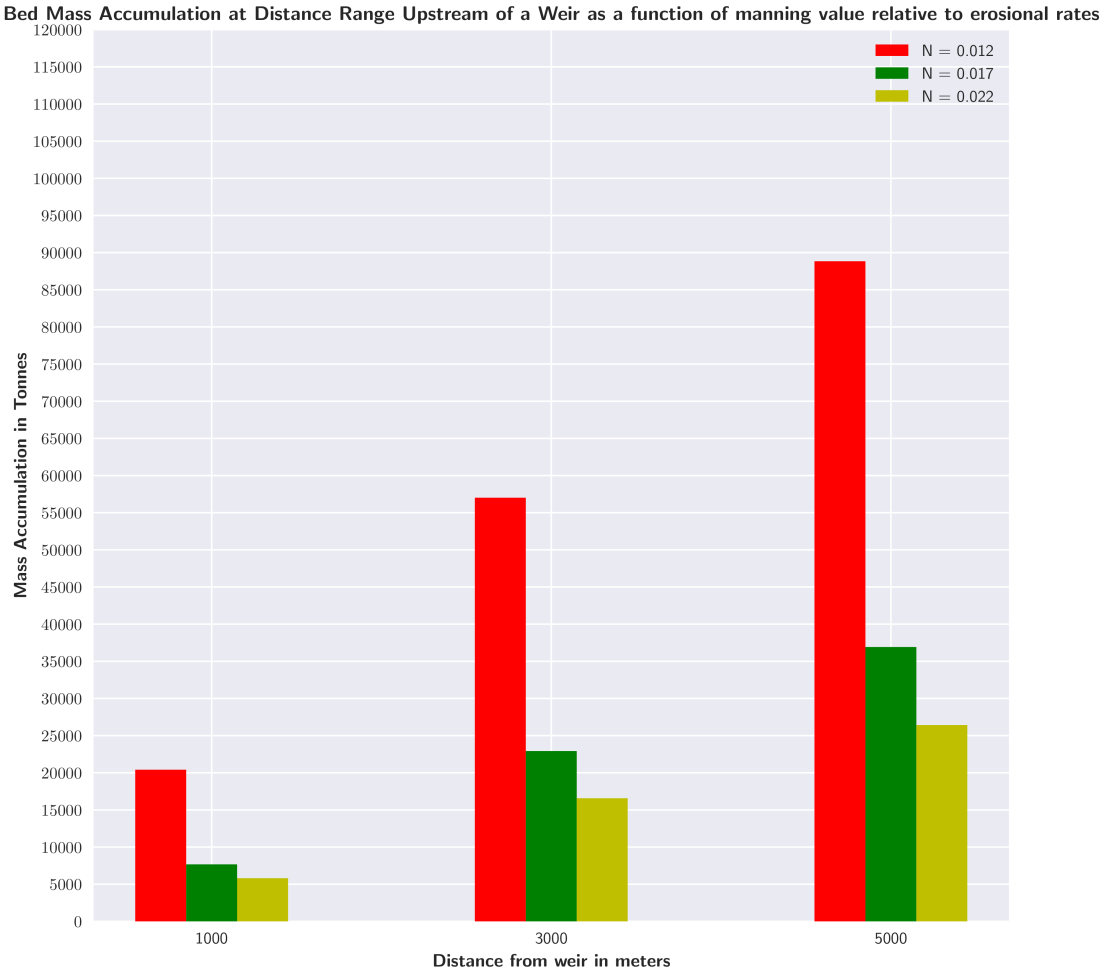

Figure A.25: Comparison of bed mass accumulation at various distances upstream with altering mannings roughness coefficient using Toffaletis equation relative to erosional rates

A.5 MODEL RESULTS: YANGS

A.5.1 Invert Change

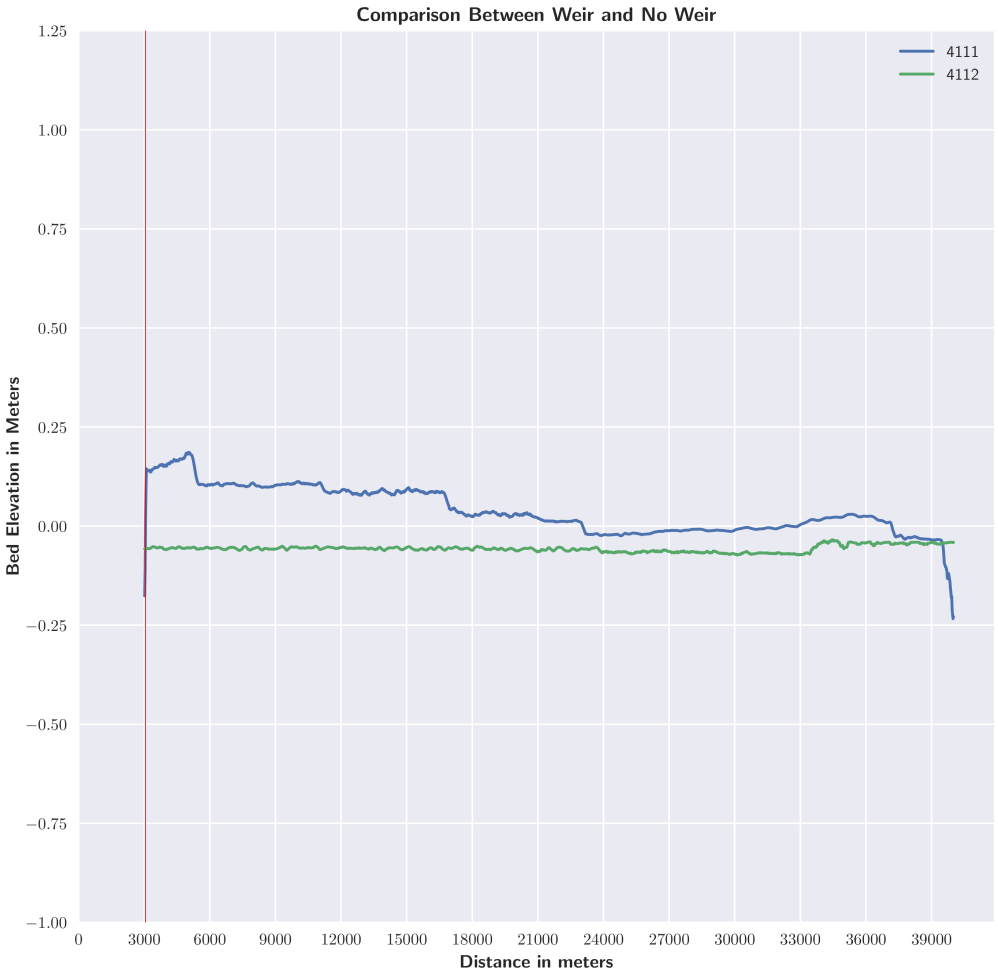

Figure A.26: Bed Elevation Comparison between 4111 & 4112: Manning Value 0.012

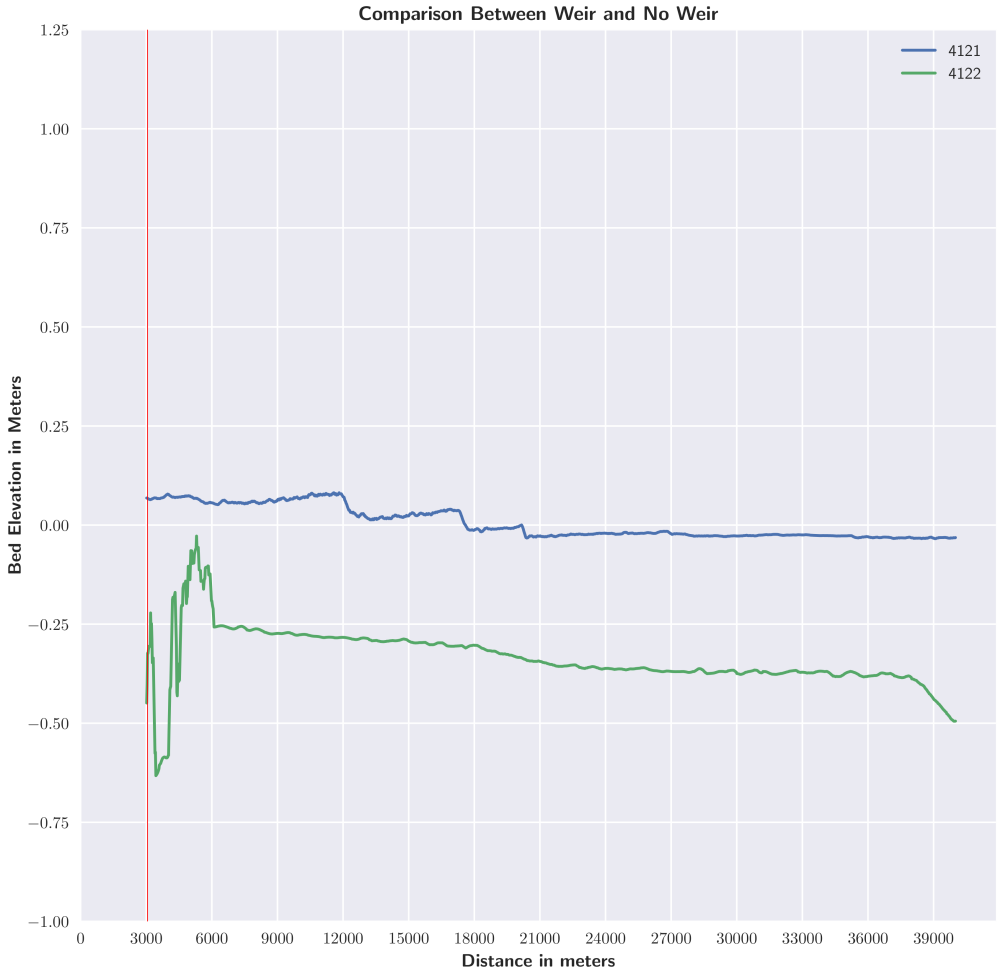

Figure A.27: Bed Elevation Comparison between 4121 & 4122: Manning Value 0.017

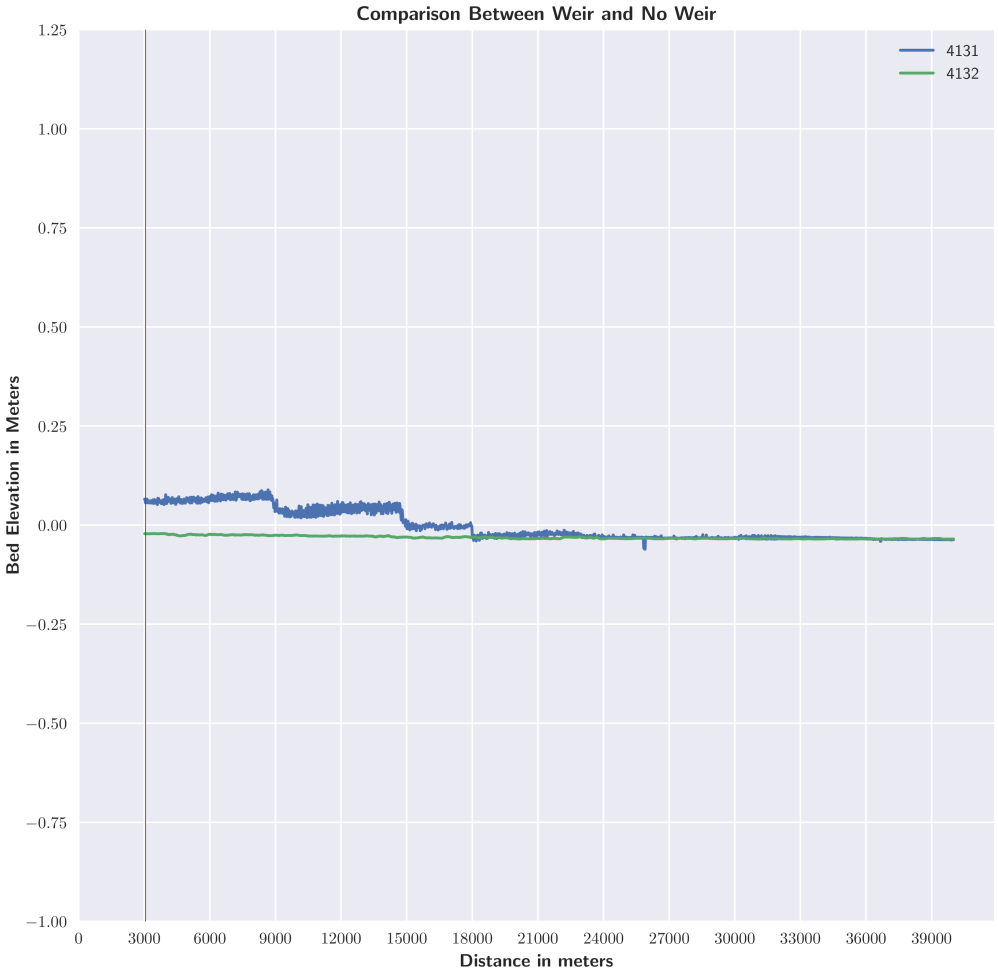

Figure A.28: Bed Elevation Comparison between 4131 & 4132: Manning Value 0.022

A.5.2 Bed Mass Change

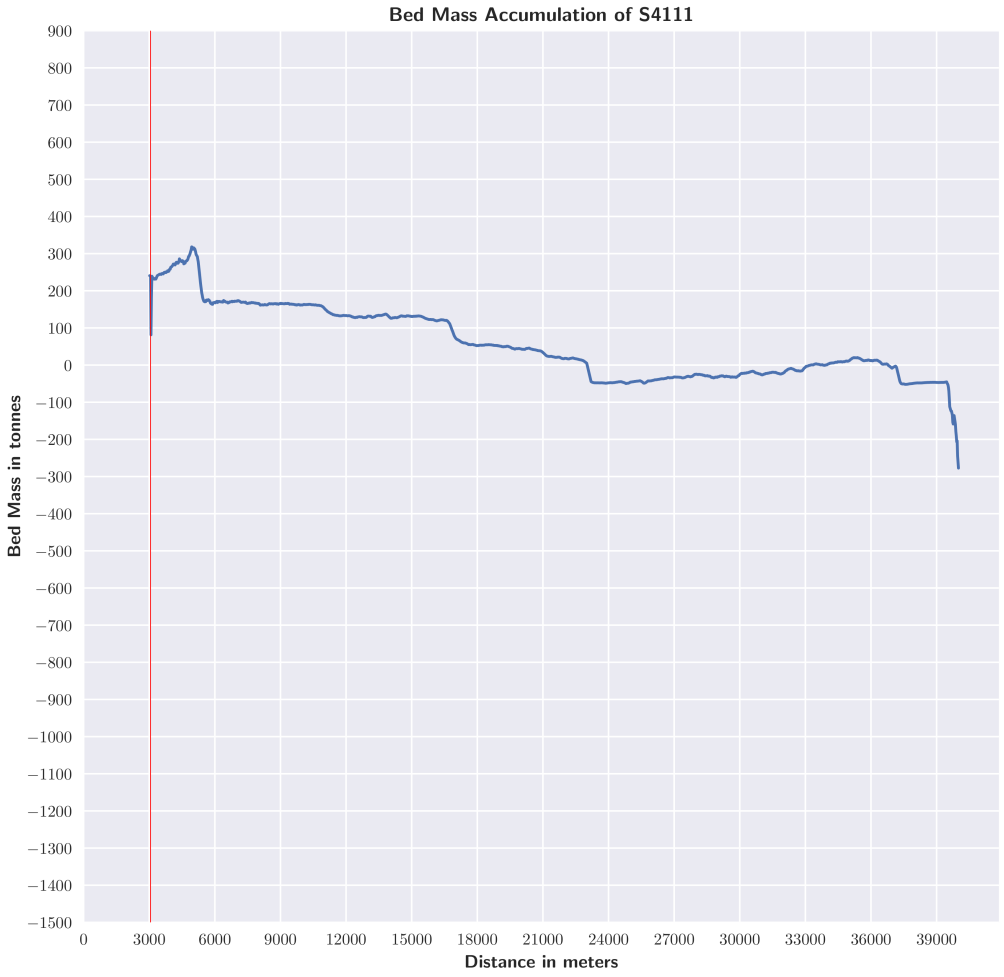

Figure A.29: Bed Mass Accumulation in Tonnes S4111

A.5.3 Time Series Upstream of Weir 20, 50, 100, 200, 500, 1000m

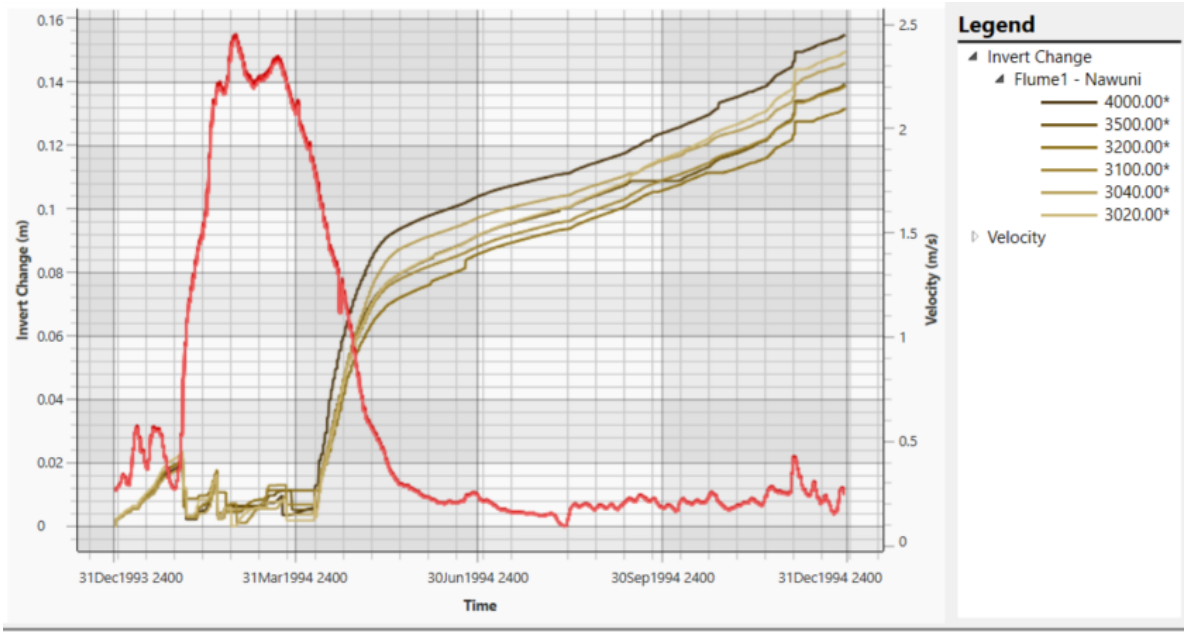

Figure A.30: Time Series Data for S4111 at locations upstream of the weir

A.5.4 Total Sediment Accumulation Upstream of Weir

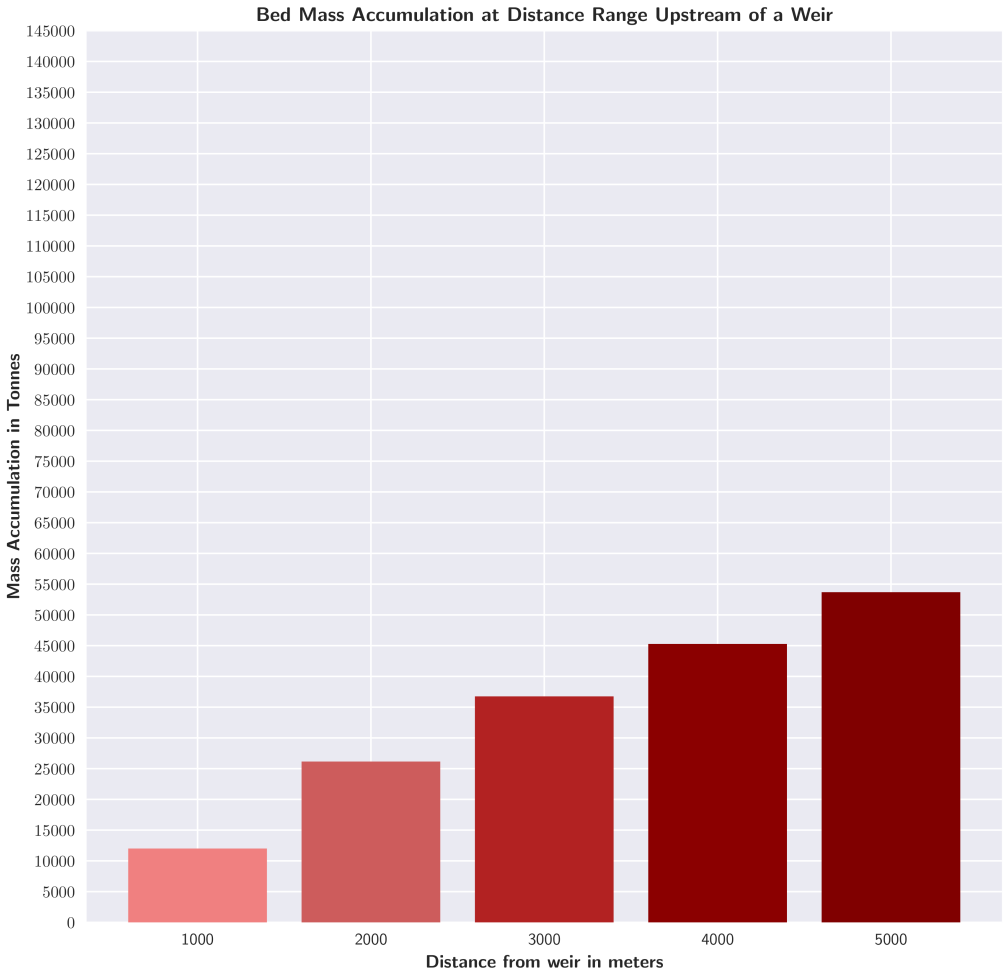

Figure A.31: Sediment Accumulation above baseline levels in tons at distances upstream of a weir

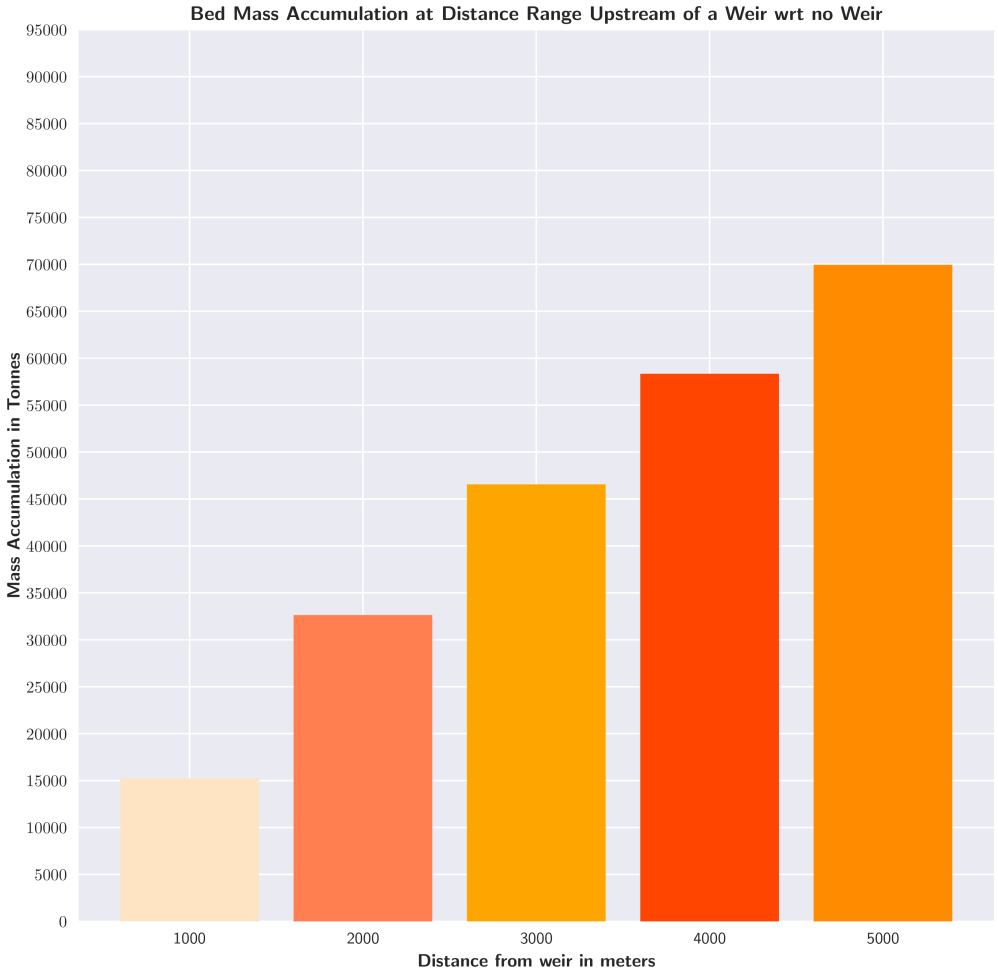

Figure A.32: Sediment Accumulation relative to erosion based on no weir at distances upstream of a weir

A.6 MODEL RESULTS: WILCOCK & CROWE

A.6.1 Invert Change

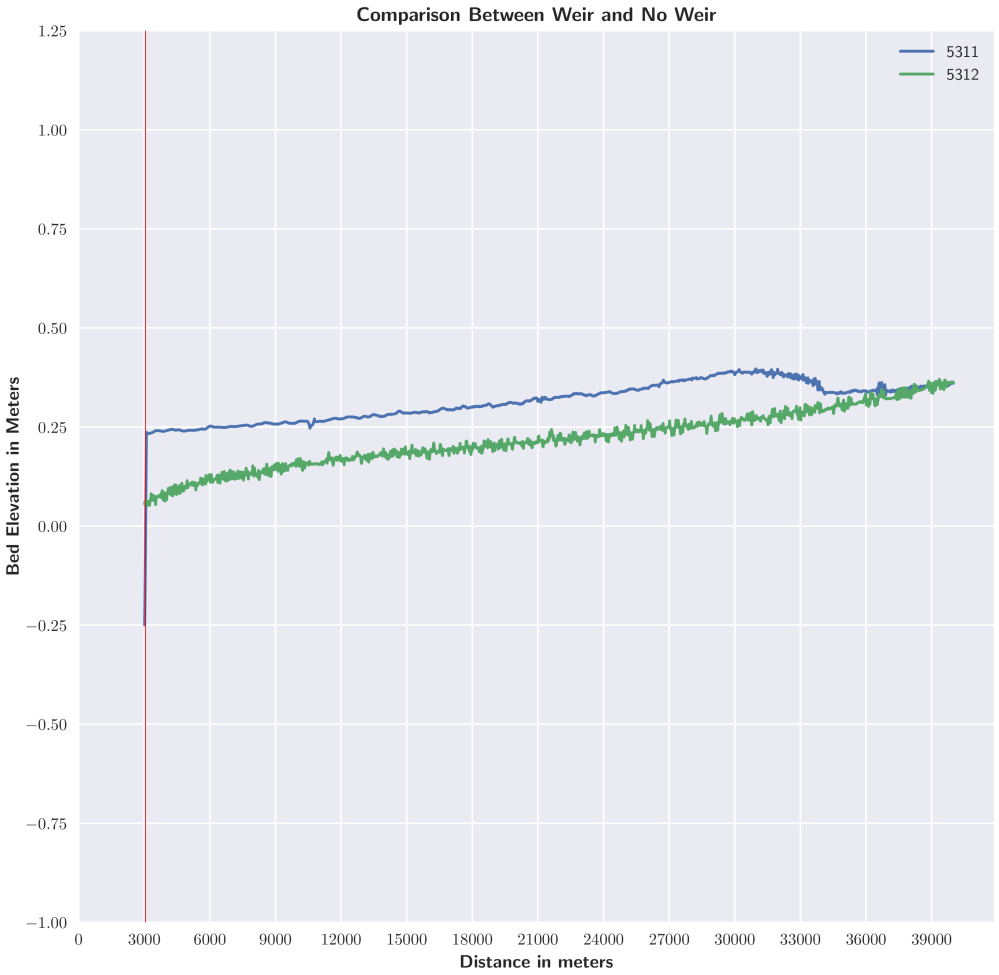

Figure A.33: Bed Elevation Comparison between 5311 & 5312: Manning Value 0.012

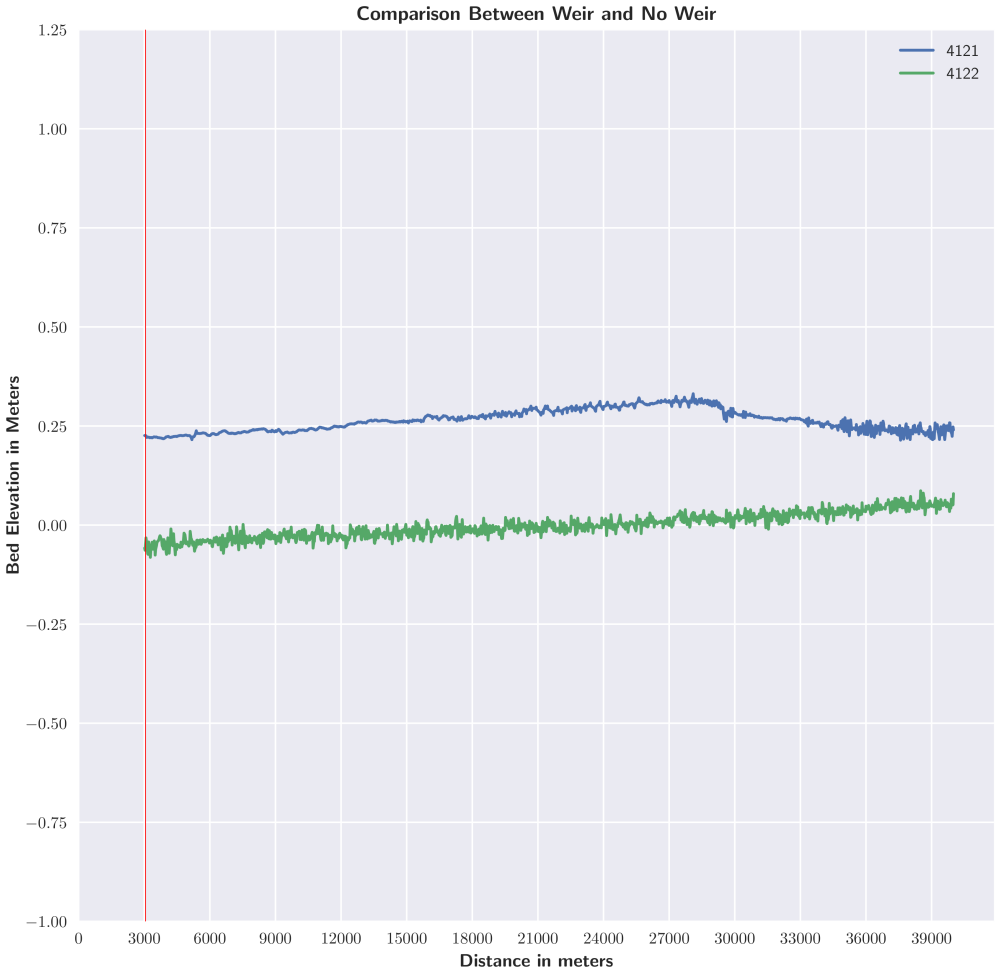

Figure A.34: Bed Elevation Comparison between 5321 & 5322: Manning Value 0.017

A.6.2 Bed Mass Change

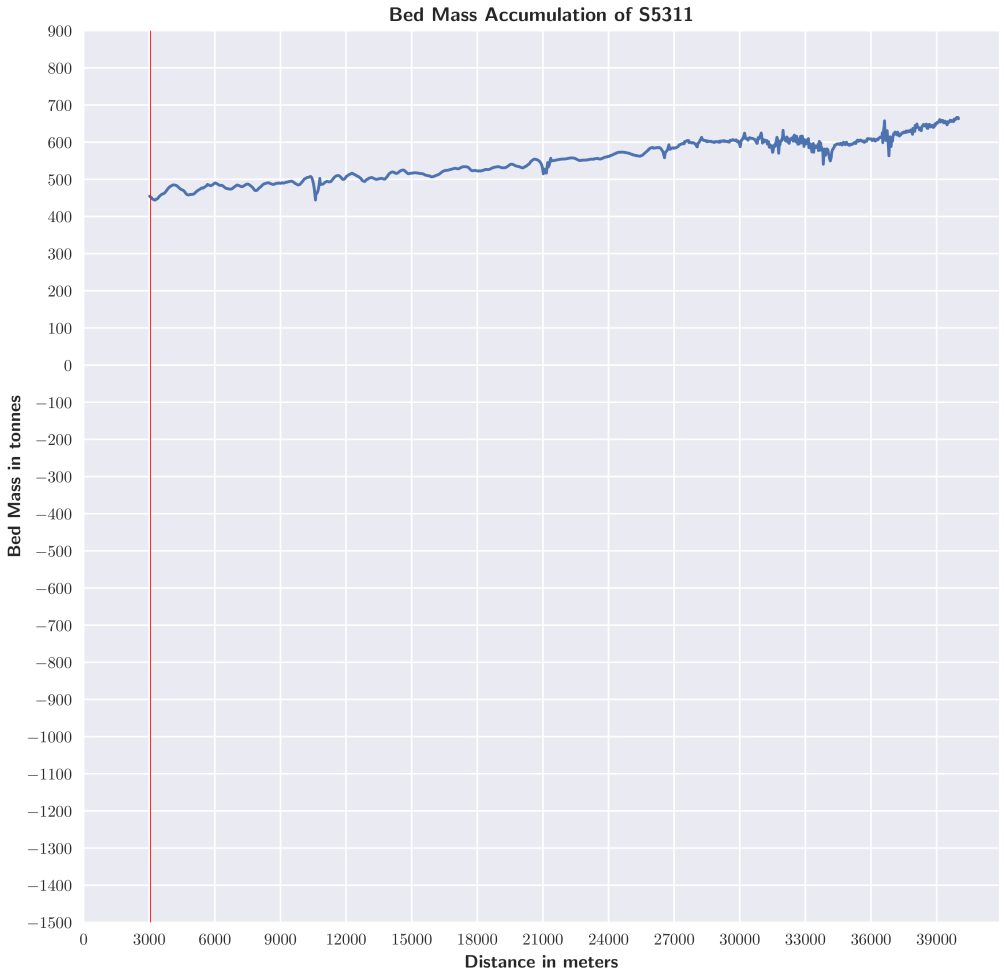

Figure A.35: Bed Mass Accumulation in Tonnes S5311

A.6.3 Time Series Upstream of Weir 20, 40, 100, 200, 500, 1000m

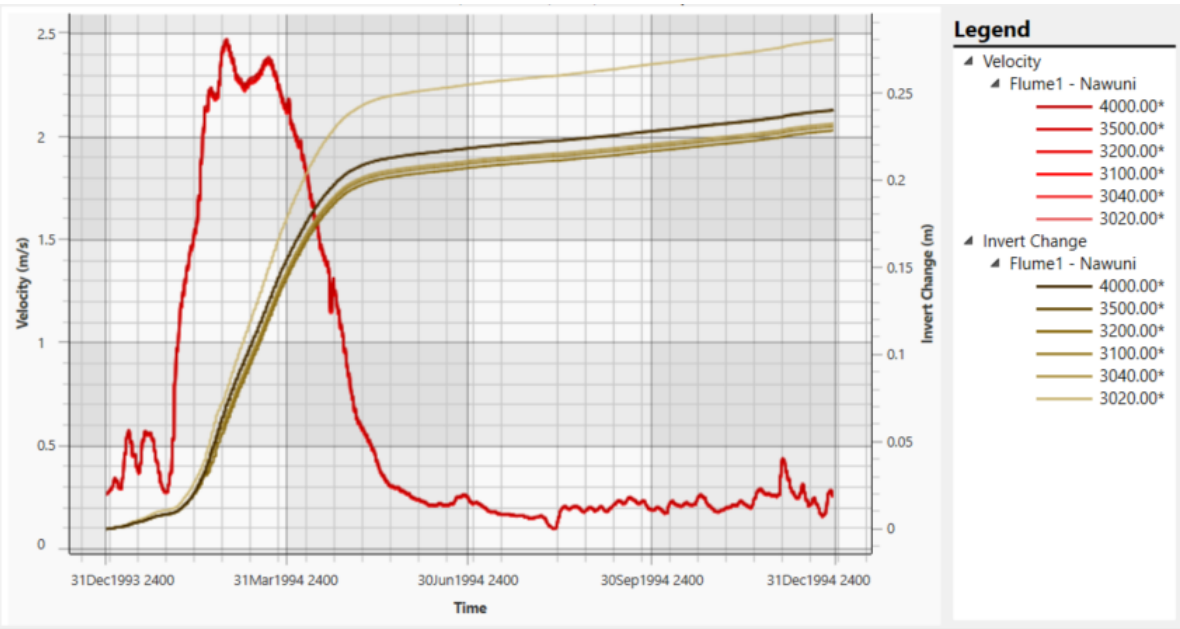

Figure A.36: Time Series Data for S5311 at locations upstream of the weir

A.6.4 Total Sediment Accumulation upstream of weir

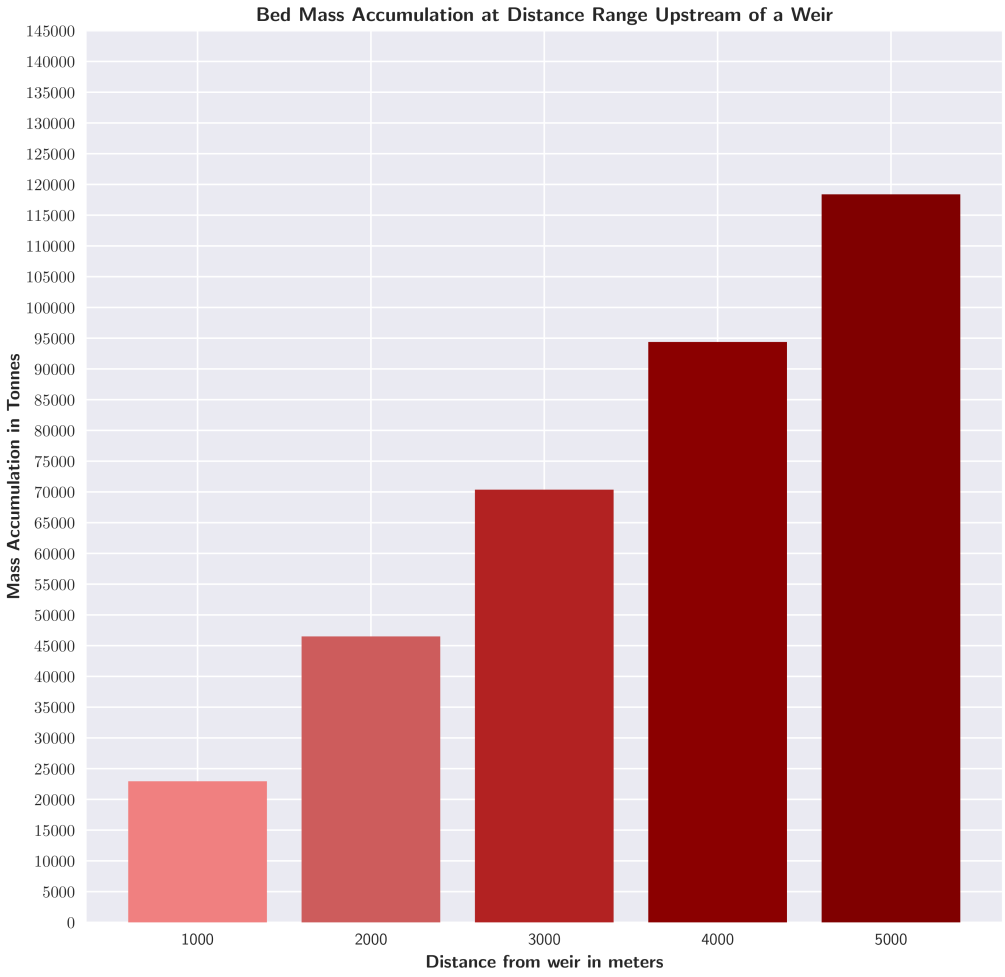

Figure A.37: Sediment Accumulation above baseline levels in tons at distances upstream of a weir

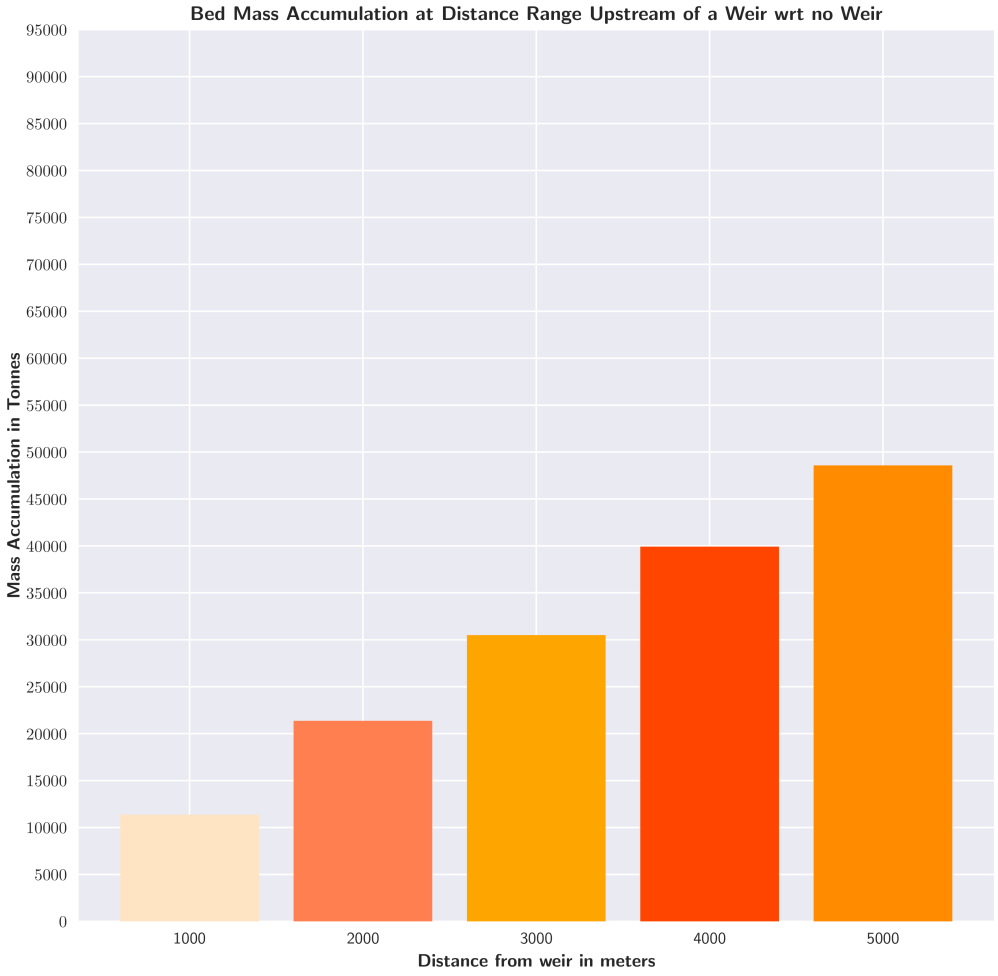

Figure A.38: Sediment Accumulation relative to erosion based on no weir at distances upstream of a weir

A.7 GRAIN BEHAVIOR

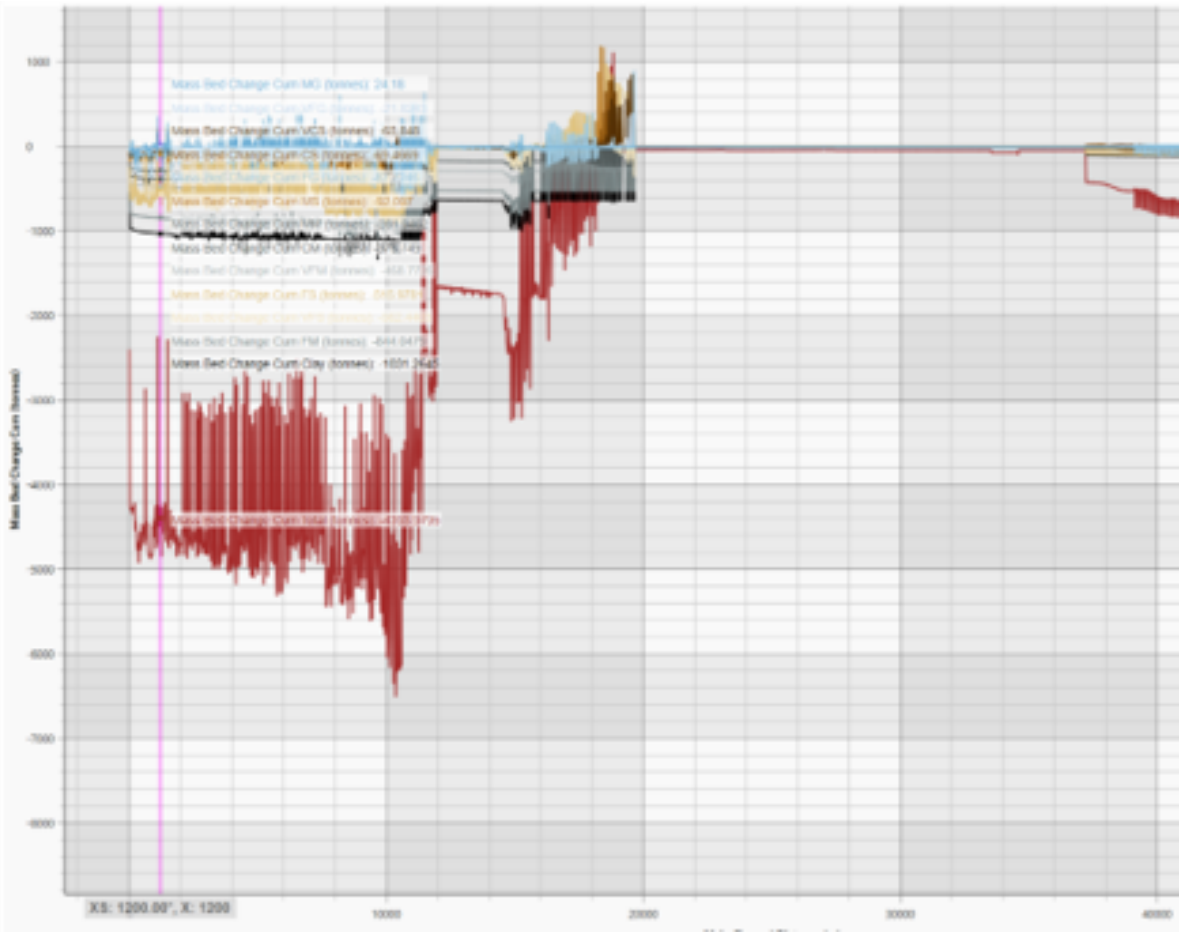

Figure A.39: Laursen Copeland Grain Behavior

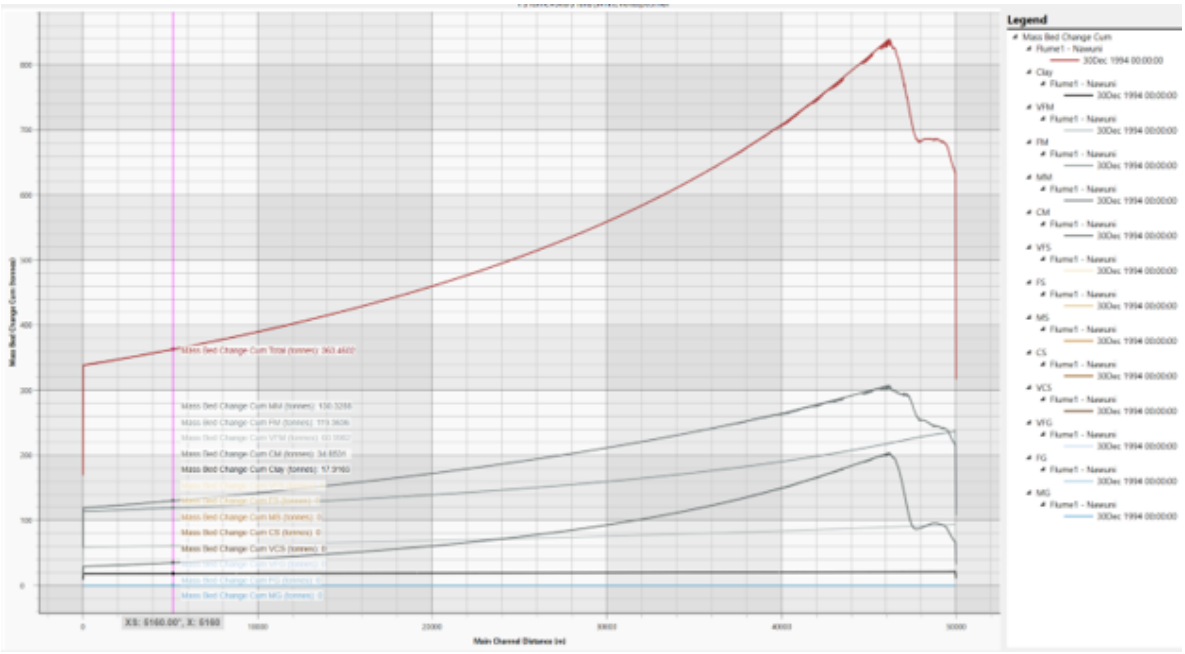

Figure A.40: Meyer Peter Muller Grain Behavior

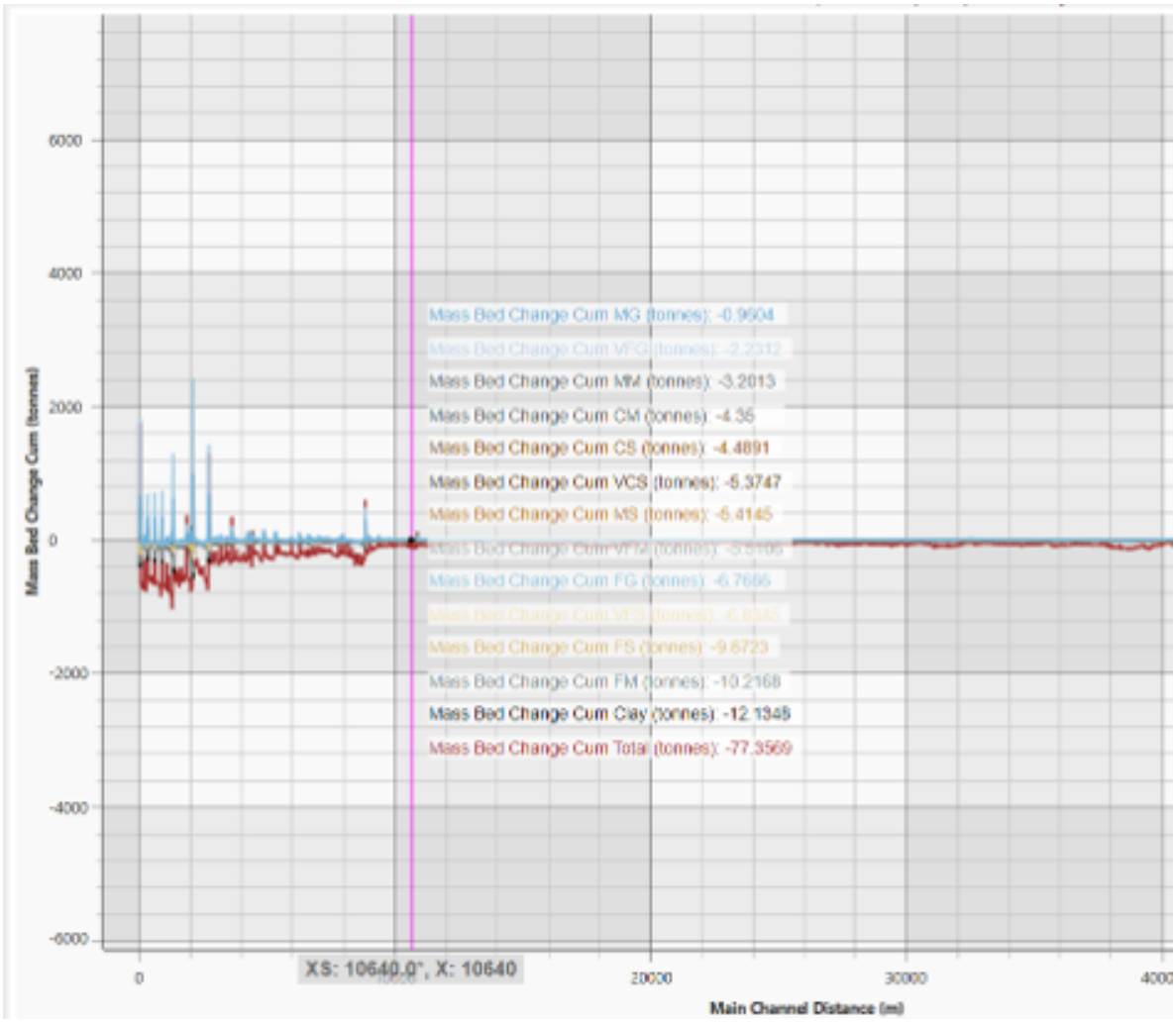

Figure A.41: toffaleti Grain Behavior

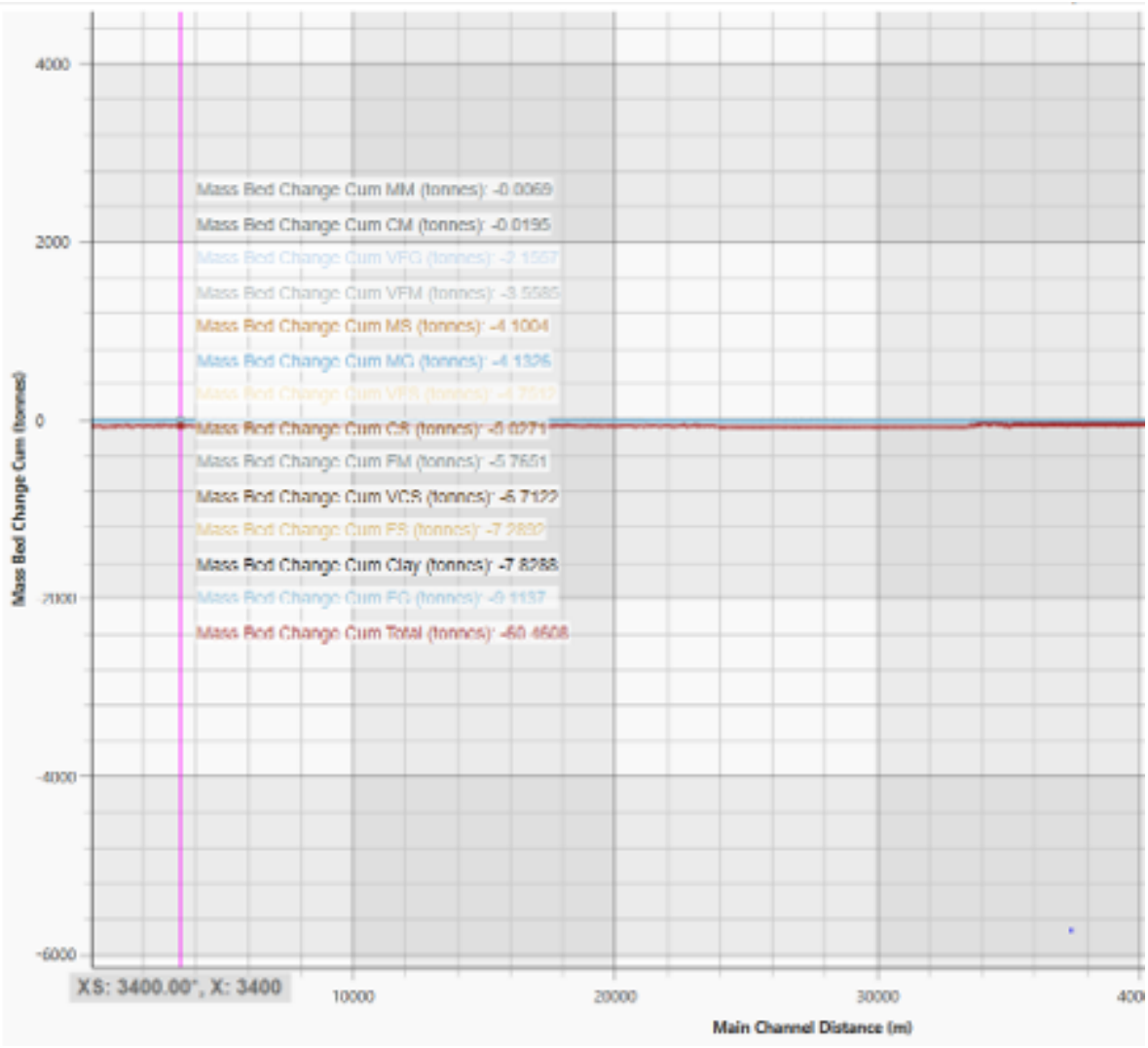

Figure A.42: Yang Grain Behavior

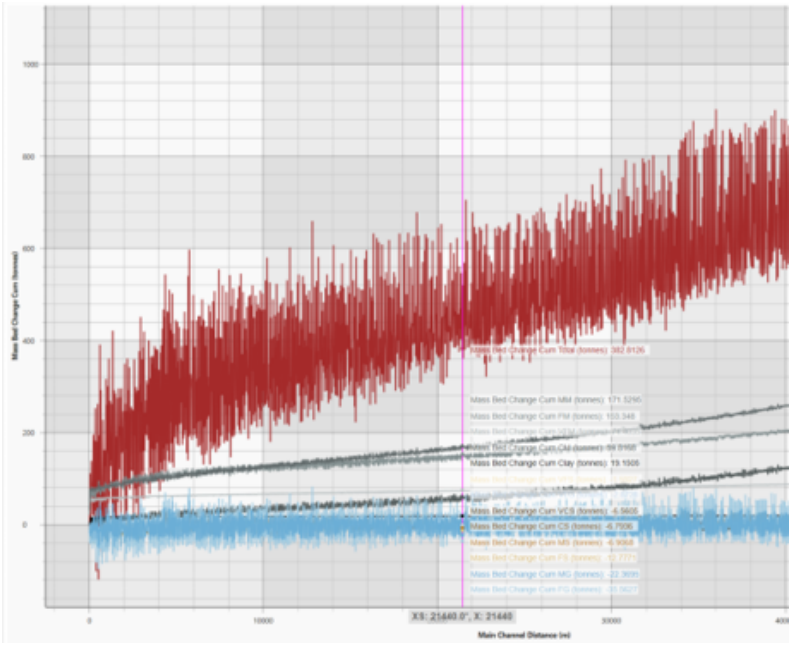

Figure A.43: Wilcock Grain Behavior

COLOPHON

This document was typeset using LaTeX. The document layout was generated using the arsclassica package by Lorenzo Pantieri, which is an adaption of the original classicthesis package from André Miede.